Energy and Climate Change 5 (2024) 100126

Contents lists available at ScienceDirect

Energy and Climate Change

journal homepage: www.sciencedirect.com/journal/energy-and-climate-change

Full Length Article

Climate ambition, background scenario or the model? Attribution of the variance of energy-related indicators in global scenarios

Alaa Al Khourdajie [a,b,*], Jim Skea [c], Richard Green [d]

[a] Department of Chemical Engineering, Imperial College London, United Kingdom
[b] International Institute for Applied System Analysis (IIASA), Austria
[c] International Institute for Environment and Development (IIED), London, United Kingdom
[d] Department of Economics and Public Policy, Imperial College Business School, Imperial College London, United Kingdom

ARTICLE INFO

Keywords:
Energy transition
Climate change mitigation
Integrated assessment models
Shapley–Owen decomposition

ABSTRACT

We attribute variations in key energy sector indicators across global climate mitigation scenarios to climate ambition, assumptions in background socioeconomic scenarios, differences between models and an unattributed portion that depends on the interaction between these. The scenarios assessed have been generated by Integrated Assessment Models (IAMs) as part of a model intercomparison project exploring the Shared Socio-economic Pathways (SSPs) used by the climate science community. Climate ambition plays the most significant role in explaining many energy-related indicators, particularly those relevant to overall energy supply, the use of fossil fuels, final energy carriers and emissions. The role of socioeconomic background scenarios is more prominent for indicators influenced by population and GDP growth, such as those relating to final energy demand and nuclear energy. Variations across some indicators, including hydro, solar and wind generation, are largely attributable to inter-model differences. Our Shapley–Owen decomposition gives an unexplained residual not due to the average effects of the other factors, highlighting some indicators (such as the use of carbon capture and storage (CCS) for fossil fuels, or adopting hydrogen as an energy carrier) with outlier results for particular ambition-scenario-model combinations. This suggests guidance to policymakers on these indicators is the least robust.

1. Introduction

Integrated assessment models (IAMs) play an increasingly critical bridging role linking the development of energy and other systems with that of the climate system [1]. IAMs differ in their approaches; "myopic" decision-making versus optimisation (with perfect foresight) over a time horizon, general equilibrium versus partial equilibrium, in addition to other aspects ([2] Annex III). But a key common characteristic is that they select technologies and practices with the aim of achieving a climate goal, either by minimising aggregate costs or by following decision rules assigned to the agents represented in the model. Almost exclusively, the climate goal used to guide the selection has been a level of cumulative carbon dioxide (CO_2) emissions (known as a carbon budget) over a time horizon either until the CO_2 net zero date (so called net zero carbon budget) or till 2100 (end-of-century budget) [3]. The use of the carbon budget is a practice adopted by the IAM modelling community; it derives from findings in physical climate science that identify a quasi- linear relationship between cumulative CO_2 emissions and global warming, but other objectives could be pursued ([2], Annex III).

Given the diversity of IAMs' underlying structures and conceptual frameworks, it is unsurprising that results vary in terms of technology adoption and utilisation. The practice has emerged, notably within the Intergovernmental Panel on Climate Change (IPCC), of categorising multiple published IAM-generated scenarios[1] according to the warming outcome in the year 2100 for a given likelihood of limiting warming to that level (e.g. scenarios that limit peak warming to 2°C with a likelihood greater than 67%). The range of results for specific indicators, such as global natural gas use, within a given scenario category are then assessed using standard descriptive statistics [4,5]. For example, in IAM-generated scenarios that limit peak warming to 2°C, the

* Corresponding author.
E-mail address: a.alkhourdajie@imperial.ac.uk (A. Al Khourdajie).

[1] Note that in the context of our paper we use the terms "IAM-generated scenarios", "model/s runs" or "IAM runs" to indicate scenario-output as what a model run gives. This is to avoid confusion with the SSP scenarios that are input socio-economic background assumptions for these models' runs, and one of the key explanatory variables in our regressions. The latter are referred to as "background scenario assumptions", "scenarios" or "SSPs".

https://doi.org/10.1016/j.egycc.2024.100126

Available online 22 January 2024

interquartile range for natural gas use in 2050 compared to 2019 lies between a 40 % decrease and a 10 % increase, with a considerably wider p5-p95 range. In other words, at the top end of the range, significant further exploration and field development is warranted; at the lower end there is less scope. Meanwhile, the global CO_2 emissions levels for the p5–p95 range are projected to decrease by 36–69 % from the 2019 levels, respectively. This means that the emissions could fall anywhere from one- to over two-thirds, roughly. What is a policymaker to make of this? These wide ranges allow decision-makers to "pick and choose" from the wide range of results available.

IAMs have been widely criticised as "black boxes". To be useful to policymakers, it is essential that there is clarity as to what conclusions are robust across models, and why and in what respect model results differ [6,7]. This paper does explicitly treat IAMs as black boxes but is intended to provide direction and focus for deeper dives into model performance and characteristics. It asks the questions: which energy system and energy indicators are robust, and which show wide variation across model runs; what are the high-level explanatory factors for these variations; and which energy indicators merit priority attention for conducting deep dives?

Our broad approach is a statistical analysis of a set of IAM runs conducted as part of a single model intercomparison project the results of which are reported in the Shared Socioeconomic Pathways (SSPs) database [8]. The database covers five SSPs that describe plausible and internally consistent futures of the global economy, population and energy service demand that result in different challenges to mitigation and adaptation. These futures revolve around five different narratives (e.g. sustainability under SSP1), which are quantified using IAMs in terms of GDP and population trajectories reflecting such narratives.

We look at a range of indicators relevant to the energy sector including primary energy supply by source, final energy demand by sector and carrier, emissions from the energy sectors, and economic indicators. We assess how much of the variance in results can be attributed to the average effect of three factors: climate ambition; background scenario assumptions (e.g. economy, demographics); and differences between the models. We also explore the unattributed portions that depend on the interaction between these. Dekker et al. [9] have also examined the sources of variation between model runs, but our paper differs in two respects. First, our regression-based analysis is explicit about the remaining variation that is not explained by these average effects. We believe that both of the following statements are conceptually useful: a) the decline in energy use as climate ambition rises and the differences in energy service demands between SSPs each contribute a similar amount to explaining the variation in primary energy across model runs; b) while predictions for nuclear power do not systematically change very much with ambition (differences between models and SSPs are much more important), some models *do* increase nuclear power in some (not all) SSPs as climate ambition increases. For indicators like this, there is a sizeable amount of variation that is not straightforward to link to differences in a single factor, and we explicitly report this, as it complicates the picture for nuclear energy as a mitigation option.

Second, we rely on runs conducted as part of a single model intercomparison project exploring the five SSPs widely used by the climate science community, which gives us a reasonably balanced panel across SSPs. Dekker et al. [9] have used the more recent IPCC AR6 Scenario Database [10] which is an unstructured database that combines runs from multiple model intercomparison projects and individual studies conducted at different points in time, often to answer different questions [4].[2] Over 90 % of those model runs are based on a single middle-of-the-road narrative; SSP2, and the vast majority of these runs are based on 5 models families leading to over-representation and hence biases in the ensemble. As we show in Fig. B1 in Appendix B, the SSPs database offers a wider and an almost-equal representation across SSPs and models, albeit not across all model-SSP combinations. The AR6 dataset is well-suited to answering questions about the variation between the wide range of results in the literature, while the SSPs database is a more balanced panel that may well be a better reflection of the variations that could come in the answer to a specific question.

We find that climate ambition has the largest impact on most energy indicators, specifically in results related to CO_2 emissions. The scenario factor plays a significant role in explaining the variability of final energy demand variables influenced by population, as well as the amounts of aggregate fossil fuels and coal coupled with CCS. Differences between models take a dominant role in explaining the variability of some energy indicators that are related to non-biomass renewables such as wind, geothermal and hydro. However, some indicators like hydrogen use, nuclear energy and geothermal, the level of carbon price, and most notably the use of CCS in all fossil fuels suffer from high variability across and/or within the models' runs, with large variation that is not straightforward to link to differences in a single factor in our analysis. This merits careful attention to the underlying scenario assumptions and model differences for informed policymaking.

The remainder of the paper is organised as follows. Section 2 describes the data and methodology. In Section 3, the empirical results are presented and discussed. Section 4 concludes by summarising the main findings, their policy implications, and providing recommendations for future research.

2. Methodology

2.1. Overview

In this paper we apply the Shapley–Owen decomposition analysis [11] in order to evaluate three drivers behind key energy indicators in long-term mitigation pathways: climate ambition, background scenario assumptions (e.g. economy, demographics) for which we use the shorthand 'scenario', and differences between the models, alongside the unattributed portions emerge from their interactions. These factors collectively shape the future evolution of the chosen key energy indicators, or any other indicator for that matter, in the IAMs' runs.

Based on the Shapley–Owen decomposition method, linear multiple regression analysis is used to attribute the respective contribution of each of these three factors to the variance of a chosen energy indicator

[2] In the AR6 Scenarios database, there are individual model runs that attempt to address specific questions. For instance, one of the model runs in Category 1 (limiting warming to 1.5C (>50 %) no or low overshoot) by model "C-ROADS-5.005", scenario "Ratchet-1.5-limCDR-noOS", focuses on the implications of applying high constraints on the scale and type of carbon dioxide removal measures available. This model run results in a very stringent CO_2 and non- CO_2 emission reductions trajectory, as well as the earliest net zero CO_2 date (2037) within the 90th percentile range. Including such a scenario in the summary statistics of, for instance, the role of biofuels is bound to result into biases in these estimates when analysed side-by-side with structured model intercomparison studies and other individual studies.

(the dependent variable) across all model runs as represented by its R^2 value.[3] The Shapley–Owen method attributes the contribution from each factor to be the increase in R^2 that comes from adding that factor to a regression. The results are averaged over all possible permutations in which the regression can be assembled. This contribution of each factor is known as the Shapley–Owen *value*. It has several attractive properties, not least that the R^2 from the overall regression is exactly decomposed into the contributions from the three factors [12]. Another important property of our approach is that we do not expect to capture all the variation between model runs via the average effects of choosing (e.g.) a particular model embodied in regression coefficients: $1 - R^2$ is the proportion of the variation in the dependent variable that is not explained by the regression (see Appendix A.1 for detailed discussion).

Other approaches in the literature on variance decomposition analysis identify the relative importance of regressors in explaining the dependent variables including sequential sums of squares and proportional marginal variance decomposition [12], and the Sobol decomposition based on functional variance analysis ([13] in the [9] paper we refer to above). The Shapley–Owen method adopted in our paper is the most appropriate in our case for 2 reasons, a) it facilitates the exogenous grouping of regressors, which, as we explain in the next section, allows us to capture nonlinear effect of climate ambition, b) studies show that Shapley value holds a comparative advantage over Sobol indices, particularly when dealing with statistically dependent or correlated input variables within sensitivity analysis. Shapley values allocate mutual contributions (be it due to correlation or interactions) of input variables individually to each variable, which might lead to more accurate and reliable sensitivity analysis results [14–16].

Similar decomposition work using the Sobol method is done by [17], where the authors attempt to disentangle the driving forces beyond mitigation scenarios such as socio-economic developments, climate system uncertainty, damage estimates, mitigation costs and discount rates. Meanwhile, [18] use decomposition analysis adapted from Index Decomposition Analysis (IDA) to identify the sensitivity factors that derive future CO_2 emissions based on SSPs characteristics. In both contributions, the authors had access to the data generating process (i.e., new IAM runs were part of the exercise), tailored to clearly reveal the role of drivers they consider, while our method does not require such access.

2.2. Data selection and pre-processing

We apply our analysis to the SSP Database [8], which contains the results of model runs based on the five SSPs developed in order to enable integrated analysis among the climate physical modelling, impact modelling and the mitigation modelling communities. The SSPs describe plausible and internally consistent futures that lead to different challenges to mitigation and adaptation. These futures evolve around the narratives of sustainability (SSP1), middle of the road (SSP2), regional rivalry (SSP3), inequality (SSP4) and fossil-fuelled development (SSP5). The physical climate dimension, and hence implicitly climate policy ambition, of these futures is captured by an earlier scenarios framework called Representative Concentration Pathways (RCPs) [19] which covers seven levels of radiative forcing by the end of the century (measured in W/m^2). These different radiative forcing levels are combined with the SSPs in a matrix structure. The SSPs model intercomparison project has six participating models and includes 126 model runs altogether. We focus on decadal years only, starting from 2020.

In terms of treating missing data due to lack of some model-SSP combinations, we adopt the approach of likewise deletion (aka Complete Case analysis) where we exclude model runs that did not report results for specific dependent variables from certain segments of our analysis and the analysis is conducted with the remaining complete cases. This efficient approach does not necessitate additional modelling or imputation given that missingness in model-SSP combinations may be deemed as Missing Completely at Random (MCAR), where the missingness is independent of both observed and unobserved data. This characteristic renders listwise deletion a less biased approach compared to scenarios where missingness might be systematically related to other factors [20]. For the same reason, we do not correct for the fact that some models have more entries for certain scenarios than others, where sampling method may induce different types of bias. Similarly, where models do not have any entries for certain scenarios (e.g. MESSAGE-GLOBIOM has no entries for SSP4 and SSP5) rather than introducing bias due to imputation they simply don't feature in the relevant analysis and hence the sample is not perfect. In explaining our findings throughout the Results and Discussion section we highlight, where needed, such cases (e.g. not all models report Primary Energy Geothermal) and how they influence the Shapley–Owen decomposition results. Appendix B.1 includes general descriptive statistics of the database, followed by a table on missing data by variable in Appendix B.3. The detailed plots in Appendix C (e.g. Fig. C4 for Primary Energy Geothermal) clearly flag models that failed to report specific variables.

In order to conduct the Shapley–Owen decomposition analysis, we perform multiple linear regression analyses where the dependent variables are the chosen key energy indicators (e.g. final energy demand for electricity), while the explanatory variables capture the three factors mentioned above. Appendix B.2 includes the full list of the energy indicators which are our dependent variables. As for the explanatory variables, we represent the model factor by a set of dummy variables that captures the modelling families, while another set of dummy variables captures the SSP families and hence the scenario factor. One model and one SSP are used as the numeraire in constructing the dummy variables. In contrast, the climate ambition factor is represented by a quadratic function of total cumulative CO_2 emissions between 2010 and 2100 and its square, computed from the variable "Emissions|CO_2" in the SSPs database. Using a quadratic function in the regressions allows for a non-linear response to stricter emissions targets.

We intentionally did not use RCP dummy variables to represent climate ambition as the baseline emissions vary so much across models even for a given RCP-SSP combination. While this could be seen as an additional source of inter-model variation, cumulative CO_2 emissions drive the climate, and the level of mitigation observed should be linked to reductions in these. At the suggestion of an anonymous referee, we undertook further diagnostic analysis by using the RCPs as dummy variables instead of quadratic cumulative CO_2 emissions as presented in Appendix E below. For most indicators, both measures yield very similar results.

The continuous variable is more effective in explaining variations in unabated fossil fuel use, as it captures differences across baseline results. RCP dummy variables are better at explaining the role of certain mitigation technologies, such as hydrogen as a final energy carrier, which rise more rapidly for the highest levels of ambition than a quadratic relationship with emissions can capture. This may suggest that neither measure is completely satisfactory, something that we reflect on in future research avenues.

2.3. Applying Shapley–Owen decomposition to mitigation scenarios

For each dependent variable (energy sector indicator), we ran seven ordinary least squares (OLS) regressions. These regressions cover all

[3] The R^2 value (aka the coefficient of determination or goodness of fit) is a measure of how well the linear regression model fits the data. It ranges from 0 to 1, with the value 1 indicating a perfect fit and the value 0 indicating no correlation whatsoever.

possible combinations of factors.[4] The first regression model, referred to as 'full model', includes all explanatory variables (three factors) as illustrated in Eq. (1) below. The subsequent regressions include all possible combinations of one or two factor(s), as presented in detail in Appendix A.2. The full model is:

$$MitInd(Amb, Scen, Mod)_i = \beta_0 + \beta_1 CuEm_i + \beta_2 CuEm_i^2 + \sum_s \gamma_1^s SSP_i^s + \sum_m \gamma_2^m Mod_i^m + u_i \quad (1)$$

where $MitInd(.)$ is the dependent variable of an energy indicator. Amb, $Scen$, Mod stand for the ambition, scenario and model factors respectively, indicating the regressors included in each regression. β_0 is the intercept term. β_1 and β_2 are the coefficients of cumulative emissions ($CuEm$) and their squared value ($CuEm^2$), which together capture the ambition factor. The Shapley–Owen decomposition method, an extension of the Shapley decomposition approach [11], allows some explanatory variables to be grouped exogenously based on prior knowledge. Cumulative emissions and their square form one group, four dummy variables for SSPs[5] the second, and five for models the third.

γ_1 and γ_2 in eq. (1) are the sets of coefficients of the dummy variables for SSP (scenario factor) and Mod (model factor) respectively. The error term is denoted by u_i. The R^2 resulting from each regression is denoted by listing the factors included in brackets: the R^2 corresponding to Eq. (1) is $R^2(Amb, Scen, Mod)$, while for a regression that includes the scenario ($\gamma_1 SSPs$) and model ($\gamma_2 Mod$) factors only it is $R^2(Scen, Mod)$.

The Shapley–Owen *value* for each factor, denoted R^2_{factor}, is computed by subtracting the R^2 for each possible regression that does not include that factor from the R^2 of a corresponding regression to which the factor has been added, then weighting the results. For example, subtracting the $R^2(Scen, Mod)$ from the full model's $R^2(Amb, Scen, Mod)$ gives the marginal impact of adding Amb given the other two factors have already been taken into account. This has a weight of 1/3 as it represents two of the six possible permutations of the full model.[6] Following all possible combinations of two or one factor(s), the Shapley–Owen value for Ambition can be computed as follows:

$$R^2_{Amb} = \frac{R^2(Amb)}{3} + \frac{R^2(Amb,\ Scen) - R^2(Scen)}{6} + \frac{R^2(Amb,\ Mod) - R^2(Mod)}{6} + \frac{R^2(Amb,\ Scen, Mod) - R^2(Scen, Mod)}{3} \quad (2)$$

The sum of all decomposed Shapley–Owen values for all three factors is given by:

$$R^2_{Amb} + R^2_{Scen} + R^2_{Mod} = R^2_{Amb,Scen,Mod} \quad (3)$$

It can be shown algebraically that this sum equals the R^2 of the full regression in Eq. (1), that is $R^2_{Amb,Scen,Mod} = R^2(Amb,\ Scen, Mod)$

Unless Eq. (1) is a perfect fit to the data, there will be a residual variation (the unattributed portions in our decomposition) that cannot be explained by the three factors collectively, given by:

$$R^2_{Resid} = 1 - R^2(Amb, Scen, Mod) \quad (4)$$

3. Results and discussion

3.1. Overview

We begin by analysing primary energy supply variables to understand how their use varies across models, scenarios and levels of climate ambition. Following this, we delve into final energy demand variables, segmented by sectors and by carriers, to shed light on consumption patterns. Subsequently, we explore key emissions variables. Lastly, we assess economic indicators such as GDP and carbon prices to discuss their interactions with our indicators.

3.2. Non-fossil energy supply

Each panel of the decomposition diagrams below follows the same design. Fig. 1 illustrates the decomposition for the variations in selected primary energy supply variables: in total and for various low-carbon sources. The solid black line with markers in the top panel shows the mean across model runs for the total primary energy supply variable. The dashed dark red line shows the median. For many of the variables we study, the median is below the mean, suggesting a tail of model runs with high values. The coloured bars run from one standard deviation below the mean value to one standard deviation above. Each bar is divided in proportion to the three Shapley–Owen values for our factors and the unexplained R^2_{Resid}. The lower end of the stacked bars may reach below the x-axis which is shown as a solid red horizontal line for $y = 0$ where relevant. While negative values are possible for a few variables, (e.g. emissions from land use and land use change), the negative values in our graphs usually just signal that the standard deviation is larger than the mean. This happens when the models' runs are sufficiently skewed and dispersed (so that means and medians diverge). The largest contribution to variations in the trajectory of aggregate primary energy supply across model runs comes from the scenarios, especially towards the end of the century, followed by climate ambition. In other words, aggregate energy levels are related to input activity level assumptions in the SSPs coupled with climate ambition. Systematic differences between models are relatively unimportant, while the relatively narrow top bar that captures residuals confirms that the average effects of the three factors explain a high proportion of the variation.[7]

When it comes to biomass (second row, left panel) the level of climate ambition plays a significant role in determining the trajectory of biomass use in, for instance, power generation and liquid fuel production, both of which are come under increasing focus when stringent targets are considered [21]. Meanwhile, bioenergy potentials differ across SSPs due to constraints related to competition over land which is determined by global demand for food consumption [22], as well as access to clean fuels in developing countries, which is largely influenced by the levels of population and GDP growth [23]. Both effects are captured by the small but increasing proportion of the scenario factor in the figure. In Fig. C1 in Appendix C below we illustrate how some models (specifically GCAM and AIM) deploy different levels of biomass under different scenarios for the same ambition level. This leads to increasing residual effects where results diverge based on model- and scenario-specific choices.

The second row, right panel in Fig. 1 focuses on primary energy generation from nuclear. It shows that the explained variations in the

[4] A regression model that includes no explanatory variables is one of the theoretical combinations considered. However, by definition, its R^2 value would be zero, hence there's no need to actually run this particular model.

[5] There are five SSPs, but one must always be chosen as the base case and is not given a dummy variable – the values of the other SSP dummies show how indicators vary relative to that base case.

[6] If one factor (say Amb) is chosen first, there are two that might be chosen second, giving two permutations. Similarly, if Amb is added last, either $Scen$ or Mod could have been chosen first, but the marginal contribution of Amb is the same in each case, and so we have another two permutations with the same marginal contribution. While there are also two permutations in which Amb is added second, its marginal contribution must be separately calculated for each of the two possible first-choice variables, giving the two terms in the middle of Eq. (2), each with half the weight of the outer terms.

[7] Of course, *all* of the variation ultimately comes from the interaction of the three factors, but we want to identify variation that only comes from particular combinations, as opposed to the expected effect of switching between models.

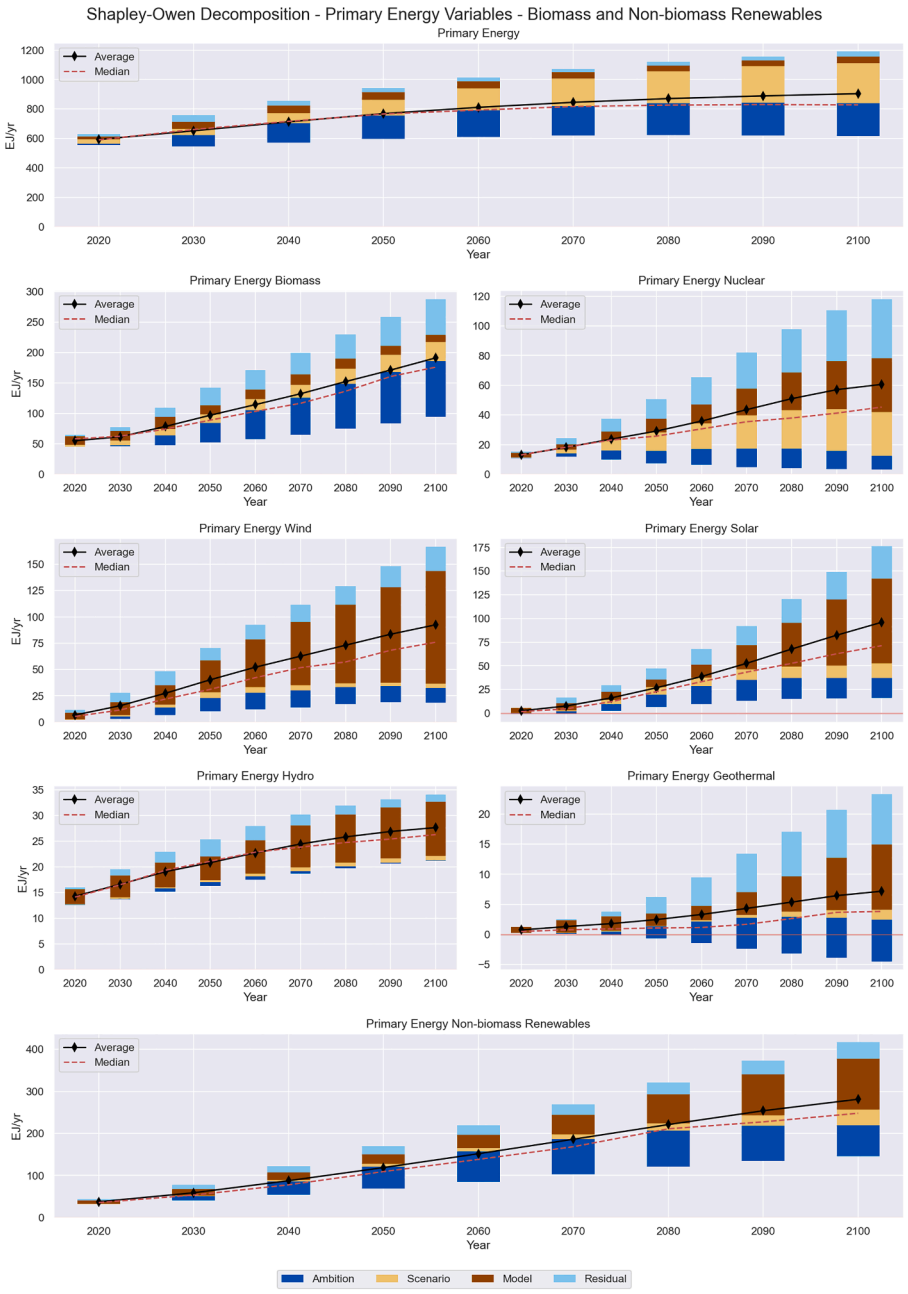

Fig. 1. Shapley–Owen decomposition – primary energy variables – total and low-carbon sources. Top panel in row 1 shows the aggregate primary energy supply, the panels in rows 2 show biomass energy supply and nuclear energy supply, the two panels in row 3 show wind energy supply and solar energy supply, while the panels in row 4 show hydro energy supply and geothermal energy supply, with the final row showing the aggregations of non-biomass renewable energy. Notice that the y-axis scale differs between panels.

first half of the trajectory are primarily driven by the scenario factor coupled with equal contributions from the model and climate ambition factors. However, as we move towards the second half of the century, differences between models become increasingly important in explaining the variability, alongside the scenario factor. The impact of climate ambition, on the other hand, remains relatively limited throughout the century. The large and increasing proportions of residuals in the decomposition are because some models increase nuclear energy supply for high ambition levels, but only in some scenarios, as we further illustrate in Fig. C2 in Appendix C below for the year 2100. For instance, models may well disagree on future trajectories of nuclear due to varying technological assumptions about learning rates or the possibility of future cost increases Rogner et al. [24,25].

The third row in Fig. 1 shows the decomposition for energy supply from wind (left panel) and solar (right panel). In both cases, differences between models are found to play a significant role in explaining the variability in their trajectories, more so in the case of wind. This suggests that the underlying assumptions in models on costs, technical progress, regional potential and maximum penetration as well as other related technologies such as batteries are what is driving the projections of these technologies [6,22]. This result aligns with Dekker et al. [9], who also find the model factor to be the dominant one in explaining the variation

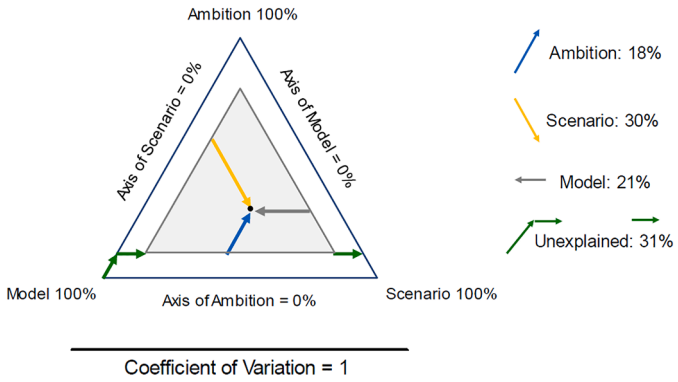

Fig. 2. Example ternary plot – summary of Shapley–Owen decomposition 2060 – nuclear energy.

in wind and solar power.[8] Climate ambition is generally more important than the choice of scenario, but the residuals are equal to or larger than its effect for most decades. As ambition rises, some models, in some scenarios, deploy noticeably more wind or solar power than average. We present more data for wind in Fig. C3 in Appendix C.

The left panel in the fourth row of Fig. 1 on hydro also shows a similar decomposition pattern to energy supply from wind, also aligned with the findings from Dekker et al. [9] Meanwhile, the right panel shows that while the dominant factor in driving the variation in geothermal energy is the model, it also increasingly driven by climate ambition towards the end of the century, coupled with very large and increasing residuals. Models vary in how they represent geothermal energy [26] as we further illustrate in Fig. C4 in Appendix C below for the year 2080; two of the models in the SSPs database do not report any results for this variable and we excluded them from this part of our analysis (as in all similar cases), as discussed in Section 2.2 above. The final row in Fig. 1 below shows the aggregations of non-biomass renewable energy supply, which collectively are driven by the level of ambition with an increasing role for differences between models towards the end of the century. A possible implication is that there is more of a consensus that high levels of ambition require more renewable energy than there is on the *type* of renewable energy required.

In addition to the decomposition diagram above, we can demonstrate the same results with adapted ternary plots. Fig. 2 gives an example, for nuclear energy in 2060. The underlying design will be repeated in ensemble diagrams below. To provide a graphical representation of variability across the model runs for a year, each side of the main outer triangle is equal to the variable's coefficient of variation (as in Fig. 1),[9] and can be compared to the thick line of unit length below it. Values below 0.5 (30 % of the sample) and above 1.5 (13 % of the sample) are truncated for legibility. The length of each edge of the outer triangle represents 100 % of the variation; the length of the edges of the inner triangle represents the proportion of the variation explained by our three factors, the R^2 of the regression. The higher the R^2, the larger the inner triangle relative to the outer. The inner triangle is a conventional ternary diagram, in which the proximity of the point to each vertex represents the corresponding factor's contribution to the explained variation in model runs. In this case, the chosen scenario does the most to explain the variation in results, and so the point is closer to the bottom right vertex of the triangle. The length of the yellow arrow from the inner triangle's axis for "scenario = 0 %", parallel to the axis of model = 0 % (or, equivalently, a line parallel to the axis of ambition = 0 %), gives its contribution. Its length can be compared either to the inner triangle (giving its relative contribution to the explained variation) or (equivalently to Fig. 1) to the outer triangle as its contribution towards explaining the overall variation across model runs. The blue and grey arrows show the contributions of the ambition and model factors, measured from their respective axes; as their contributions are similar, the point is close to the line that bisects the bottom-right vertex and the "scenario = 0 %" axis. The combined length of the three green arrows gives the share of variation that is unexplained. The inner triangle is positioned so that if the three factors each have the same contribution, their point will be at the intersection of the three lines bisecting each vertex, whatever the level of unexplained variation.

Fig. 3 below shows a set of adapted ternary plots for the year 2060 used to summarise some of the results in Fig. 1 above. The figures illustrate both the variability in the estimates of each indicator (e.g. Geothermal has the largest relative variability) and the level of residuals (e.g. lowest for Primary energy).

3.3. Energy supply from fossil fuels

In Fig. 4 we show the Shapley–Owen decompositions for the energy supplied from fossil fuels with and without carbon capture and storage (CCS). Looking at the top panel which shows the aggregate fossil fuels (with and without CCS) and all panels on the left in the following rows which show aggregate and individual unabated fossil fuels (i.e. without CCS), the variation of their trajectories is very dependent on the level of ambition. Given that fossil fuels account for the majority of CO_2 emissions this is unsurprising. For the unabated use of gas and of oil, ambition is slightly less important, though still capable of explaining around half of the end-century variation between model runs. Systematic differences between models are more important for these two technologies than for coal or the total of fossil fuel use, perhaps suggesting different views about the ease of switching between fuels [27]. The share of variation left to the residuals is also higher for oil and gas than for coal, which we illustrate in Figs. C5–C7 in Appendix C.

The panels on the right show the use of fossil fuels with CCS. In the cases of aggregate fossil fuels use, gas and coal, the choice of scenario has more pronounced impact than in the cases without CCS, while differences between models are small. This is driven by the impact of different levels of population and GDP on energy demand. The majority of model runs show fossil fuel use declining by the end of the century, but a few have continued increases. The level of climate ambition is surprisingly unimportant as an across-the-board driver of CCS with fossil energy, either for the individual fuels or overall. Generally, ambition plays a bigger role mid-century than it does late in the 21st century. Since oil is mostly used for transport and CCS is better suited for stationary uses, the amount of oil burned with CCS, which is only reported by three models, is relatively small and quite dependent on the model used. Across the fossil fuel with CCS results, however, a much higher proportion of the variation across model runs remains unexplained, implying that some models choose high levels of CCS, but only for high levels of ambition or energy demand. We further illustrate the differences across scenarios and models in Figs. C8–C10 in Appendix C below.

Fig. 5 below shows individual ternary plots for the year 2060 for the indicators above, as well as combined fossil fuel use with and without CCS, in aggregate and individually. In these latter cases our findings are aligned with those of [9].

3.4. BECCS and CCS

Fig. 6 covers the decomposition for three variables related to the use of carbon capture and storage. For primary energy use with BECCS (top

[8] Note that in discussing our results we draw similarities, where possible, with findings in Dekker et al. [9]. We believe this has the added value of illustrating how despite the different methods (namely Shapley–Owen decomposition, and Sobol decomposition) and different databases and approach to the analysis, some trends persist. However, this exercise is only feasible for a small set of indicators assessed by both papers, and in a few cases the different approaches to capturing the scenario factor affect the results.

[9] The coefficient of variation (CV) is a standardised measure of dispersion defined as the ratio of the standard deviation to the mean.

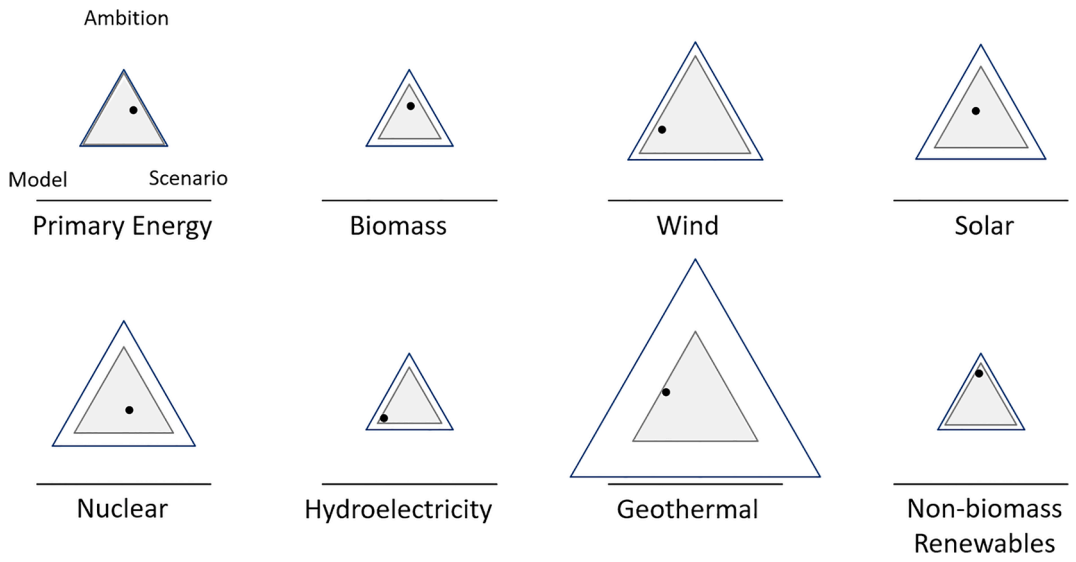

Fig. 3. Ternary plot – summary of Shapley–Owen decomposition 2060: primary energy, overall and from low-carbon sources.

panel), the level of climate ambition is the most significant factor in explaining variability throughout the century. This is in line with the depiction of bioenergy use with CCS as a crucial option for mitigation in the underlying literature, particularly in the energy sector [6,28]. The scenario and model factors have increasing and equal contributions to the variability, albeit to a limited extent. The overall decomposition here is, not surprisingly, aligned with the decomposition of the overall biomass energy supply in Fig. 1 above, hence follows the same rationale for these model and scenario factors, as well as the residuals. As would be expected, this overall pattern is mirrored to a large extent for CO_2 emissions from BECCS (middle panel). The main difference is that there is little consistent variation between models in the amount of carbon to be captured for a given scenario and level of ambition.[10]

As for the overall CO_2 through CCS (bottom panel), climate ambition continues to play an important role in explaining the variability of CCS throughout the century. However, the scenario factor, particularly towards the second half of the century, becomes the largest contributor to the overall decomposition. CCS is needed in high ambition model runs and in scenarios with higher underlying energy demand (e.g. SSP5) where the amount of carbon stored tends to rise [27], as we show in Fig. C11 in Appendix C below. Given the small number of indicators discussed in this section, we do not provide a ternary plot here.

3.5. Final energy

Fig. 7 below shows the decomposition of final energy variables in total and for selected energy carriers, specifically electricity and hydrogen. Starting with total final energy use (top panel), the figure shows that by the end of the century, the largest proportion of the variation across model runs is explained by the assumptions embedded in the scenarios; scenarios with higher population and GDP would systematically require more energy. Climate ambition is also important: higher levels of ambition imply lower energy use. Systematic differences between models are relatively unimportant, while the relatively narrow residual confirms that the three factors explain a high proportion of the variation.

Looking at the absolute level of electricity consumption (second row), the decomposition shows that model runs are influenced by the chosen scenario, particularly towards the end of the 21st century. This is driven by the effect of different levels of population and GDP growth on overall energy demand. Additionally, the differences across models become increasingly prominent, as we further show in Fig. C12 in Appendix C. When it comes to climate ambition, its influence results in more electricity overall in many high-ambition model runs but also more efficient use of electricity (in the sense of a smaller amount per dollar of GDP). These forces tend to cancel out yielding a seemingly unimportant effect of climate ambition on the absolute amount of electricity used. These forces are also coupled with a few relatively high levels of electricity use in model runs with high emissions (Fig. C12 in Appendix C) which explains why the residual here is higher than in the case of total final energy use (top panel).

For electrification (the share of electricity in final energy use – third row), climate ambition is explicitly more important, explaining over half of its variation. Mechanistically, this is because the denominator (final energy) is heavily influenced by ambition while the numerator (electricity) is seemingly not, as discussed above. This effect is reinforced by the fact that it is generally more efficient to provide energy services via electricity, resulting in a fall in final energy as a by-product of electrification. Differences between models remain important, while the socioeconomic scenario is less so, as we further show in Fig. C13 in Appendix C below.

When it comes to hydrogen consumption by final energy users (bottom row), during the first half of the century, the level of climate ambition plays the most significant role. However, as we move towards the end of the century, differences across models become increasingly important. The socioeconomic background scenarios also play an increasingly important role in determining the trajectory of hydrogen in the final energy mix. These trends are consistently accompanied by increasingly large residuals, as hydrogen only reaches a large scale in a few model-scenario combinations, and in these cases the relationship between ambition and hydrogen use is too non-linear to be captured by our quadratic approach, as discussed in Appendix E. We further illustrate the differences between models in Fig. C14 in Appendix C below, noting the large number of outliers and that not all models reported hydrogen in the SSPs database. Additional results on other final energy carriers such as liquids, solids, gases, and heat can be found in Appendix D. The ternary plot for all final energy variables (both carriers and sectors) is provided in the next Section.

3.6. Final energy by sector

At the level of end-use sectors, our three factors capture most of the

[10] A side calculation revealed that the amount of biomass primary energy burned per tonne of CO_2 captured differs between (and usually within) models.

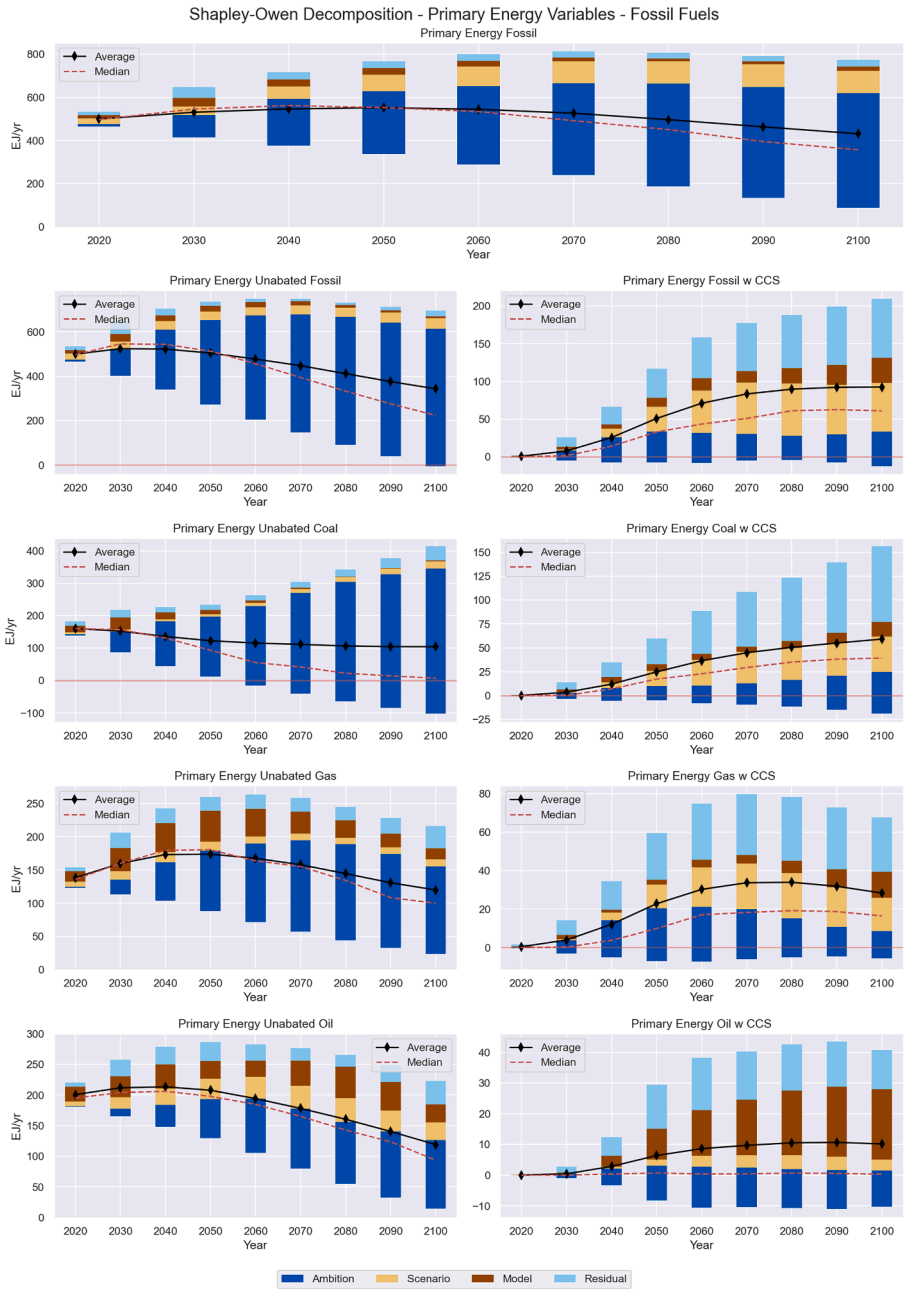

Fig. 4. Shapley–Owen decomposition – primary energy variables – fossil fuels with and without CCS. Top panel shows aggregate fossil fuel use with and without CCS. All panels on the left show the different sources of unabated fossil fuels, while all panels on the right are the corresponding duels with CCS. Notice that the y-axis scale differs between panels.

variation in the results (Fig. 8). Starting with the industry sector (top panel), the largest proportion of variations is explained by differences between the four models that report this output, as further illustrated in Fig. C15 in Appendix C. The dominance of non-electric fuels in this sector, such as oil, gas or feedstocks, makes decarbonisation challenging and results depend on underlying assumptions in the models, such as the role of indirect electrification via hydrogen or the constraints on electrifying the chemical industry due to the dominance of feedstock in its processes [29]. This is further confirmed by [9], where the model factor plays the most significant role in all fuels used in this sector. The background scenario and climate ambition factors play a moderate role in explaining the variability throughout the century, given the influence of population and GDP assumptions on the demand for industrial production, while since industry is a "hard-to-decarbonise" sector, there is relatively little reduction in emissions, even with high levels of ambition.

As for final energy demand in the combined residential and commercial sector (second panel) the largest proportion of variations in this sector's trajectory is consistently explained by the scenario factor. The different projections of population and GDP directly affect the underlying demands. Cooling demand and the use of appliances, especially in developing countries, are expected to rise to levels that will compensate for the reduction in heating demand due to electrification, efficiency improvements, or climate change impacts [30]. The model factor becomes increasingly more important towards the end of the century as different calibrations in the four models reporting the variable affect their attempts to meet space and water heating and cooking demand via electrification or the use of biofuels [22], see Fig. C16 in Appendix C below.

The variations in the trajectory of final energy demand in the

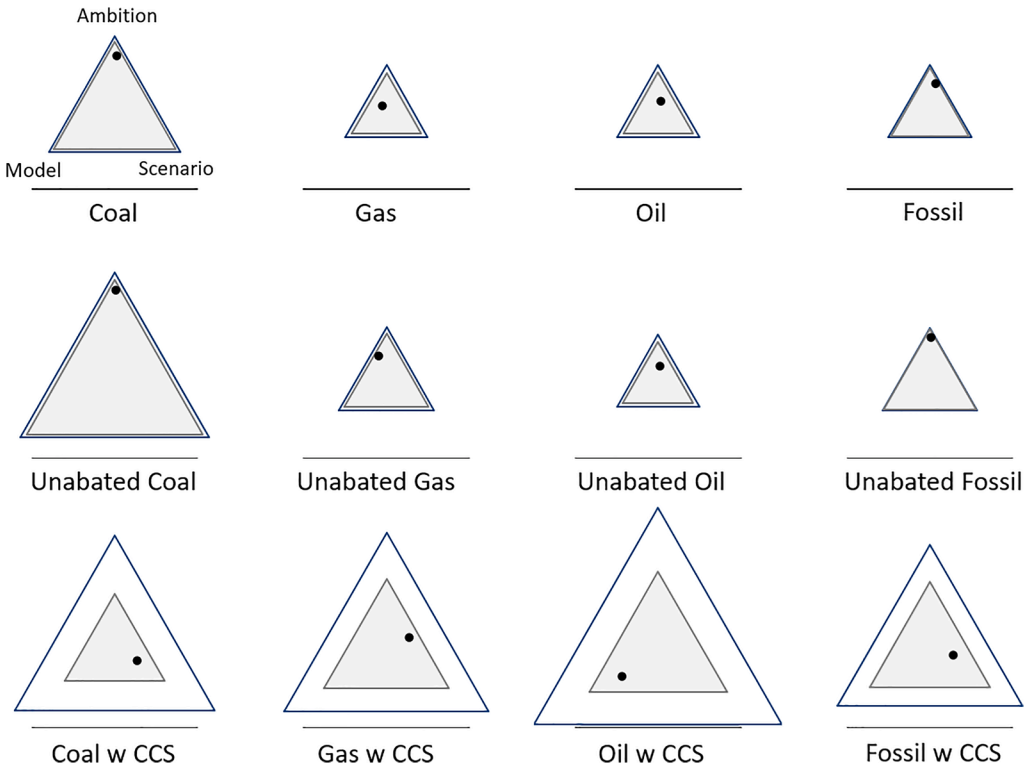

Fig. 5. Ternary plot – summary of Shapley–Owen decomposition 2060: primary energy from fossil fuels, overall, unabated and with CCS.

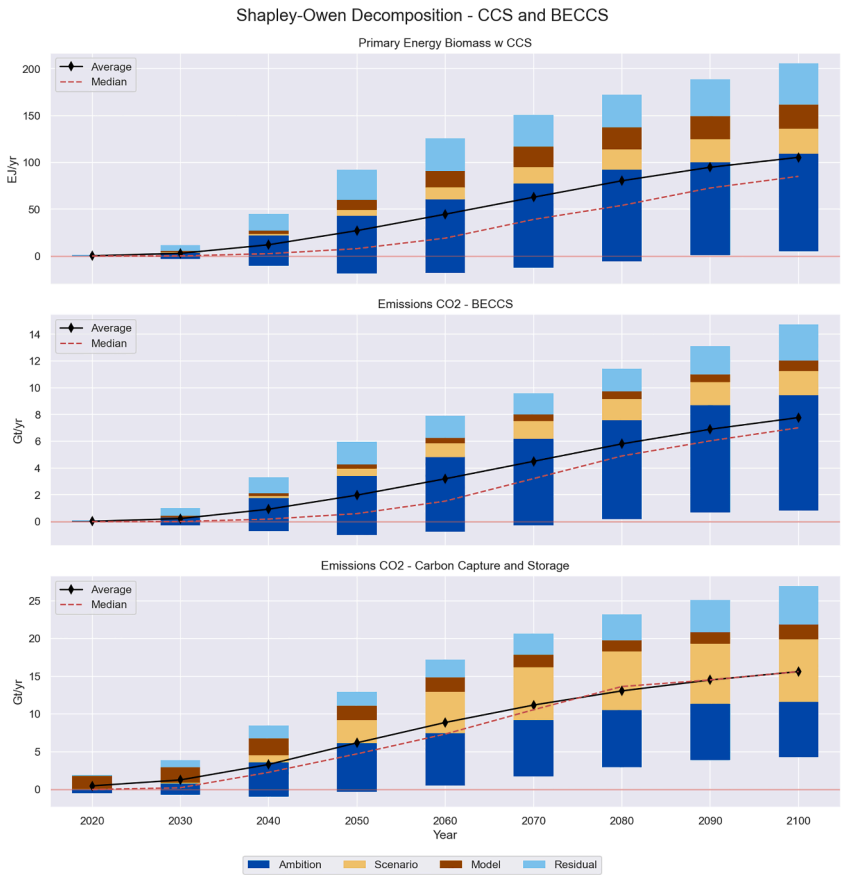

Fig. 6. Shapley–Owen decomposition – CCS and BECCS. Top panel shows primary energy use with BECCS, middle panel shows CO_2 emissions resulting from BECCS use, and the bottom panel shows CO_2 emissions through CCS. Notice that the y-axis scales and units differ between panels.

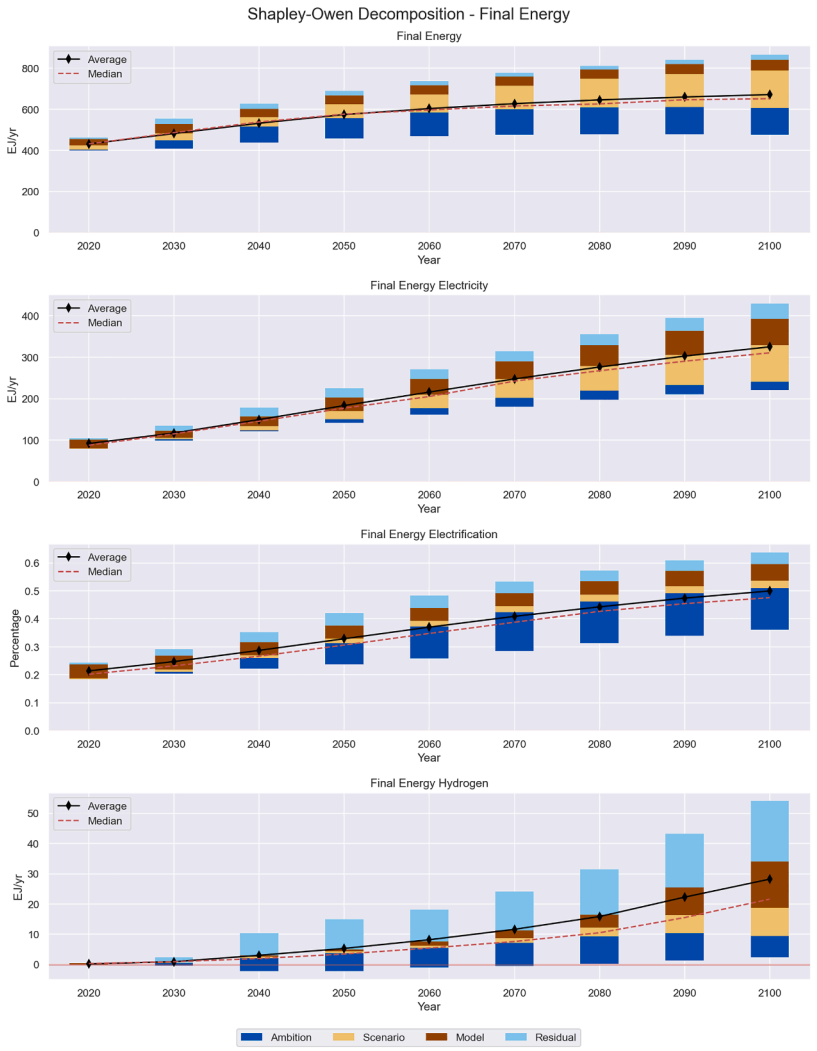

Fig. 7. Shapley–Owen decomposition - final energy. Top panel shows aggregate final energy, second row shows electricity, third row shows electrification (share of electricity in aggregate final energy), and bottom row shows hydrogen. Notice that the y-axis scale differs between panels.

transportation sector (final panel), are mostly explained by the model factor in the first half of the century, while in the second half the scenario factor followed by climate ambition increasingly explains the variation; see Fig. C17 in Appendix C below for more details. This is not surprising, as the level of demand drives the evolution of the sector, coupled with how the sector will evolve in terms of electrified mobility directly or indirectly via hydrogen and adoption of different transport modes such as public transport [29,31]. Perhaps unsurprisingly, in both cases of buildings and transport, we find the scenario is more important than in [9], given that we have a much more even spread across SSPs (something they suggest would be a good topic for further research).

Fig. 9 below shows individual ternary plots for the year 2060 for each sector and carrier discussed in the results above, as well as the four carriers reported in Appendix D.

3.7. Emissions

Fig. 10 below illustrates the decomposition for CO_2 and non-CO_2 GHG emission variables. The overall trend, illustrated by the mean curves, for all emission variables decreases through the 21st century at varying reduction rates. The median curves slightly deviate from the means for all variables implying a slightly left-skewed distributions across model runs. The climate ambition factor explains almost all the variability of overall CO_2 emissions (top panel), those from fossil fuels and industry specifically (second row, left panel) and emissions of the Kyoto gases[11] (third row). This is hardly surprising, given that our definition of climate ambition is so closely aligned with the levels of CO_2 emissions and that CO_2 emissions dominates the Kyoto Gases. When it comes to CO_2 emissions from land use (second row, right panel), the role of the factors in explaining the variability changes dramatically and varies throughout the century. The significance of land use in our analysis is due to the use of reforestation (for instance) to allow burning more fossil fuels while still meeting climate goals. The model factor is the most important at first but declines later, while there are large residuals. As discussed in Fig. 1 above some models differ across scenarios in the rate at which biomass deployment increases with ambition leading to increasing residuals. We further illustrate the large uncertainties across models in Fig. C18 in Appendix C below.

Emissions of methane (CH_4, last row, left panel) and nitrogen (N_2O, last row, right panel) come from the energy sector (e.g., fugitive emissions of methane from natural gas production) and from agriculture. Climate ambition remains the largest factor in explaining their

[11] A basket of 7 greenhouse gases which includes Carbon dioxide (CO_2), Methane (CH_4), Nitrous oxide (N_2O), Hydrofluorocarbons (HFCs), Perfluorocarbons (PFCs), Sulphur hexafluoride (SF_6), and Nitrogen trifluoride (NF_3).

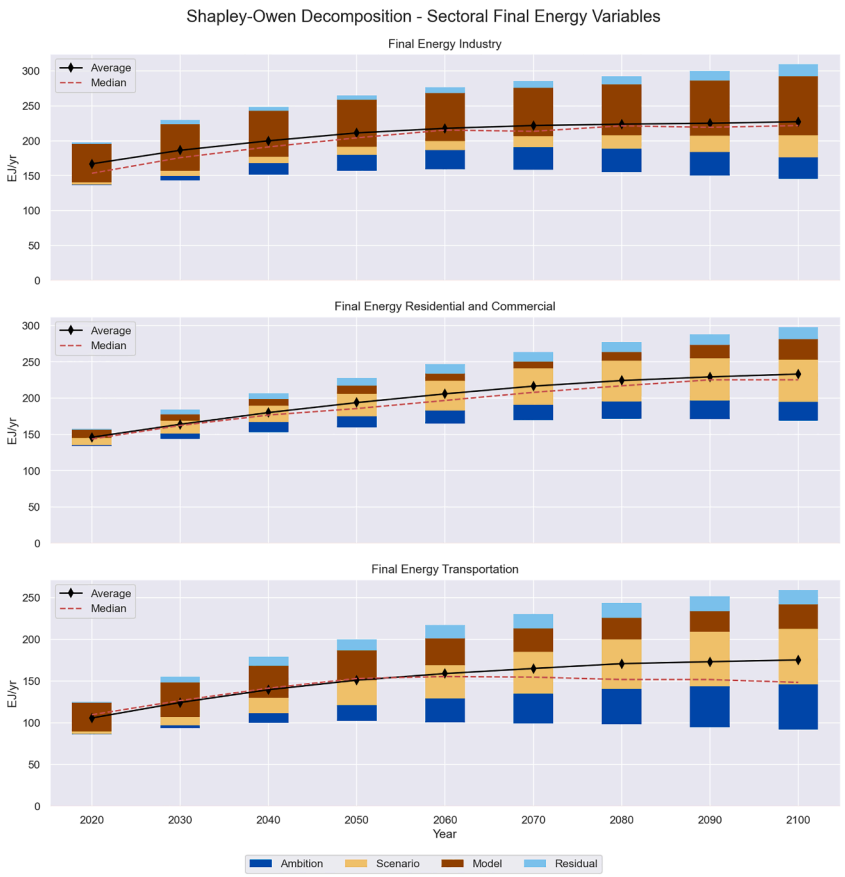

Fig. 8. Shapley–Owen decomposition – sectoral final energy. Top panel shows final energy demand in the industry sector, middle panel in the combined residential and commercial sector, and the bottom panel in transportation. Notice that the y-axis scale differs between panels.

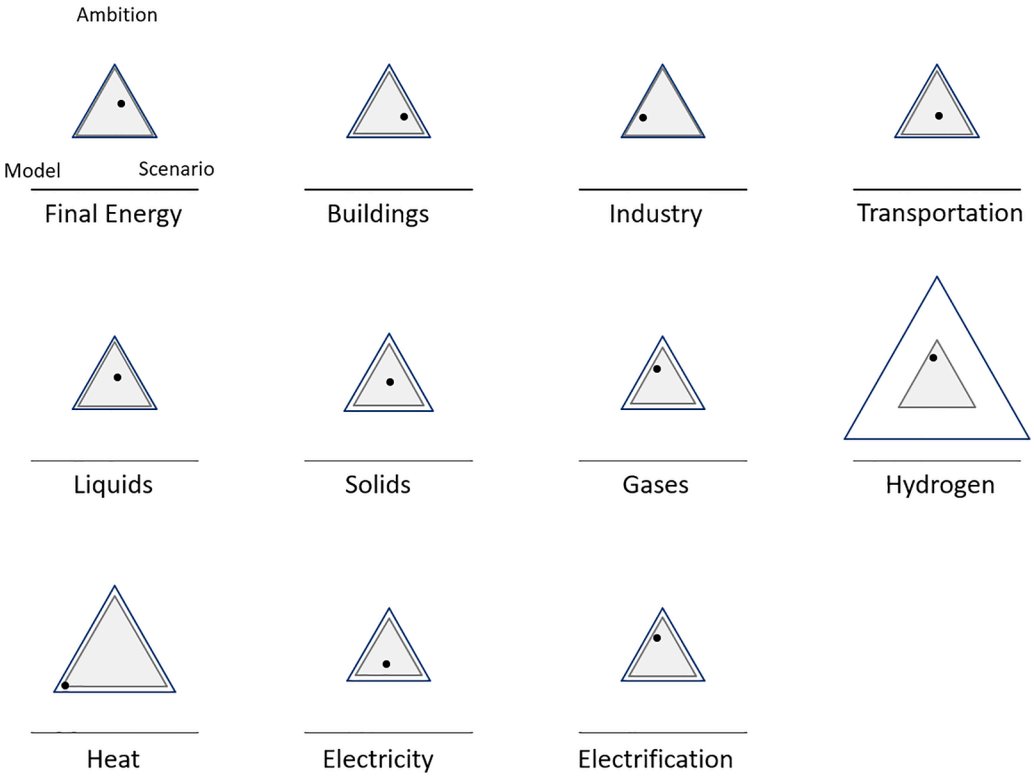

Fig. 9. Ternary plot – summary of Shapley–Owen decomposition 2060: final energy, overall, by sector and by carrier.

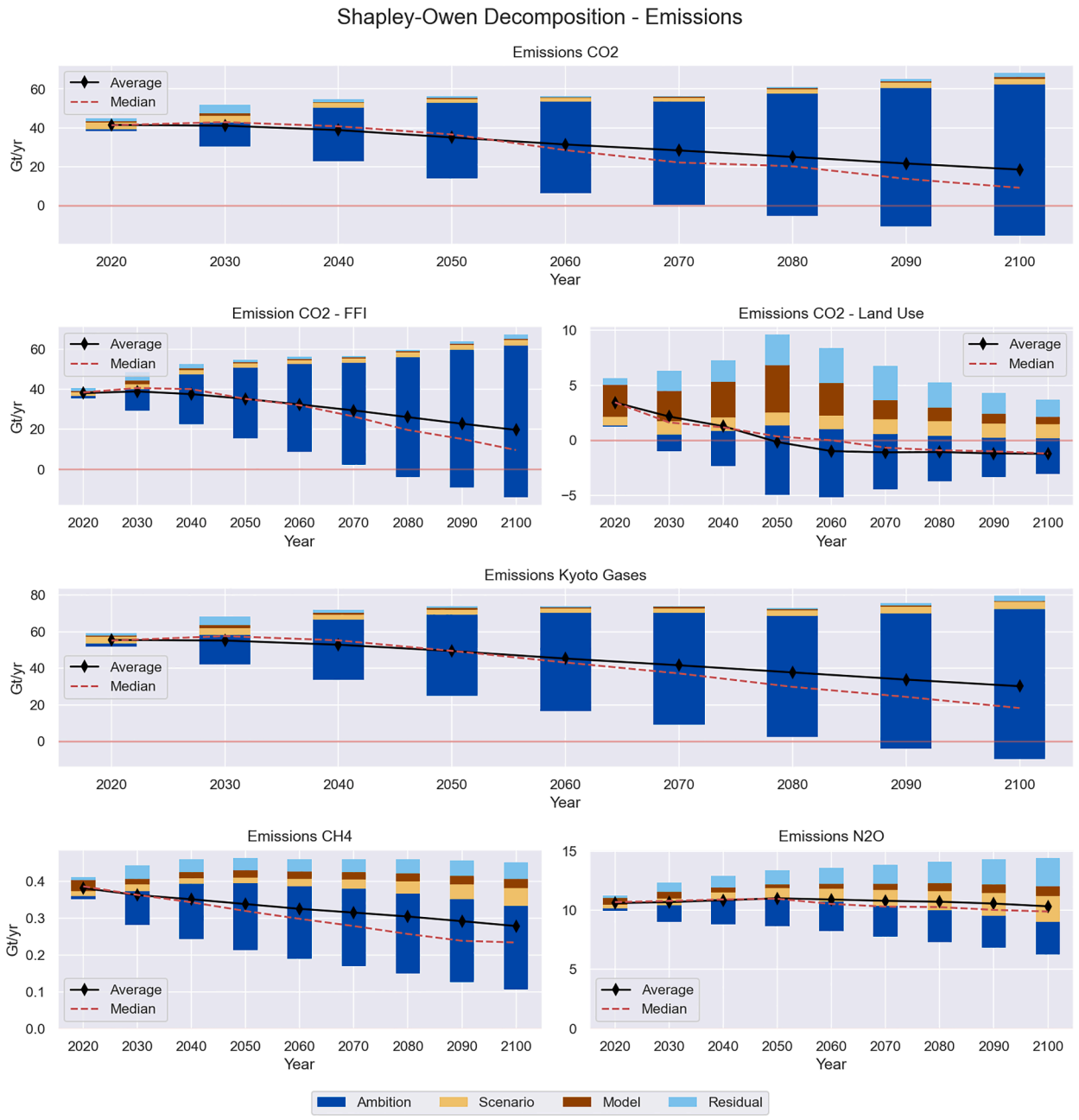

Fig. 10. Shapley–Owen decomposition – emissions. Top panel shows CO_2 emissions, panels in the second row show disaggregated CO_2 emissions into fossil fuel and industry (FFI) and land use, the panel in the third row shows Kyoto gases, while the bottom row panels show CH_4 and N_2O. Notice that the y-axis scale differs between panels.

variability, slightly less so in the case of N_2O. This is given their significant contribution to the Kyoto gases basket as well as high warming potential [32]. In both cases, the role of the scenario factor is more pronounced than in the other panels, as population growth and food demand are strong drivers for these emissions [8]. Residuals are relatively smaller for CH_4 than for land use CO_2 emissions, while those for N_2O are greater, particularly by the end of the century. Nonetheless, they are also largely driven by the same underlying uncertainties [33]. Our findings here are aligned with those of [9].

Just like the decomposition plot above, the individual ternary plots in Fig. 11 below show the dominant contribution of climate ambition to 2060 results for CO_2 emissions and the Kyoto gases.

3.8. Economic variables

Our data include two economic variables, the price of carbon and the level of GDP. The price of carbon (Fig. 12 below, top panel) is endogenous, and very non-linear in the level of ambition: some model runs produce 2100 carbon prices of over $2000 per tonne of CO_2 for high levels of ambition, and in two cases, the values are an order of magnitude higher (see Fig. C19 in Appendix C below). This means that over half the variation in the results for 2100 is unexplained by our approach. The explained variation is split approximately evenly between model and ambition. Across the model runs as a group, no scenario has a systematically higher or lower carbon price than any other. The distribution of results is highly skewed, with many runs having very low carbon prices and, for some models, those with a high level of ambition having very high prices. Consequently, the median of results is close to zero,

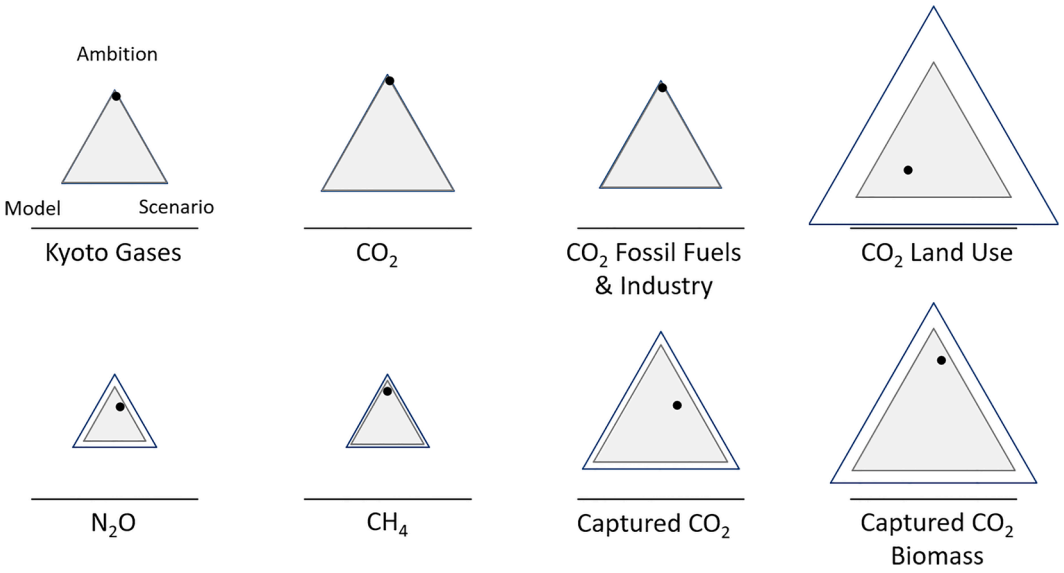

Fig. 11. Ternary plot – summary of Shapley–Owen decomposition 2060: emissions.

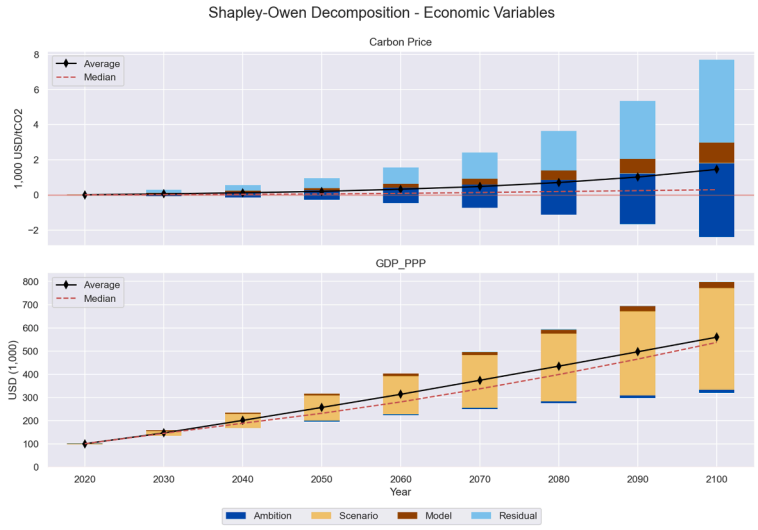

Fig. 12. Shapley–Owen decomposition – economic variables. Top panel shows carbon prices, while the bottom panel shows GDP_{PPP}. Notice that the y-axis scale differs between panels.

while the mean is approaching \$2000/tCO_2 by 2100.

GDP rises over the century in all scenarios, but at rates that depend on the scenario: this factor accounts for over 90 % of the variation in the data from 2040 onwards. Unlike carbon prices, two of the six models treat GDP as an exogenous input, while for the others, it is an output that depends on the level of ambition. For these models, action to curb emissions results in very slightly lower GDP and explains the very small variability attributable to model and ambition.[12] Costs of climate change impacts are not accounted for, given that these models' runs are based on cost-effectiveness IAMs. We further show the variability across scenarios in Fig. C20 in Appendix C.

3.9. Cross-sector comparisons

We complement our earlier discussion by grouping together those indicators that are most affected by each of the three factors in turn or have particularly high residuals. Climate ambition plays the largest role in explaining many energy-related indicators, illustrated in Fig. 13 below. It explains almost all the variability in most emissions results. On one level, this is not surprising given that we measure ambition in terms of the cumulative CO_2 emissions that dominate the Kyoto gases, but a given cumulative target still allows some variation between scenarios (though not, we find, models) in the middle of the century. When it comes to the primary energy mix, climate ambition has a role in determining the trajectory of biomass (with and without CCS) and some non-biomass renewable use (solar), while its impact on nuclear energy is very limited. This is also true for the use of unabated fossil fuels which needs to be phased out for achieving the climate goals. Final energy variables, particularly those that will take a prominent role in the decarbonisation of the energy system (e.g., hydrogen, electrification), are also mostly influenced by the level of climate ambition.

[12] The elasticity of GDP with respect to emissions is less than 0.1 in most cases where we compare "adjacent" model runs (e.g. SSP1-19 and SSP1-26) for the same model, with exceptions for some of the low-GDP SSP3 model runs and for the WITCH-GLOBIOM 3.1 model.

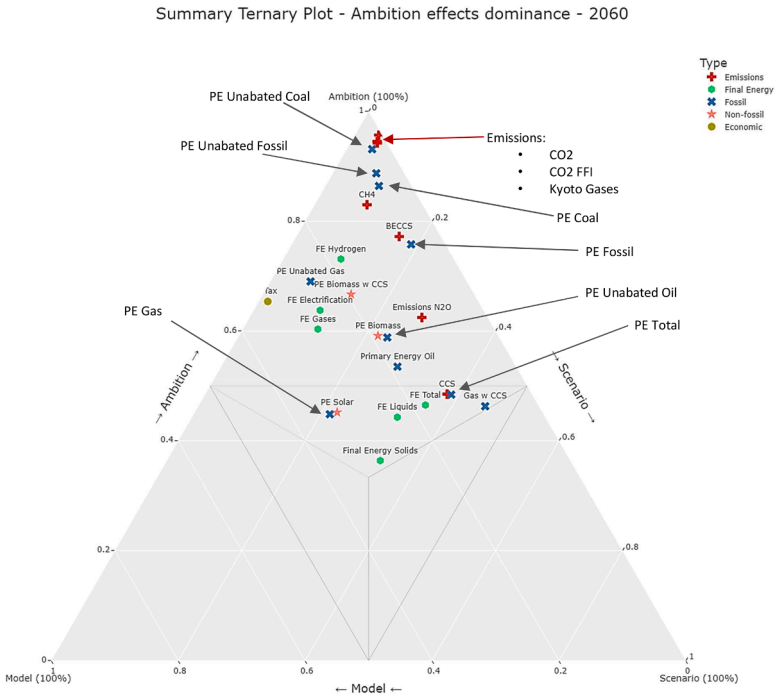

Fig. 13. Ternary plot – focus on the climate ambition factor effects 2060.

The impact of differences between scenarios (Fig. 14 below) is likely to be most pronounced for energy indicators that are influenced by population and GDP growth, such as final energy use. This is the case for final energy use in transport and (residential and commercial) buildings, although not in industry, where the choice of model has a greater effect on its outputs. The use of nuclear and coal with CCS are also driven by the choice of scenario, adopted as a means of meeting emissions targets when energy demands are high, but also have high residuals, showing that the interaction between these factors is more important than any single one of them.

Finally, differences between models (Fig. 15 below) take a dominant role in explaining the variability of some of the energy indicators that may depend on modellers' assessment of their future potential, such as the non-biomass primary energy renewables of geothermal, wind and hydro. There are also significant inter-model differences in predictions for CO_2 emissions from land use, as well as final energy use in the

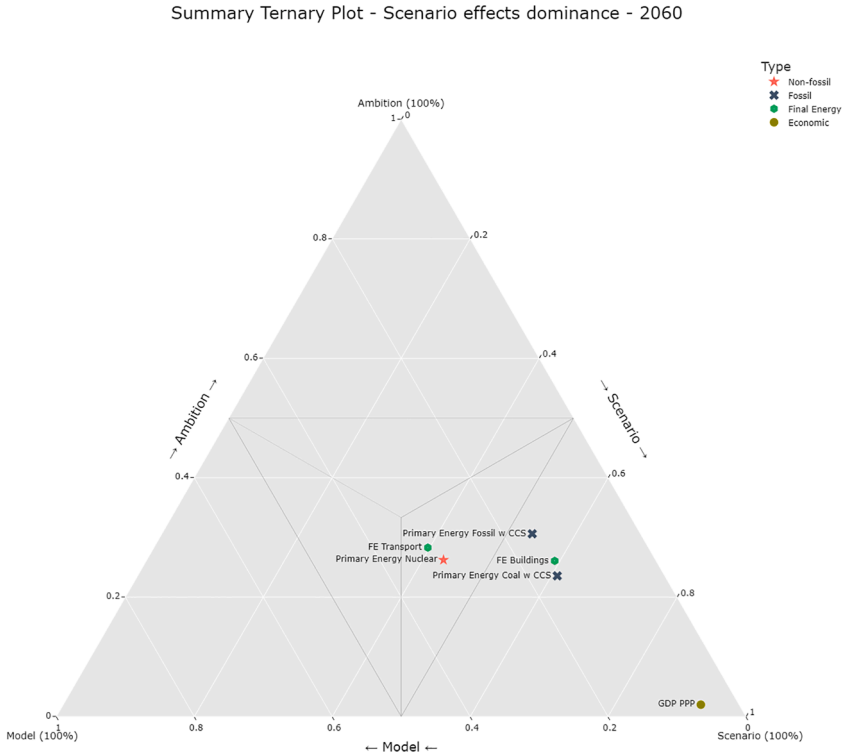

Fig. 14. Ternary plot – focus on the scenario factor effects 2060.

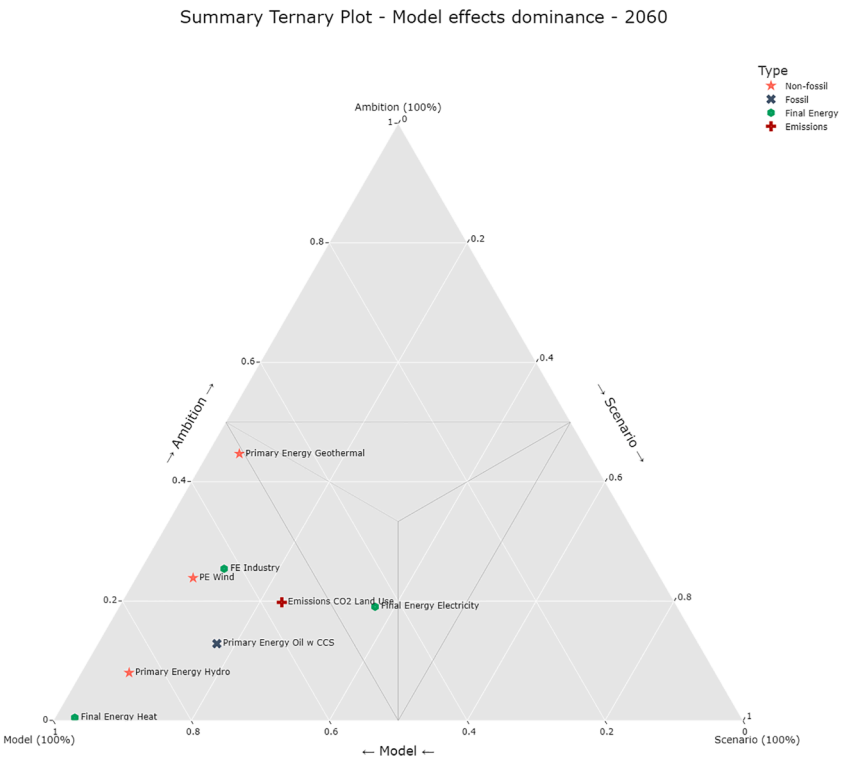

Fig. 15. Ternary plot – focus on the model factor effects 2060.

industry sector and heat.

CO_2 emissions from land use is one of the indicators with a high residual share, showing that we cannot explain their variability well from the average effect of climate ambition or the chosen model or scenario. While actions such as reforestation can be used to create large amounts of negative emissions, this is only for some combinations of ambition, model and scenario. The same is true of the (potentially expensive) application of CCS to fossil fuels, nuclear energy and use of hydrogen. The varying use of such expensive technologies feeds through into the carbon price,[13] and this is the mitigation indicator with the highest average proportion of unexplained residuals.

4. Conclusions and policy implications

In this paper we conduct a decomposition analysis to evaluate the drivers behind key energy indicators in long-term mitigation scenarios that are generated using integrated assessment models (IAMs). We identify three key drivers: climate ambition, model, and socioeconomic background scenario, which collectively shape the future evolution of the chosen key energy indicators in these scenarios. The Shapley–Owen decomposition method based on the proportion of variation explained in a set of multiple regressions attributes the contribution of each factor to the variation in a chosen energy indicator, while explicitly calculating the proportion of variation that is not so easily explained. We apply this analysis to a set of IAMs' runs conducted as part of a single model intercomparison project, the results of which are reported in the SSPs database. The paper asks: which energy system indicators are robust, and which show wide variation; and what are the high-level explanatory factors for the variance in results across model runs; which energy indicators merit priority attention for conducting deep dives?

Our paper contributes to a new and growing body of literature on understanding the driving forces behind key finding from climate mitigation scenarios ensemble. Such analyses include various elements: the structure of the ensemble itself, data availability, as well as the representation of models and scenarios (SSPs in our case). Each of these elements could represent a challenge in undertaking an ex-post analysis like ours here. Methodologies to undertake decomposition analyses may provide consistent insights even when they differ, as we demonstrated above in a few cases when comparing our results to those of Dekker et al., [9]. Most of our results are robust to the choice between the use of cumulative CO_2 emissions or RCP dummy variables as a measure of climate ambition, but some results do change, explaining a mix of increased and decreased proportions of the variations in our energy indicators. One avenue for future research is adopting a hybrid approach, or a more complex functional form, that incorporates both measures. An anonymous referee suggested that the Shared Climate Policy Assumptions approach of Kriegler et al. [34] might also be used in this way. Other approaches involve creating a structured scenarios ensemble to create a more systematic dataset on which a decomposition analysis can be run (e.g. [18]). Ultimately, our work underscores the imperative for both methodological advances and community consensus in debiasing scenario ensembles and decomposition analyses, as argued for by recent contributions like [4,5], to support policymakers in understand the underlying driving forces, biases and uncertainties behind these results.

Our analysis highlights the importance for policymakers not to solely rely on the usual results of mitigation scenario indicators or stop at considering uncertainties, but also seek to understand the underlying driving forces behind these results. This is critical for informed policy decisions that take into account the factors that shape the outcomes of these model runs and the level of robustness and confidence in those outcomes.

Our analysis has indicated that robust energy system messages can be derived from integrated assessment modelling. It is clear, perhaps unsurprisingly, that high levels of climate ambition as measured by cumulative CO_2 emissions over the 21st century are associated with high levels of emissions reductions in the energy sector for every decade

[13] The models calculate the carbon price as a shadow cost of mitigation, the marginal cost (over a business-as-usual alternative) per tonne of carbon of the most expensive mitigation method used in a given scenario.

throughout the century. Climate ambition also drives total fossil fuel energy use and the unabated use of coal, gas and oil. The use of coal or gas with CCS, however, depends on a mix of climate ambition and scenario (affecting the overall energy service demand to be met), with large residuals showing that some models are much more aggressive than others in adopting them as the demand for clean energy rises. Predictions for the use of oil with CCS are generally low and depend on the model chosen, with large residuals. The overall use of gas is most affected by ambition (particularly at the end of the century), but the scenario and (earlier in the century) model are also important, with a residual element of around one-fifth. In other words, the picture is much less clear than for coal and oil.

The overall use of non-biological renewables is, unsurprisingly, very strongly driven by climate ambition as, to a lesser extent, is biomass for energy. But the use of specific forms of renewable energy is much more model-driven. This is especially the case for wind and hydro, whereas ambition has more influence on solar in the middle of the century, alongside a sizeable residual. Nuclear energy is higher (on average) for greater ambition, scenarios with greater energy service demand and in some models; their relative influence varies over the century but residuals of around one-third show that particular combinations can have outsized effects. Climate ambition appears responsible for half the variation in the use of BECCS in the second half of the 21st century, with residuals gradually falling to one-fifth.

The pattern for final energy demand is very sector specific. Residential and commercial energy demand, and transport energy demand are highly scenario-dependent whereas industrial energy is much more affected by model differences. Hydrogen use has some of the highest residuals, with ambition driving a quarter to a third of the variation mid-century, replaced by model differences by 2100. Electricity demand needs careful interpretation. Total electricity demand is largely driven by background scenario and model. But electrification, as measured by the share in final energy demand, is heavily linked to climate ambition, which requires both an increasing share of energy services to be met through electricity, and the efficiency with which they are provided to increase.

Policymakers can take three broad messages from this analysis:

a) The broad direction of energy system change, reduced use of fossil fuels, especially coal and oil, and the rise of renewables is a robust feature of ambitious climate scenarios.
b) For final energy demand, the key is to look at the social and economic change implied by background scenarios - this is as important as the level of climate ambition.
c) For the use of specific forms of renewable energy such as wind, solar and hydro, and for nuclear, there are no clear messages from the analysis. Here, non-scenario-based assessment is needed, along with a much more in-depth, rigorous analysis of model differences.

Some models produce “outlier” results in some scenarios for some levels of climate ambition; our analysis shows where this happens, and where that rigorous analysis should be focused.

Funding

Alaa Al Khourdajie and Jim Skea were supported by the Engineering and Physical Sciences Research Council, United Kingdom, grant/award no. EP/P022820/1. Alaa Al Khourdajie was also supported by the European Union’s Horizon Europe research and innovation programme under grant agreement no. 101056306 (IAM COMPACT).

CRediT authorship contribution statement

Alaa Al Khourdajie: Conceptualization, Data curation, Formal analysis, Methodology, Project administration, Software, Validation, Visualization, Writing – original draft. **Jim Skea:** Conceptualization, Formal analysis, Methodology, Writing – original draft, Validation, Visualization. **Richard Green:** Conceptualization, Formal analysis, Methodology, Visualization, Validation, Writing – original draft.

Declaration of competing interest

The authors declare the following financial interests/personal relationships which may be considered as potential competing interests:

Alaa Al Khourdajie reports financial support was provided by the Engineering and Physical Sciences Research Council. Jim Skea reports financial support was provided by the Engineering and Physical Sciences Research Council.

Data availability

Shared on GitHub: https://github.com/AlKhourdajie/SSPs_decomposition.

Acknowledgements

We would like to thank Raphael Slade and Iain Staffell from Imperial College London, Centre for Environmental Policy, for their helpful comments and suggestions at early stages of the paper. We also thank two anonymous referees for their thoughtful and constructive comments on our manuscript. The feedback they provided helped us improve the quality and clarity of our work, and refining our arguments, including the diagnostics in Appendix E. Participants at the Toulouse Energy and Climate Conference, June 2022, and the IAEE European Conference, Athens, September 2022, and seminar audiences at the University of Luxembourg and at Imperial College London in July 2023 gave helpful comments. Any remaining errors or issues are solely our own.

Appendices

Appendix A

A.1 The Shapley decomposition and Shapley–Owen decomposition methods

The Shapley decomposition method, or Shapley value method, is grounded in cooperative game theory but used here to decompose the relative importance of different regressors in explaining the variation of a dependent variable. The underlying premise of the Shapley method is to think about the regressors of a model as players and the quality of a model fit as a total value to maximise under various coalitions. In cooperative game theory terms, the Shapley value measures the worth of a player as the marginal increase in the value of an objective when they join a group of players (a coalition), averaged over all possible orderings in which the final coalition could be formed. Applied to regression analysis, the Shapley value averages the increase in R^2 from adding another regressor over all possible subsets of predictors in a model. This is advantageous in the case of multicollinearity as it includes the possibility of competitive influence among predictors in any subset [35,36].

In some cases, explanatory variables are exogenously organised into groups, whose composition is known *a priori* to the researchers, or into dummy variables to capture categorical variables. Both cases apply in our paper, where for instance the ambition factor is a group of two explanatory variables (the cumulative emissions variable and its squared value). In such cases, a generalisation of the of the Shapley decomposition approach, known as the Shapley–Owen decomposition or Shapley–Owen *value* is used in order to adjust the processing of the information about decomposed R^2, such that the resulting values of groups can be interpreted as assigned to the group directly rather than the variables [11]. The solution assigned to each group is calculated comparatively on average over all possible combinations of predictors in the regression. It produces a unique solution satisfying general requirements of Nash equilibrium [35].

To demonstrate the Shapley–Owen decomposition concept applied to a simple regression analysis, consider a regression model given by:

$$y_i = \beta_0 + \sum_{j=1}^{p} \beta_j x_{ji} + \varepsilon_i \tag{A.1}$$

where y_i is the dependent variable, β_0 is the intercept term, β_j is the coefficient of an explanatory variable x_{ji}, and ε_i is the error term. Working first with individual regressors, the Shapley value of a particular regressor j is based on the computation of all 2^p possible models for each possible combination of models with up to k regressors. Hence the Shapley value is the marginal contribution of adding regressor x_j to the model weighted by the number of permutations of this sub-model, given by:

$$R^2_{Shapley} = \sum_{T \subseteq Z\{x_j\}} \frac{k! \,.\, (p-k-1)!}{p!} \left[R^2\left(T \cup \{x_j\}\right) - R^2(T)\right] \tag{A.2}$$

where T is a model with k regressors excluding x_j, and Z is the set containing all possible models with different combinations of regressors. Without loss of generality, the above simple case can be extended to a regression model where explanatory variables are exogenously grouped. This gives the Shapley–Owen value, where only combinations of regressors containing either all or none of the members of each group are included in the permissible set Z, and $T \cup \{x_j\}$ must be replaced with $T \cup \{g(x_j)\}$, where $g(x_j)$ denotes the regressors in the same group as x_j, in Eq. (A2).

Following Grömping [12] we verify in our results that our analysis satisfied the proposed Desirability Criteria for decomposition of R^2. These are (a) Proper decomposition where the model variance is decomposed into shares, with the sum of all shares equal to the model variance, (b) non-negativity where all shares assigned to regressors must be non-negative and (c) ensuring non-zero shares of all regressors with a non-zero coefficients.[14]

A.2 Regressions used to apply the Shapley–Owen decomposition method to mitigation scenarios

Following up on Section 2.3 above we present here all seven regression models included in the analysis. For each dependent variable (energy indicator), a Shapley–Owen decomposition analysis is conducted by running seven linear ordinary least squares (OLS) regressions. These regressions cover all possible combinations of factors.[15] The first regression model, referred to as 'full model', includes all explanatory variables (three factors) as illustrated in Eq. (A3) below. The subsequent three regression models Eqs. (A.4)–(A.6) include all possible combinations of two factors, i.e. eliminating one factor in each model. The last three regression models Eqs. (A.7)–(A.9) include one factor each, eliminating two factors in each model. These regression models are as follows:

$$MitInd(Amb, Scen, Mod)_i = \beta_0 + \beta_1 CuEm_i + \beta_2 CuEm_i^2 + \sum_s \gamma_1^s SSP_i^s + \sum_m \gamma_2^m Mod_i^m + u_i \tag{A.3}$$

$$MitInd(Amb, Scen)_i = \beta_0 + \beta_1 CuEm_i + \beta_2 CuEm_i^2 + \sum_s \gamma_1^s SSP_i^s + u_i \tag{A.4}$$

$$MitInd(Amb, Mod)_i = \beta_0 + \beta_1 CuEm_i + \beta_2 CuEm_i^2 + \sum_m \gamma_2^m Mod_i^m + u_i \tag{A.5}$$

$$MitInd(Scen, Mod)_i = \beta_0 + \sum_s \gamma_1^s SSP_i^s + \sum_m \gamma_2^m Mod_i^m + u_i \tag{A.6}$$

$$MitInd(Amb)_i = \beta_0 + \beta_1 CuEm_i + \beta_2 CuEm_i^2 + u_i \tag{A.7}$$

$$MitInd(Scen)_i = \beta_0 + \sum_s \gamma_1^s SSP_i^s + u_i \tag{A.8}$$

$$MitInd(Mod)_i = \beta_0 + \sum_m \gamma_2^m Mod_i^m + u_i \tag{A.9}$$

where $MitInd(.)$ is the dependent variable of a energy indicator. $Amb, Scen, Mod$ stand for the ambition, scenario and model factors respectively, indicating the regressors included in each regression. β_0 is the intercept term. β_1 and β_2 are the coefficients of cumulative emissions ($CuEm$) and their squared value ($CuEm^2$), which together capture the ambition factor. The Shapley–Owen decomposition method allows explanatory variables to be

[14] Note that there is an additional criterion in the literature "Exclusion: the share allocated to a regressor with a coefficient = 0 should be 0". However, Grömping [12] argues that such a condition is not reasonable due to the fact that a regressor has a coefficient equal to zero does not imply that this regressor has no direct influence on other regressors. We note that none of our regressors has a coefficient of zero in any regression.

[15] A regression model that includes no explanatory variables is one of the theoretical combinations considered. However, by definition, its R^2 value would be zero, hence there's no need to actually run this particular model.

sometimes grouped exogenously based on prior knowledge, an example is capturing the non-linear effects of the ambition factor here, for which we provide rational at the end of Section 2.2. above as well as Appendix E. Exogenously grouping variables under Shapley–Owen methodology is an extension of the Shapley decomposition approach [11]. γ_1 and γ_2 are the sets of coefficients of the dummy variables for *SSP* (scenario factor) and *Mod* (model factor) respectively. Each coefficient represents the estimated effect of the corresponding explanatory variable on the dependent variable, holding all other variables constant. The error term is denoted by u_i. The R^2 resulting from each regression is denoted by listing the factors included in brackets: the R^2 corresponding to Eq. (1) is $R^2(Amb, Scen, Mod)$, while for Eq. (A.6) it is $R^2(Scen, Mod)$.

Appendix B

B.1: The SSPs database descriptive statistics

In this section we present general descriptive statistics of the SSPs Database [8].

See Fig. B1

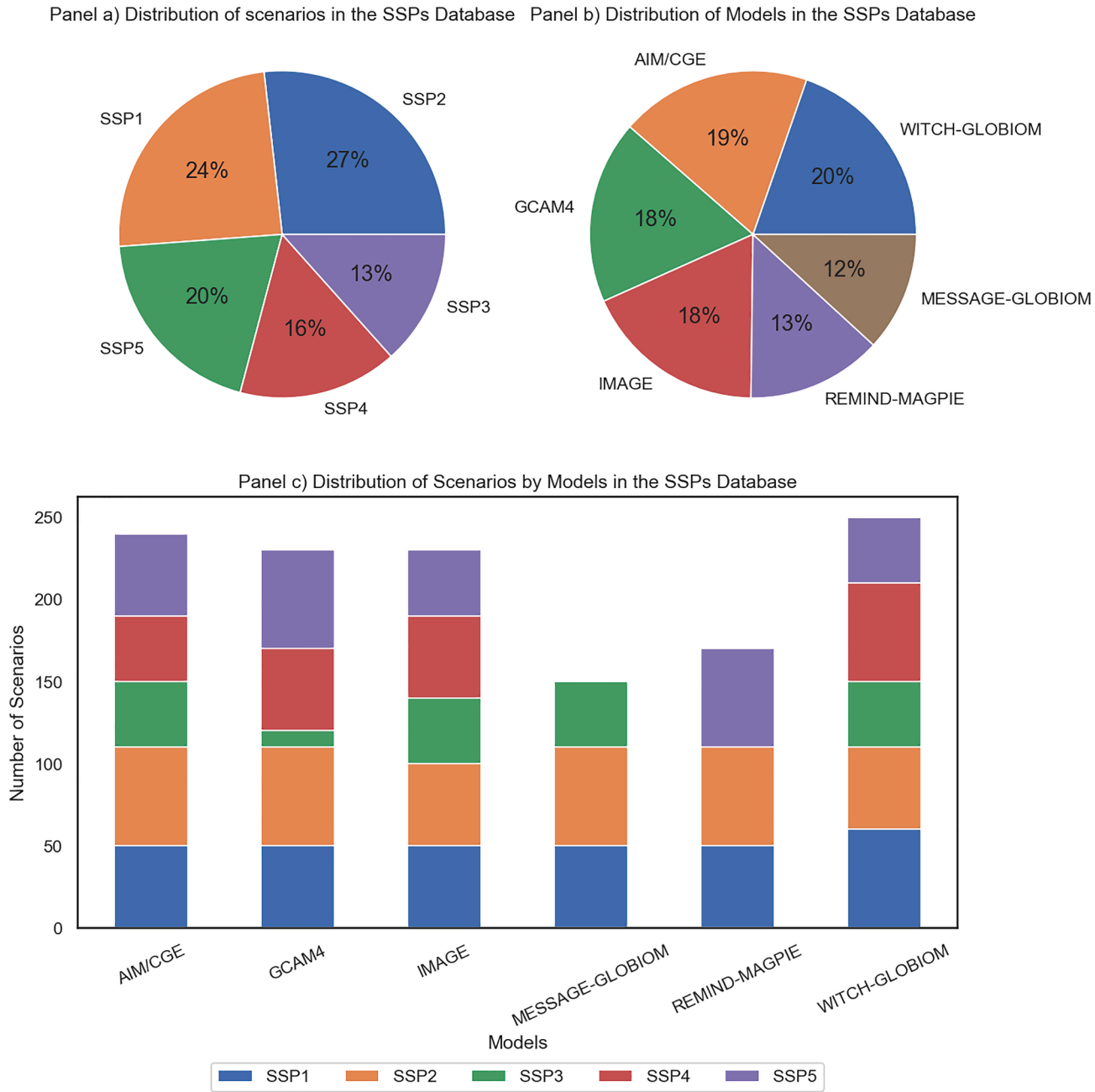

Fig. B1. The distribution of the scenarios and models in the SSPs database. Panel a) Distribution of scenarios in the SSPs database, Panel b) Distribution of models in the SSPs database, and Panel c) Distribution of scenarios by models in the SSPs database. Note that in the SSPs database each model usually runs a subset of a selected SSP. For instance, a model run labelled SSP1-19 (in line with the nomenclature of the SSPs-RCPs matrix) indicates that run represents the combination of the socio-economic assumptions captured by SSP1 quantifications, and the radiative forcing illustrated by the radiative forcing scenario RCP1.9 [37]. We aggregate such SSPs subsets and focus on the SSPs component (i.e. SSP1-19 becomes SSP1), given the rationale mentioned in the methodology Section 2.2 above for not using RCPs as a proxy for climate ambition.

B.2: List of energy-relevant indicators

List of energy-relevant indicators and their description

Variable name	Database variable label	Description
Non-fossil primary energy supply variables		
Primary energy supply	Primary Energy	Total primary energy supply
Biomass energy supply	Primary Energy|Biomass	Total primary energy supply from biomass sources
Nuclear energy supply	Primary Energy|Nuclear	Total primary energy supply from nuclear sources
Wind energy supply	Primary Energy|Wind	Total primary energy supply from wind sources
Solar energy supply	Primary Energy|Solar	Total primary energy supply from solar sources
Hydro energy supply	Primary Energy|Hydro	Total primary energy supply from hydro sources
Geothermal energy supply	Primary Energy|Geothermal	Total primary energy supply from geothermal sources
Non-Biomass Renewables energy supply	Primary Energy – Non-Biomass Renewables (computed for this analysis)	Total primary energy supply from non-biomass renewable sources. This is computed as the aggregate of nuclear, wind, solar, hydro and geothermal
Energy supply from fossil fuel variables		
Fossil energy supply	Primary Energy|Fossil	Total primary energy supply from fossil fuel sources
Fossil energy supply with CCS	Primary Energy|Fossil w/CCS	Total primary energy supply from fossil fuel sources with carbon capture and storage
Unabated fossil energy supply	Primary Energy|Fossil wo/CCS	Total primary energy supply from fossil fuel sources without carbon capture and storage
Coal energy supply	Primary Energy|Coal	Total primary energy supply from coal sources
Coal energy supply with CCS	Primary Energy|Coal|w/CCS	Total primary energy supply from coal sources with carbon capture and storage
Unabated coal energy supply	Primary Energy|Coal wo/CCS	Total primary energy supply from coal sources without carbon capture and storage
Gas energy supply	Primary Energy|Gas	Total primary energy supply from gas sources
Gas energy supply with CCS	Primary Energy|Gas w/CCS	Total primary energy supply from gas sources with carbon capture and storage
Unbated gas energy supply	Primary Energy|Gas wo/CCS	Total primary energy supply from gas sources without carbon capture and storage
Oil energy supply	Primary Energy|Oil	Total primary energy supply from oil sources
Oil energy supply with CCS	Primary Energy|Oil w/CCS	Total primary energy supply from oil sources with carbon capture and storage
Unabated oil energy supply	Primary Energy|Oil wo/CCS	Total primary energy supply from oil sources without carbon capture and storage
CCS and BECCS variables		
Biomass energy supply with CCS	Primary Energy|Biomass w/CCS	Total primary energy supply from biomass sources with carbon capture and storage
CO_2 emissions from biomass with CCS	Emissions|CO_2|Carbon Capture and Storage Biomass	CO_2 from biomass sources with carbon capture and storage
CO_2 emissions with CCS	Emissions|CO_2|Carbon Capture and Storage	CO_2 emissions from all sources with carbon capture and storage
Final energy variables		
Total final energy	Final Energy	Total final energy use
Electricity consumption	Final Energy|Electricity	Total final energy consumption from electricity
Electrification	Final Energy - Electrification (computed for this analysis)	The share of electricity in final energy use (computed variable)
Hydrogen consumption in final energy	Final Energy|Hydrogen	Total final energy consumption from hydrogen
Gases consumption in final energy	Final Energy|Gases	Total final energy consumption from gases
Heat consumption in final energy	Final Energy|Heat	Total final energy consumption from heat sources
Liquids consumption in final energy	Final Energy|Liquids	Total final energy consumption from liquids
Solids consumption in final energy	Final Energy|Solids	Total final energy consumption from solids
Final energy variables by sector		
Industry sector final energy consumption	Final Energy|Industry	Final energy consumption by the industrial sector
Residential and Commercial sector final energy consumption	Final Energy|Residential and Commercial	Final energy consumption by the residential and commercial (buildings) sectors
Transportation sector final energy consumption	Final Energy|Transportation	Final energy consumption by the transportation sector
Energy sector emissions		
CO_2 emissions	Emissions|CO_2	Total CO_2 emissions
CO_2 emissions from fossil fuels and industry	Emissions|CO_2|Fossil Fuels and Industry	CO_2 emissions from fossil fuel sources and industrial processes
CO_2 emissions from land use	Emissions|CO_2|Land Use	CO_2 from land use changes
Kyoto gases emissions	Emissions|Kyoto Gases	Total emissions of Kyoto gases
CH_4 emissions	Emissions|CH_4	Total emissions of CH_4
N_2O emissions	Emissions|N_2O	Total emissions of N_2O
Economic variables		
Carbon Price	Price|Carbon	Price of carbon
GDP_{PPP}	GDP PPP	Gross Domestic Product at Purchasing Power Parity

B.3 List of variables with missing data runs

List of variables with missing data runs

Variable name	Missing data runs
Emissions CO_2 Carbon Capture and Storage	6
Emissions CO_2 Carbon Capture and Storage Biomass	7
Final Energy Heat	25
Final Energy Hydrogen	49
Final Energy Solar	64
Final Energy Industry	42
Final Energy Residential and Commercial	42
Primary Energy Biomass with CCS	7
Primary Energy Fossil with CCS	6
Primary Energy Coal with CCS	6
Primary Energy Gas with CCS	7
Primary Energy Oil with CCS	64
Primary Energy Geothermal	48
Price of Carbon	12

Note that number of maximum observations for reported variables in all runs is 126.

Appendix C

See the Figs. C1, C2, C3, C4, C5, C6, C7, C8, C9, C10, C11, C12, C13, C14, C15, C16, C17, C18, C19, C20

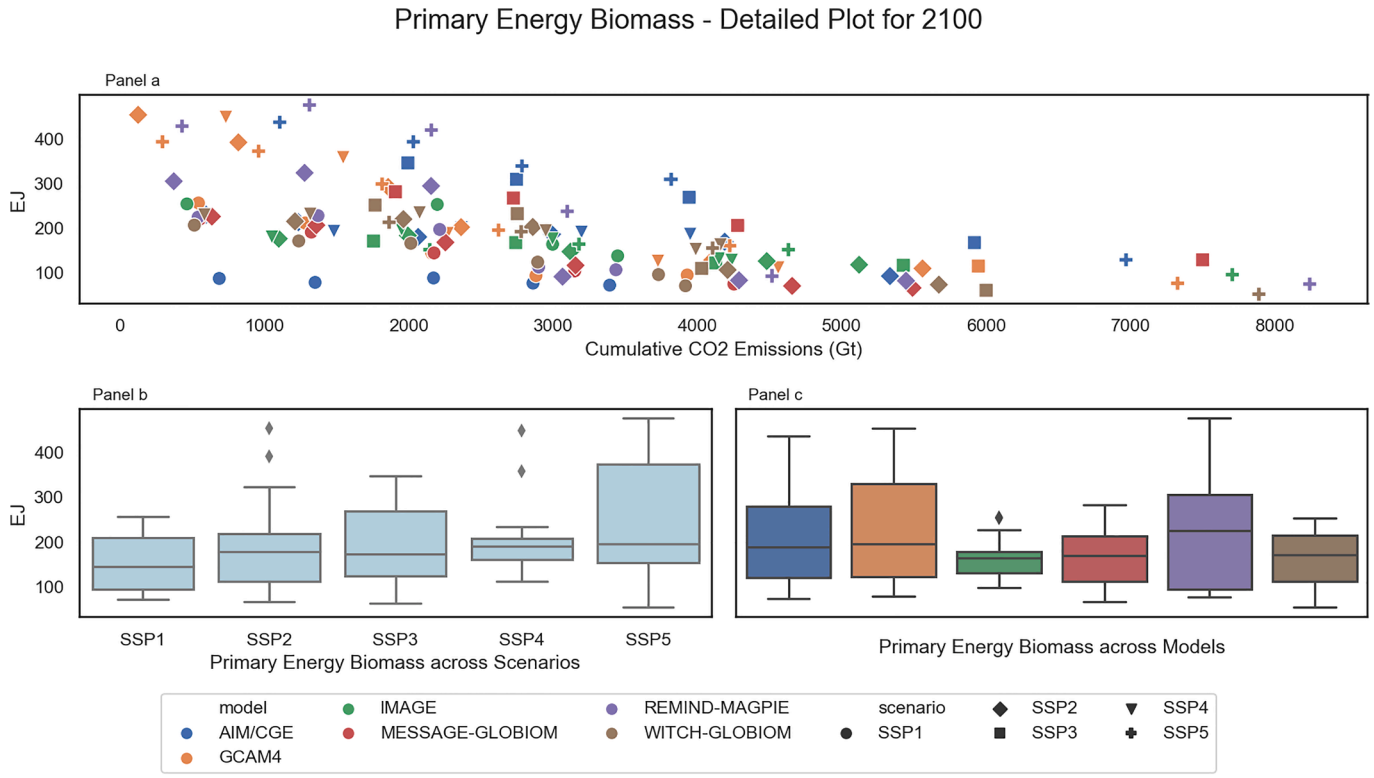

Fig. C1. The variability of primary energy supply from biomass across models and scenarios in the SSPs database, year 2100. In these plots, Panel a shows the spread of the energy indicator in question for different levels of cumulative CO_2 emissions, across different models (indicated by the colours in the legends) and across different (indicated by symbols in the legends). Panel b shows a box plot of the energy indicator across scenarios. Panel c shows a box plot of the energy indicator across models, where the colours follow the models' colours in the legends. As the figure illustrates, the spread across the models is large due to model-specific choices in biomass deployment, as discussed in Section 3.2 above in relation to Fig. 1.

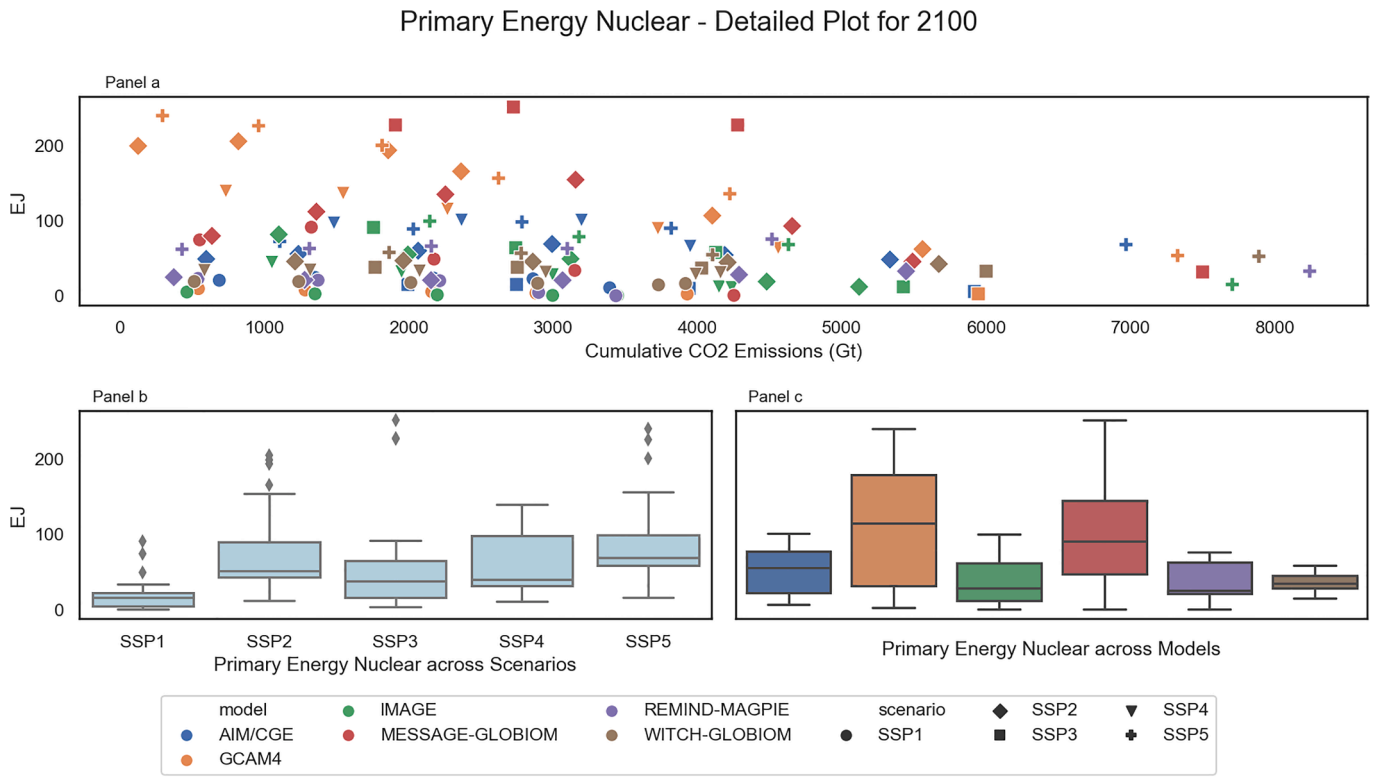

Fig. C2. The variability of primary energy generation from nuclear across models and scenarios in the SSPs database, year 2100. As the figure illustrates, the spread across model runs for some model is large, as discussed in Section 3.2 above in relation to Fig. 1. The spread across scenarios is also large.

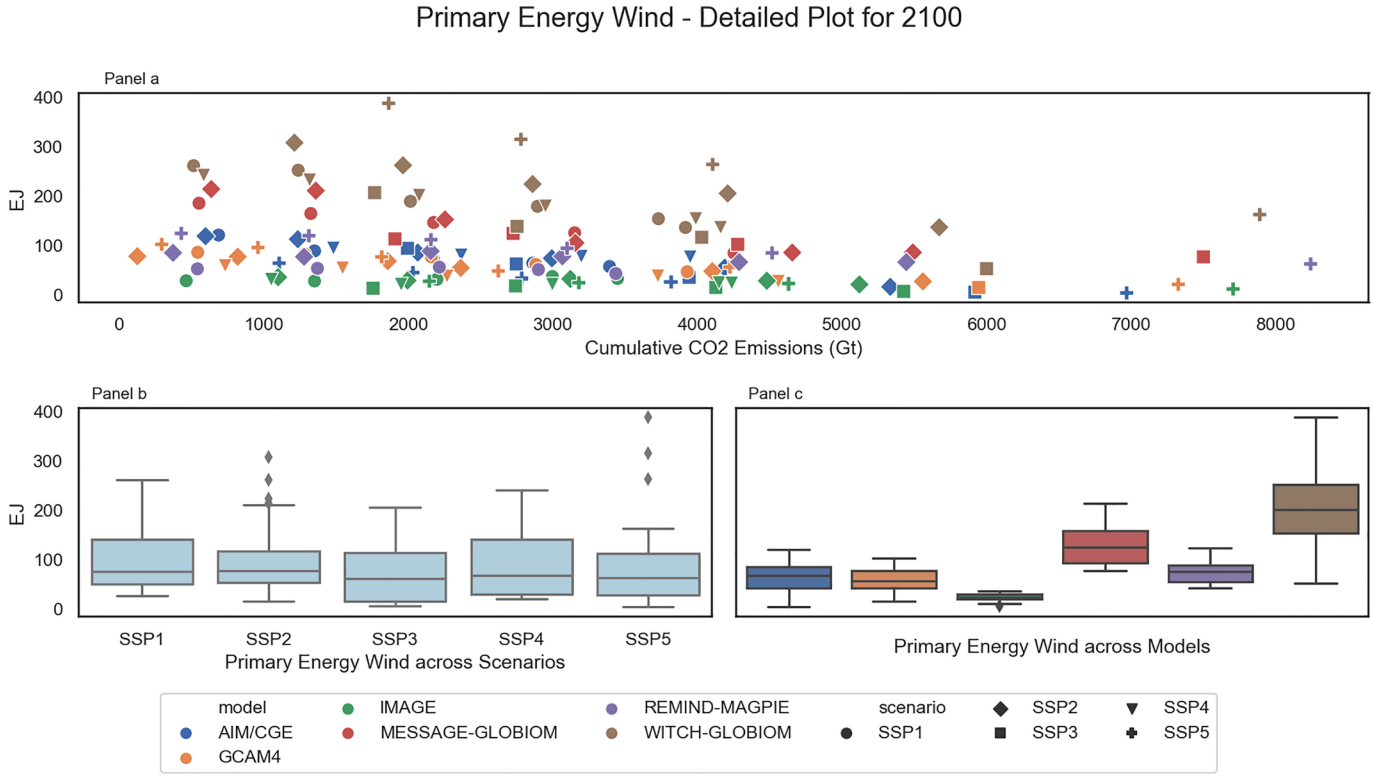

Fig. C3. The variability of primary energy supply from wind across models and scenarios in the SSPs database, year 2100. As the figure illustrates, the spread across models is large, as discussed in Section 3.2 above in relation to Fig. 1.

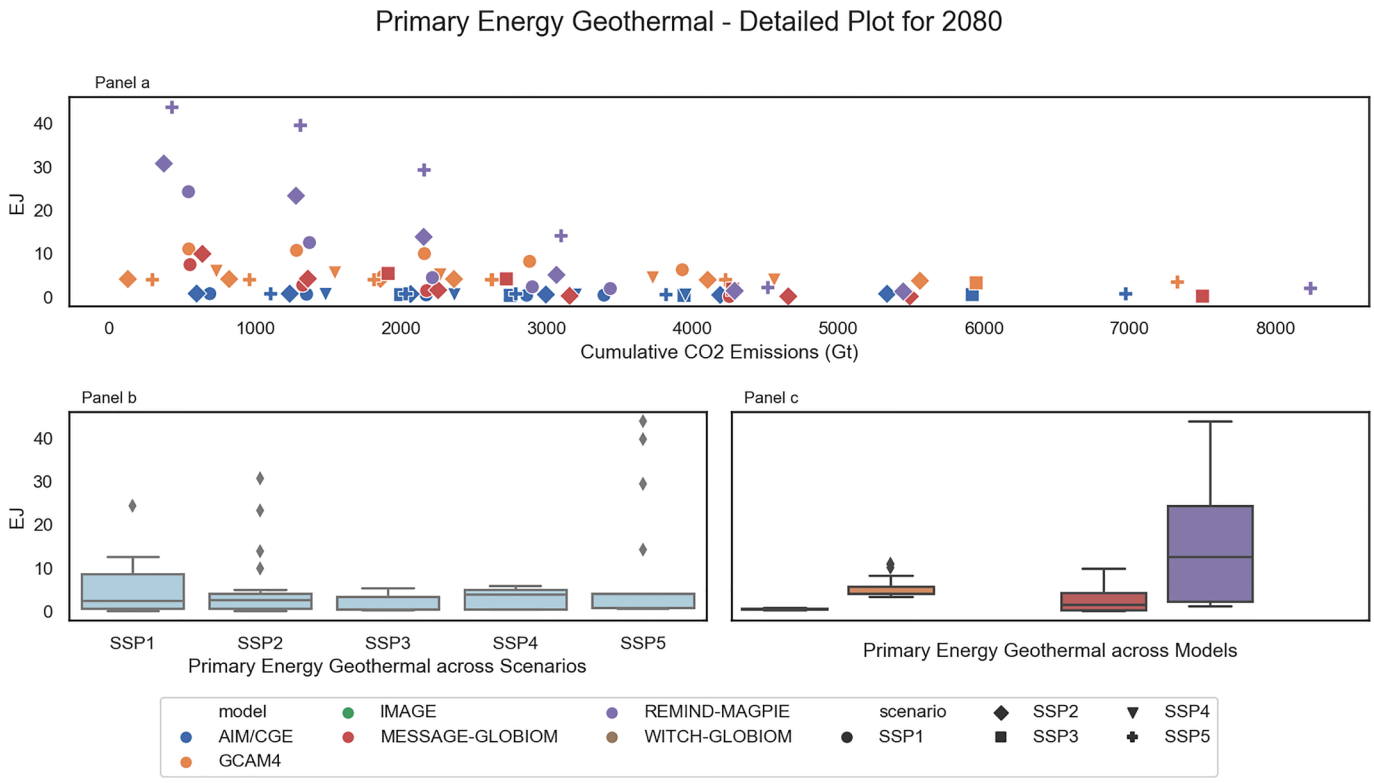

Fig. C4. The variability of primary energy supply from geothermal across models and scenarios in the SSPs database, year 2080. As the figure illustrates, the spread across models is large and not all models provide results for geothermal energy, as discussed in Section 3.2 above in relation to Fig. 1.

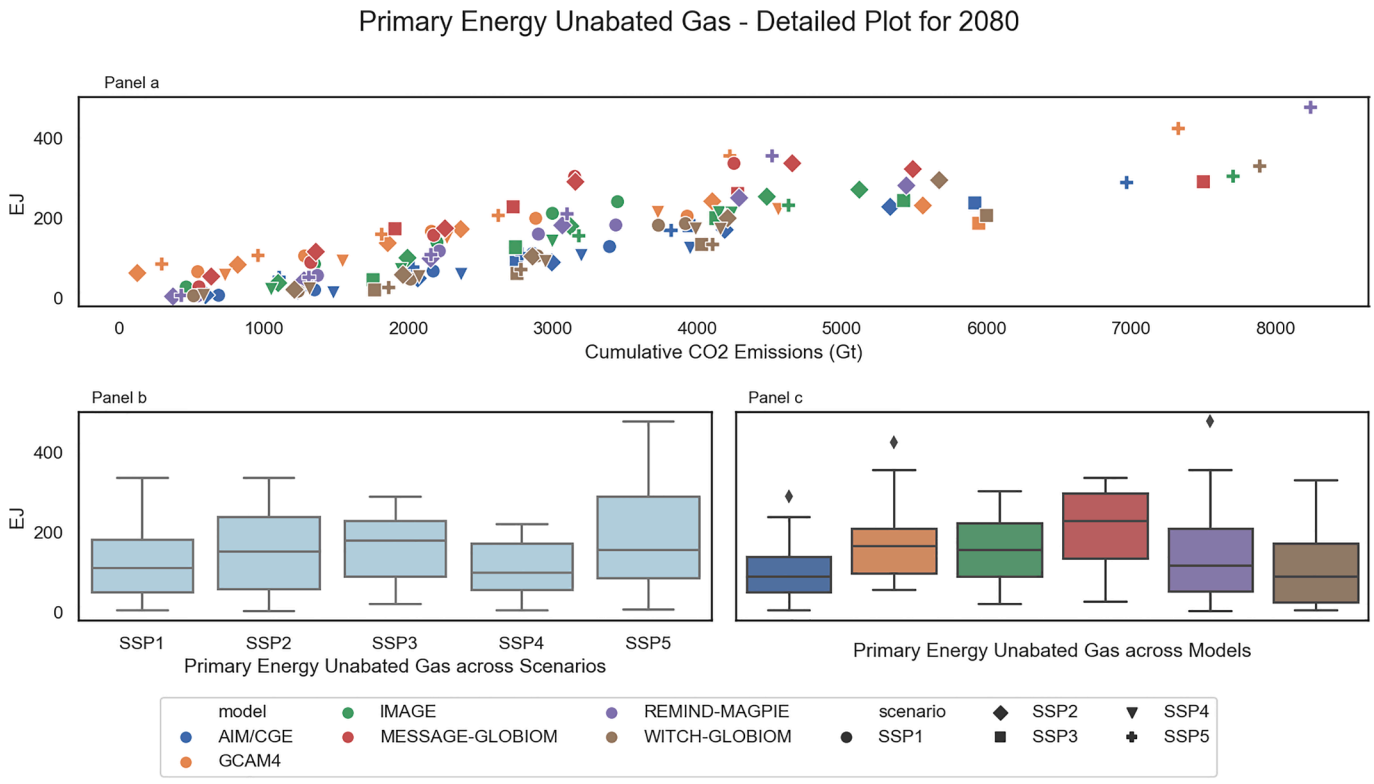

Fig. C5. The variability of primary energy supply from gas without CCS across models and scenarios in the SSPs database, year 2080. As the figure illustrates, the spread within some models (notably GCAM and REMIND) is somewhat large, as discussed in Section 3.3 above in relation to Fig. 4.

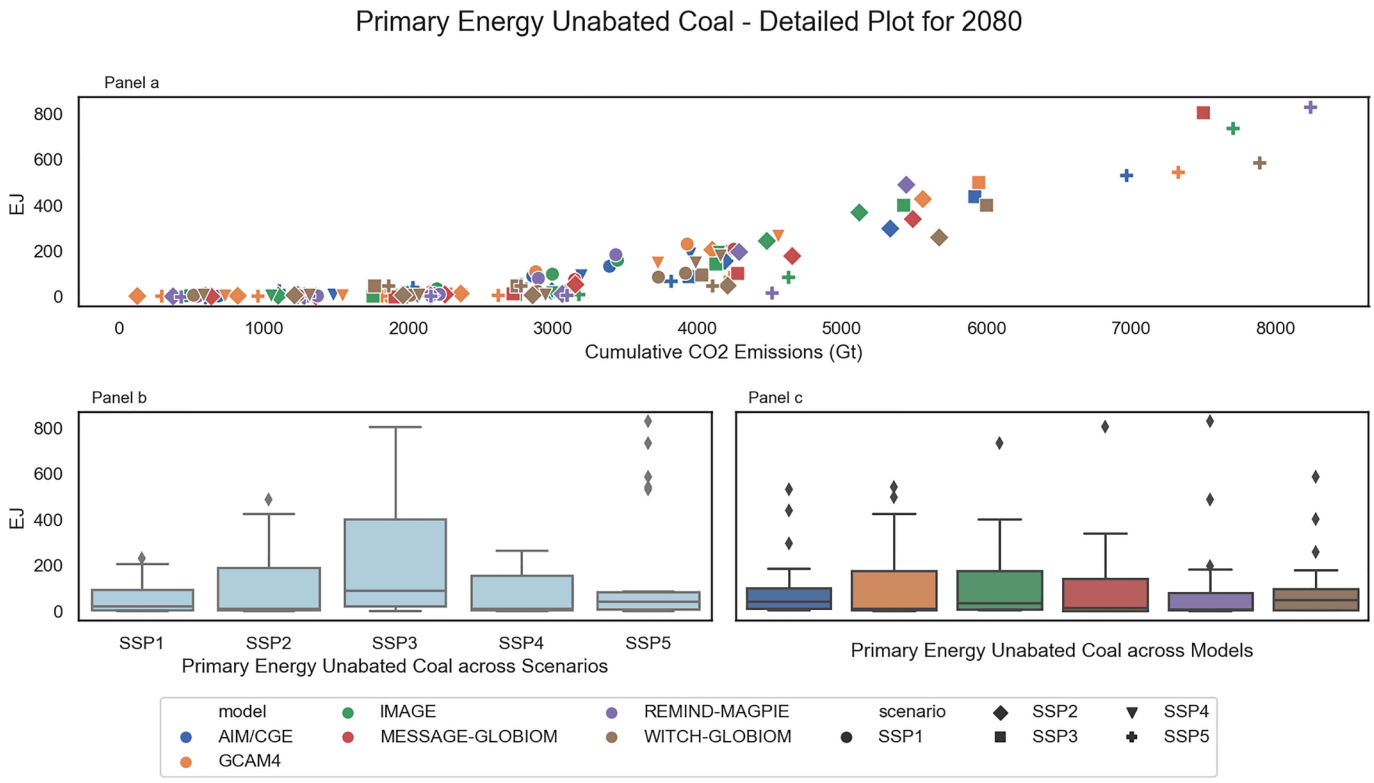

Fig. C6. The variability of primary energy supply from coal without CCS across models and scenarios in the SSPs database, year 2080. As the figure illustrates, the spread across models is limited with a not insignificant number of outliers, as discussed in Section 3.3 above in relation to Fig. 4.

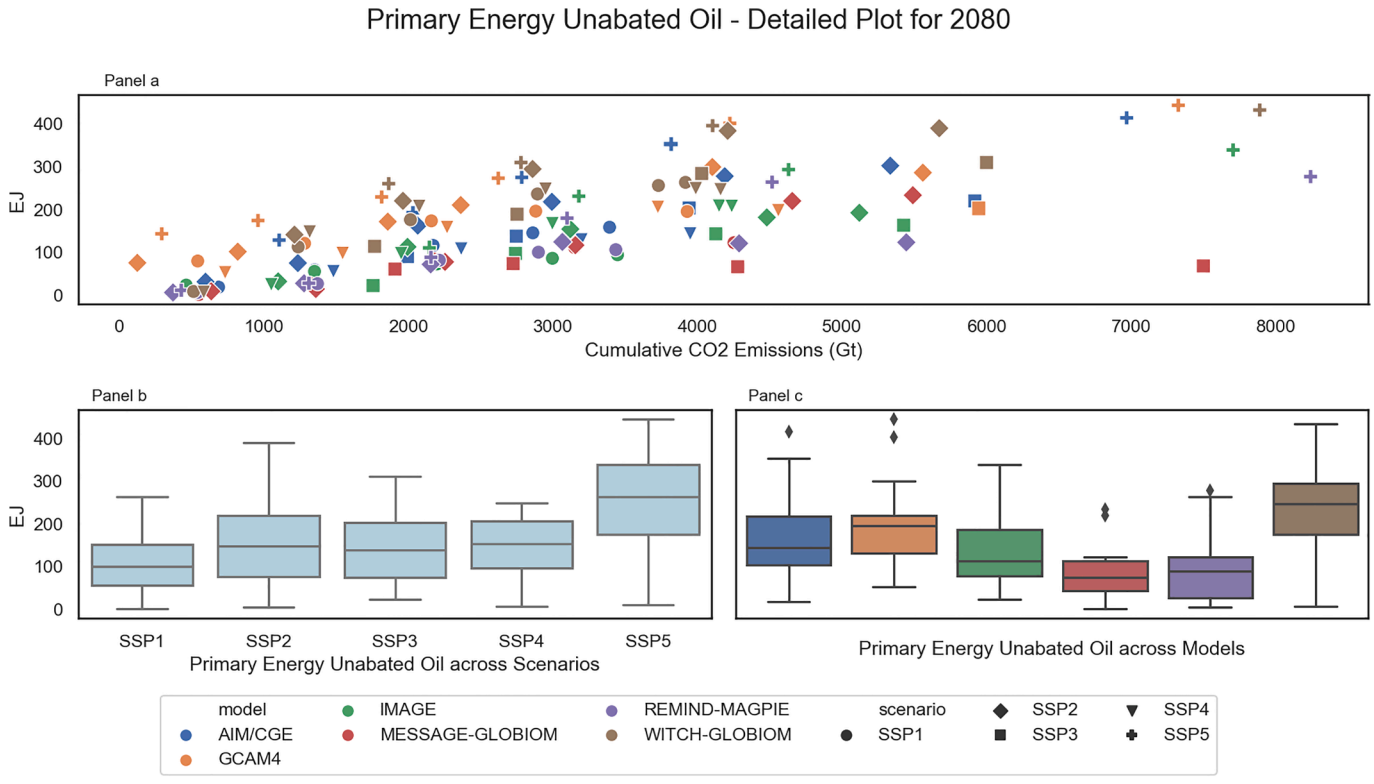

Fig. C7. The variability of primary energy supply from oil without CCS across models and scenarios in the SSPs database, year 2080. As the figure illustrates, the spread across models is somewhat large, as discussed in Section 3.3 above in relation to Fig. 4.

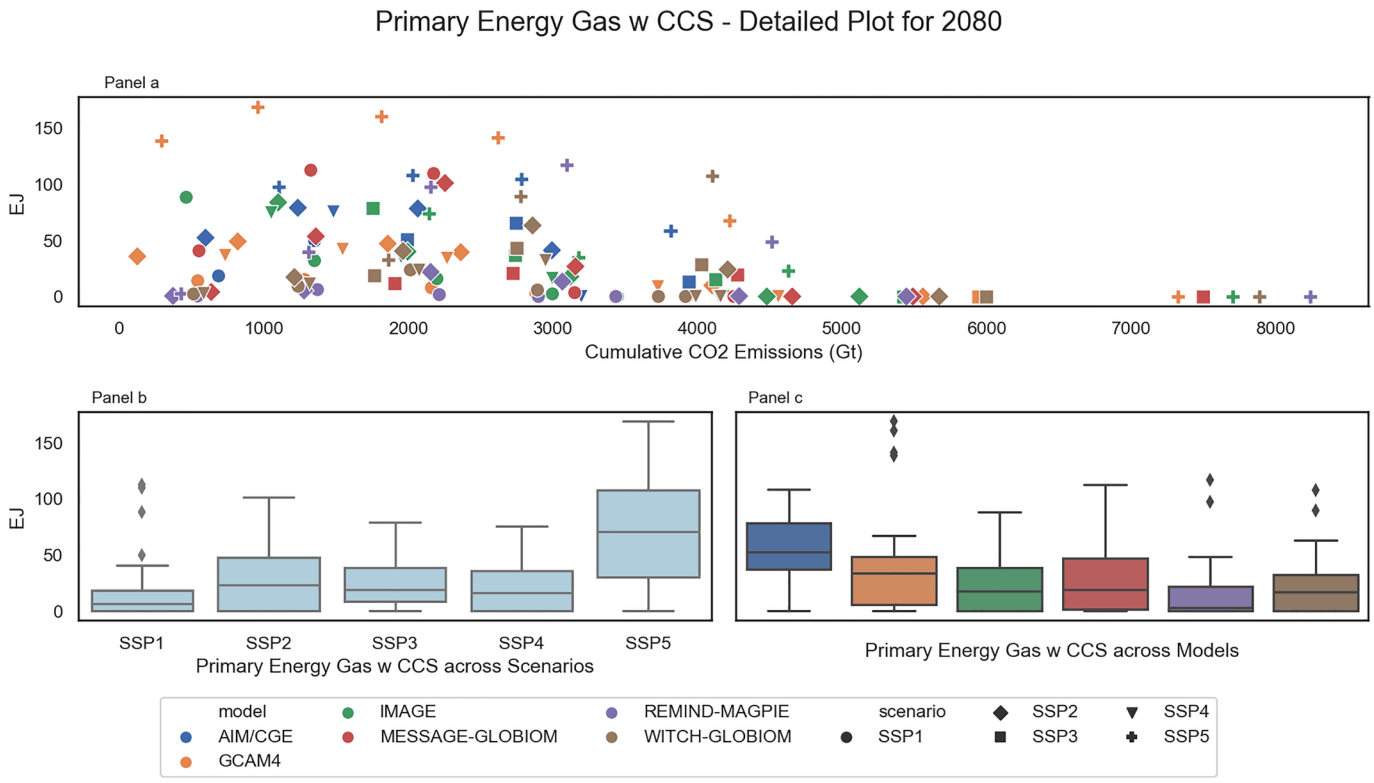

Fig. C8. The variability of primary energy supply from gas with CCS across scenarios and models in the SSPs database, year 2080. As the figure illustrates, the spread across scenarios is large, as discussed in Section 3.3 above in relation to Fig. 4.

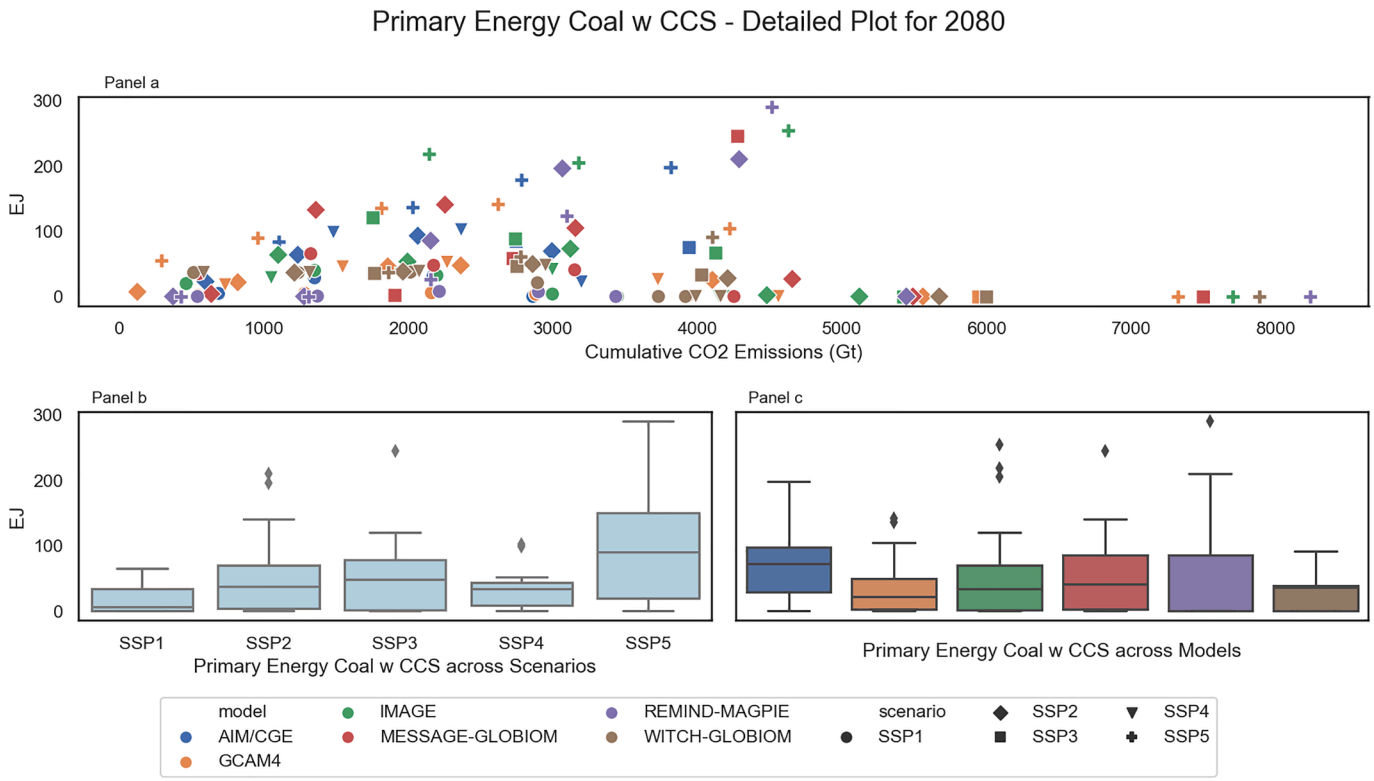

Fig. C9. The variability of primary energy supply from coal with CCS across scenarios and models in the SSPs database, year 2080. As the figure illustrates, the spread across scenarios is large, as discussed in Section 3.3 above in relation to Fig. 4.

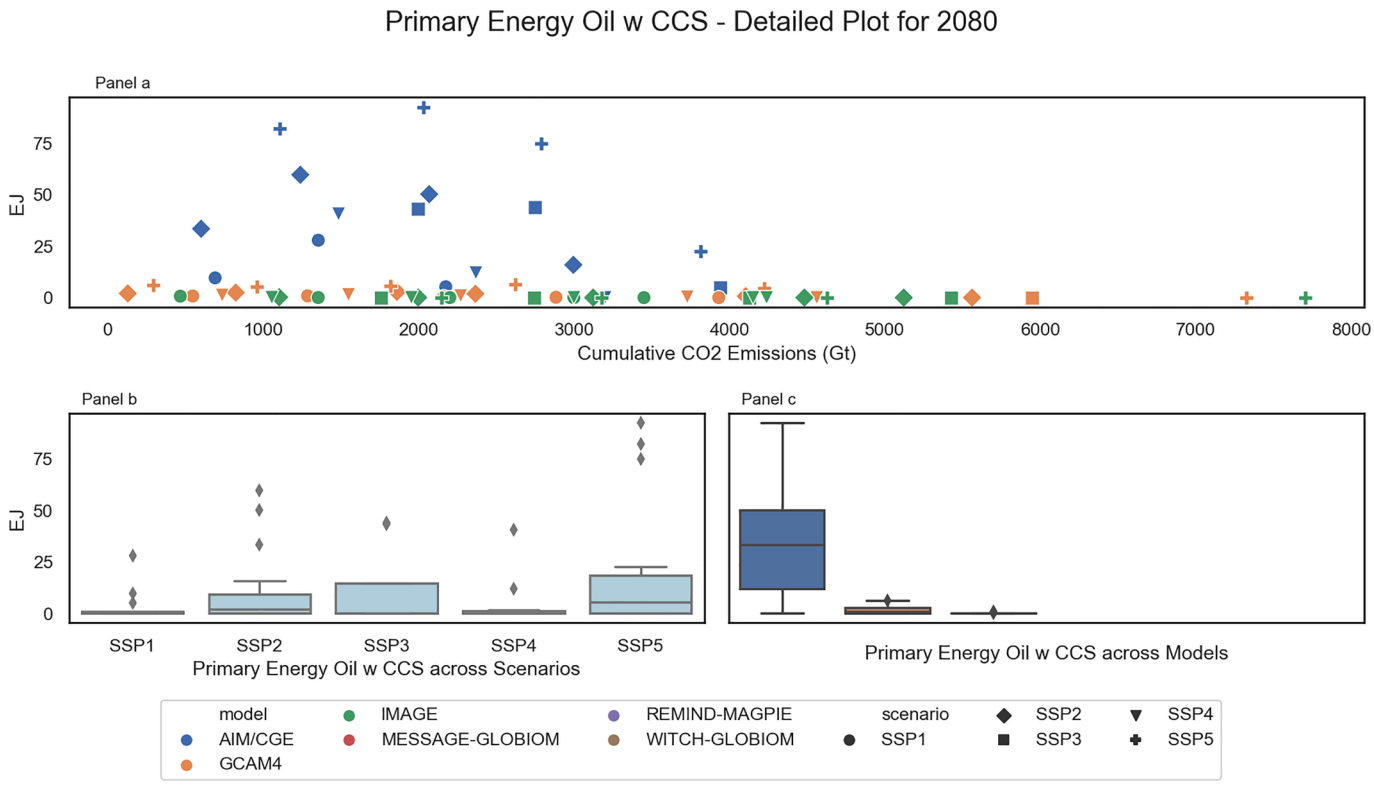

Fig. C10. The variability of primary energy supply from oil with CCS across scenarios and models in the SSPs database, year 2080. As the figure illustrates, the spread scenarios is large, and only three models report values for this variable where each differs from the next by an order of magnitude, as discussed in Section 3.3 above in relation to Fig. 4.

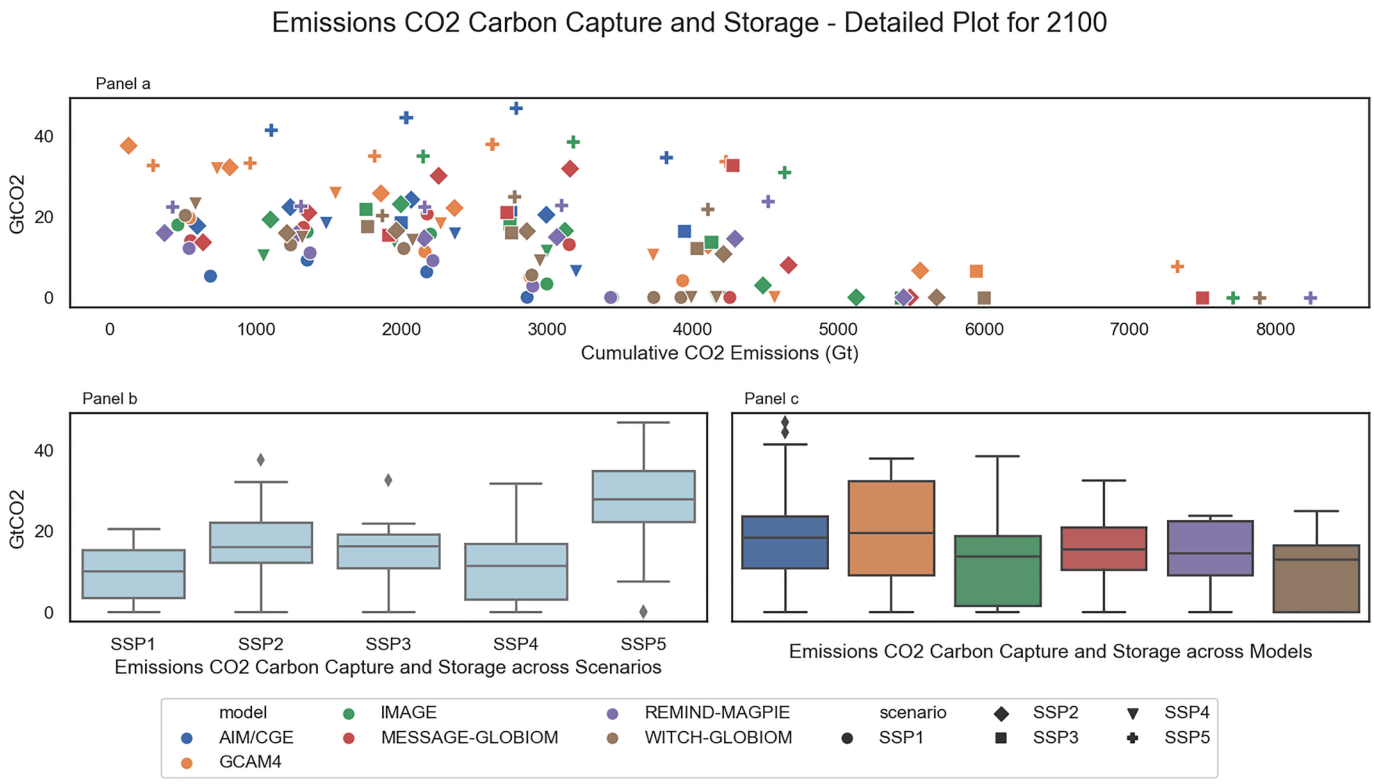

Fig. C11. The variability of CCS across scenarios and models in the SSPs database, year 2100. Related to the discussion in Section 3.4 above, Fig. 6.

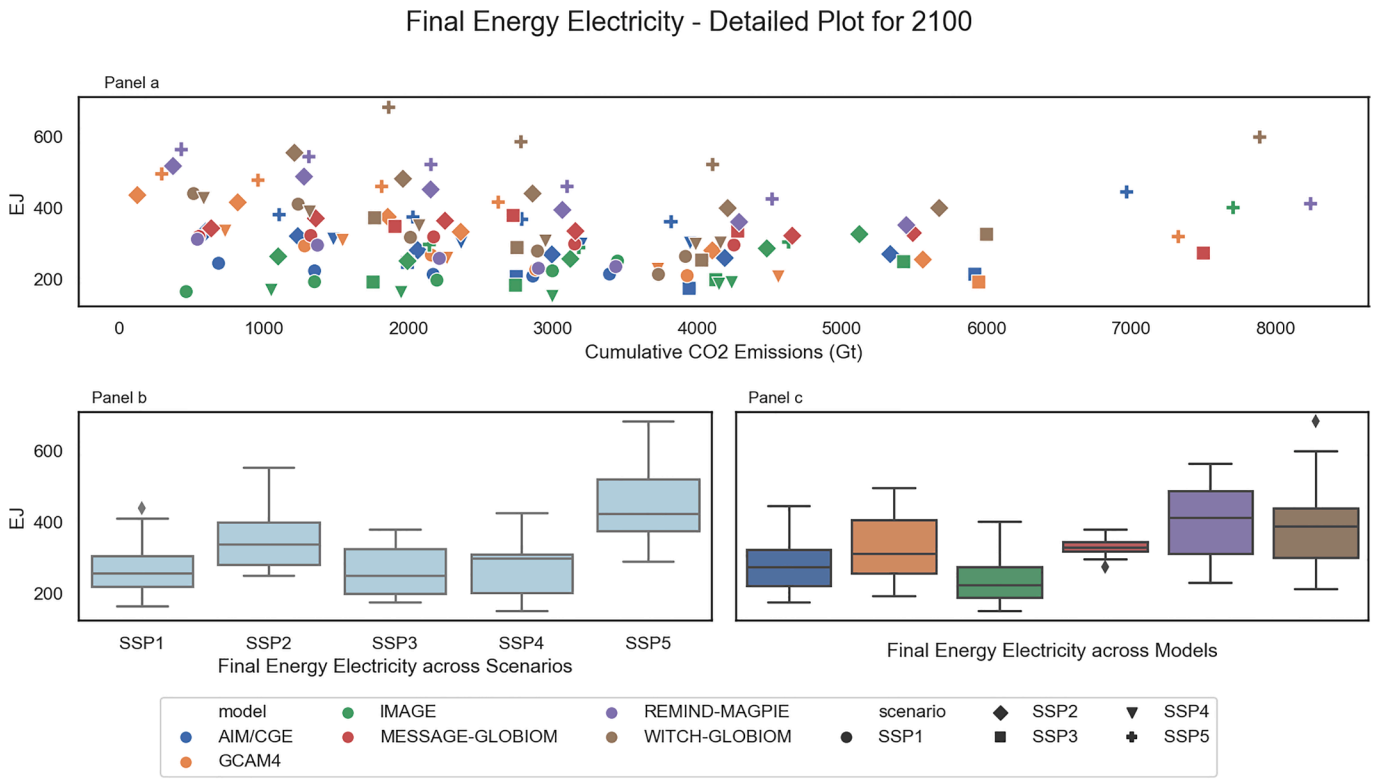

Fig. C12. The variability of the absolute level of electricity consumption in final energy, across models and scenarios in the SSPs database, year 2100. Related to the discussion in Section 3.5 above, Fig. 7.

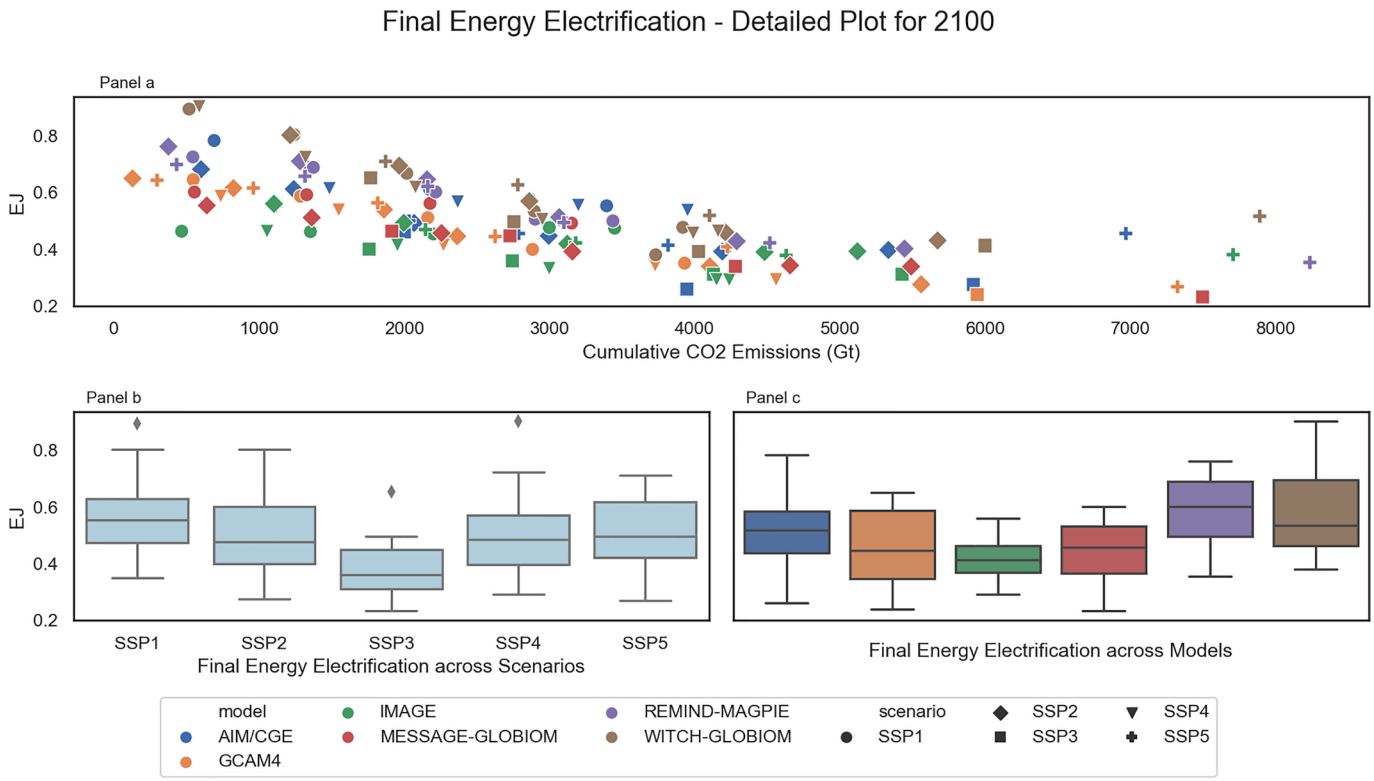

Fig. C13. The variability of electrification across models and scenarios in the SSPs database, year 2100. Related to the discussion in Section 3.5 above, Fig. 7.

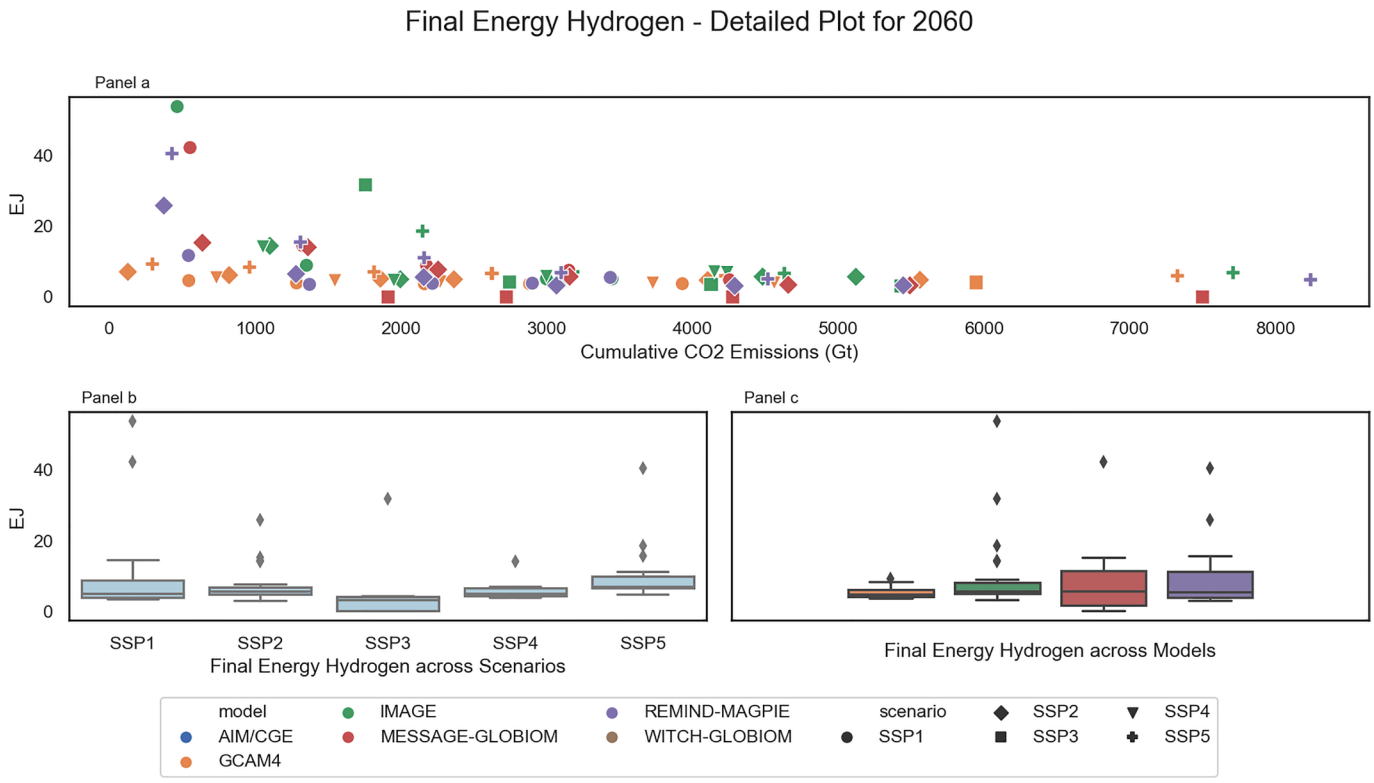

Fig. C14. The variability of hydrogen consumption across models and scenarios in the SSPs database, year 2060. Related to Section 3.5 above, Fig. 7.

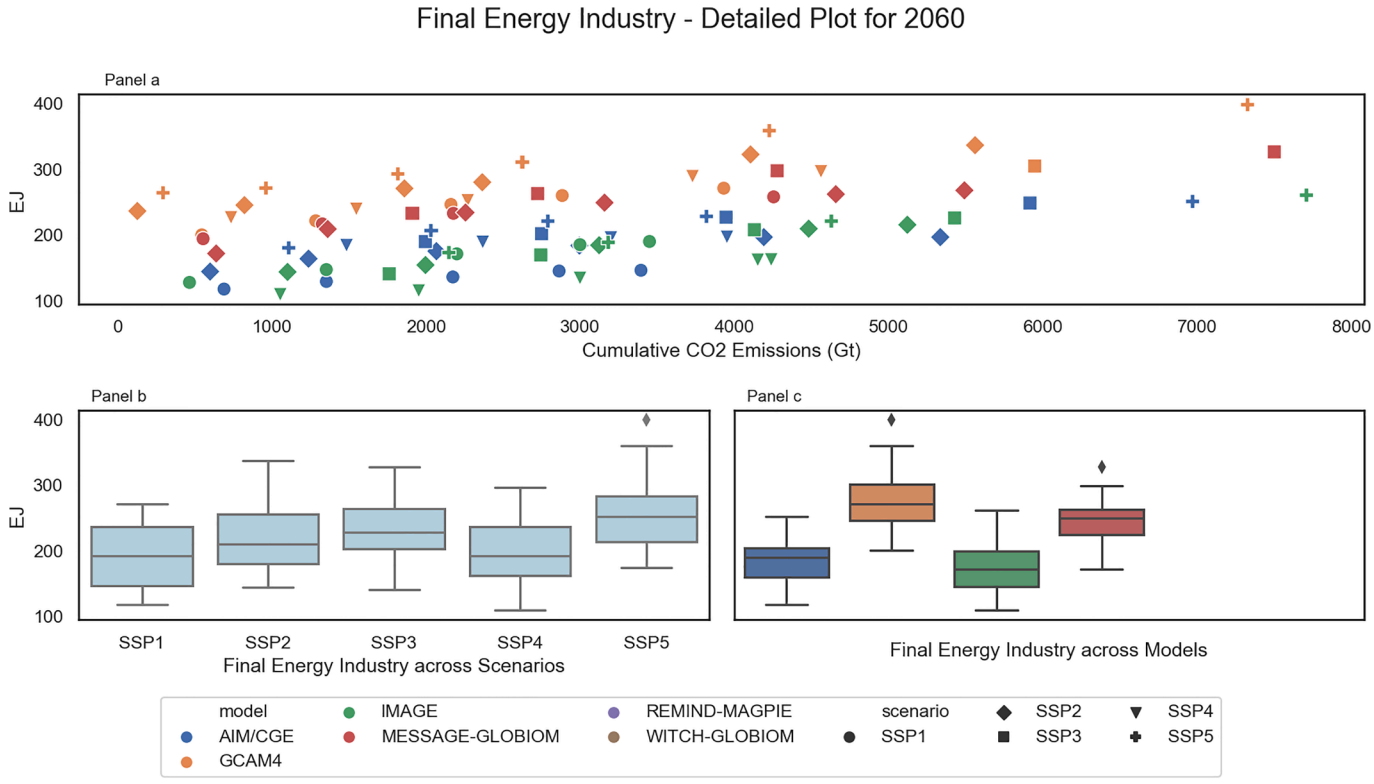

Fig. C15. The variability of final energy demand in the industry sector, across models and scenarios in the SSPs database, year 2060. Related to Section 3.6 above, Fig. 8.

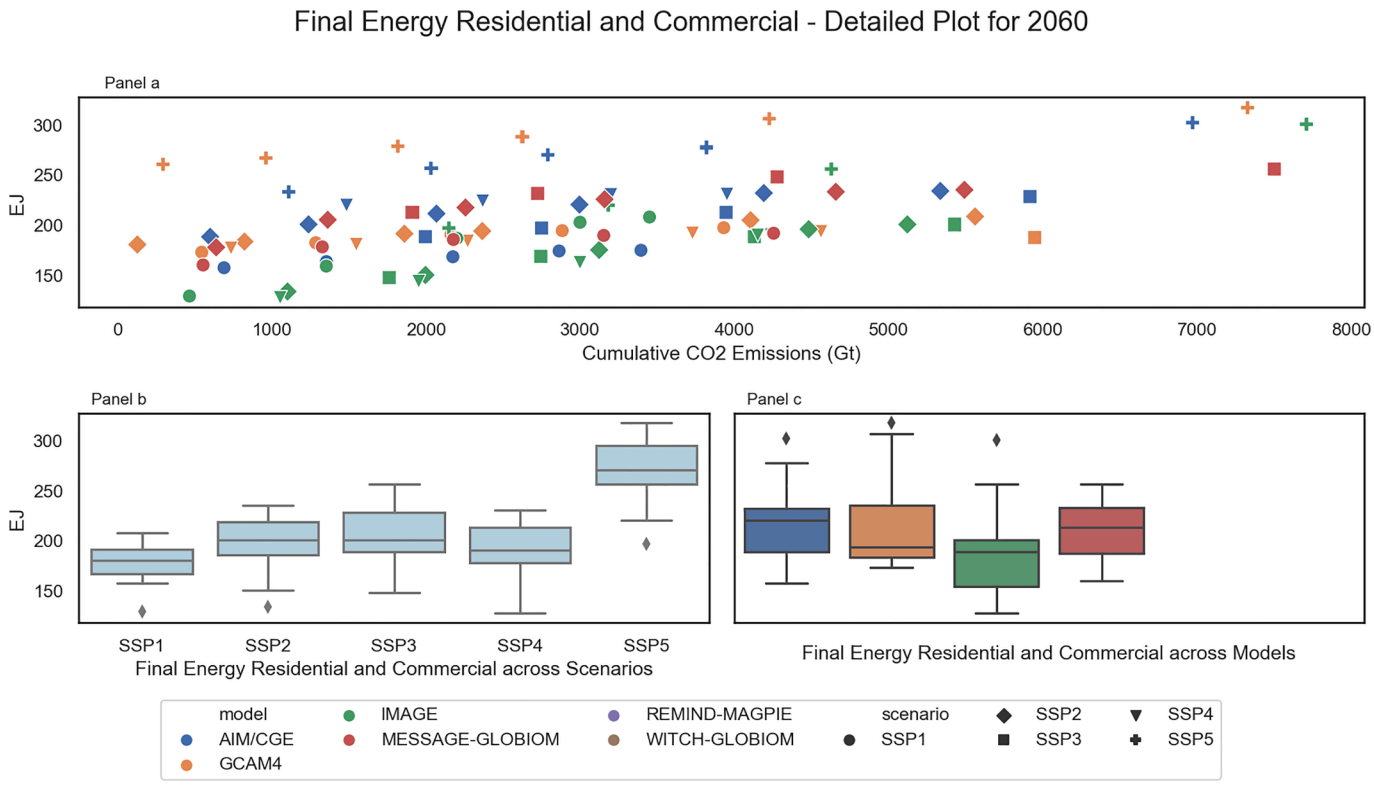

Fig. C16. The variability of final energy demand in the combined residential and commercial sector, across models and scenarios in the SSPs database, year 2060. Related to Section 3.6 above, Fig. 8.

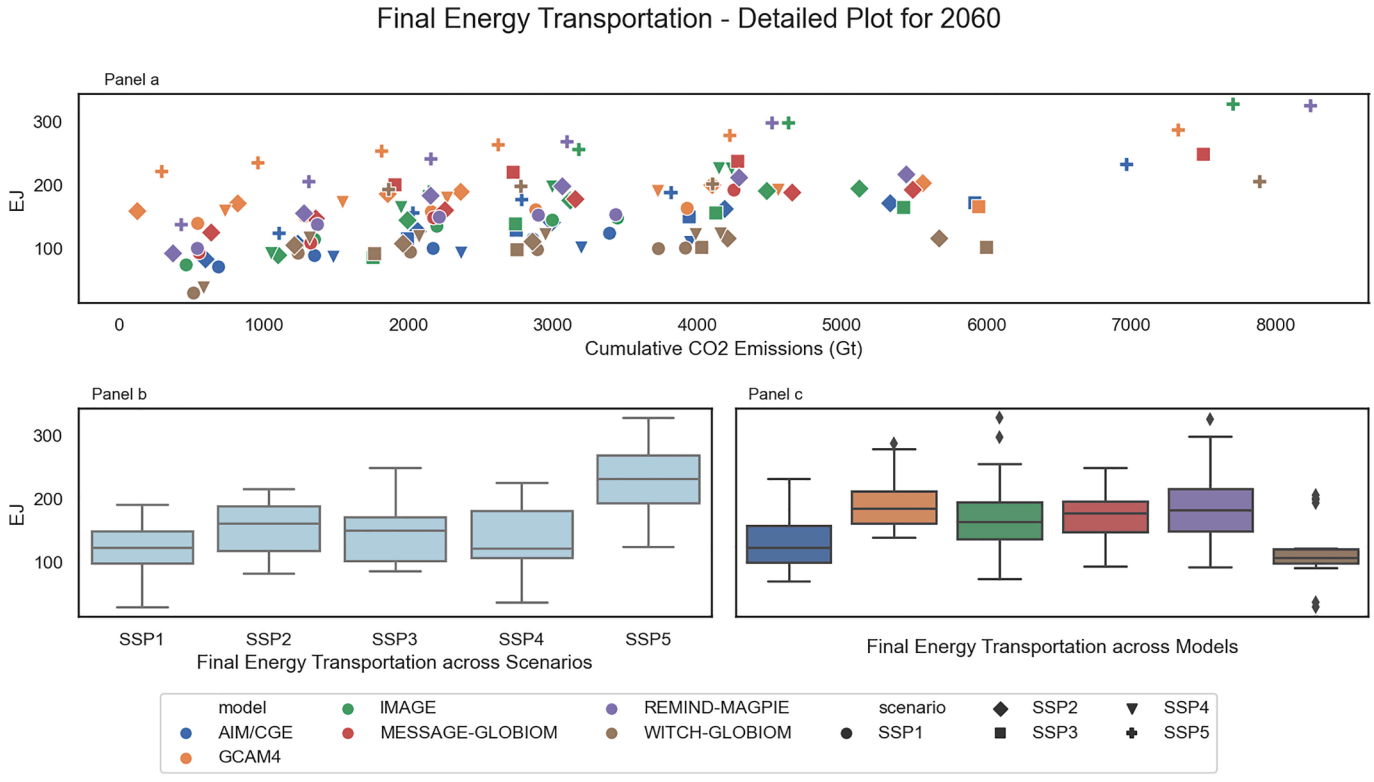

Fig. C17. The variability of final energy demand in the transportation sector, across models and scenarios in the SSPs database, year 2060. Related to Section 3.6 above, Fig. 8.

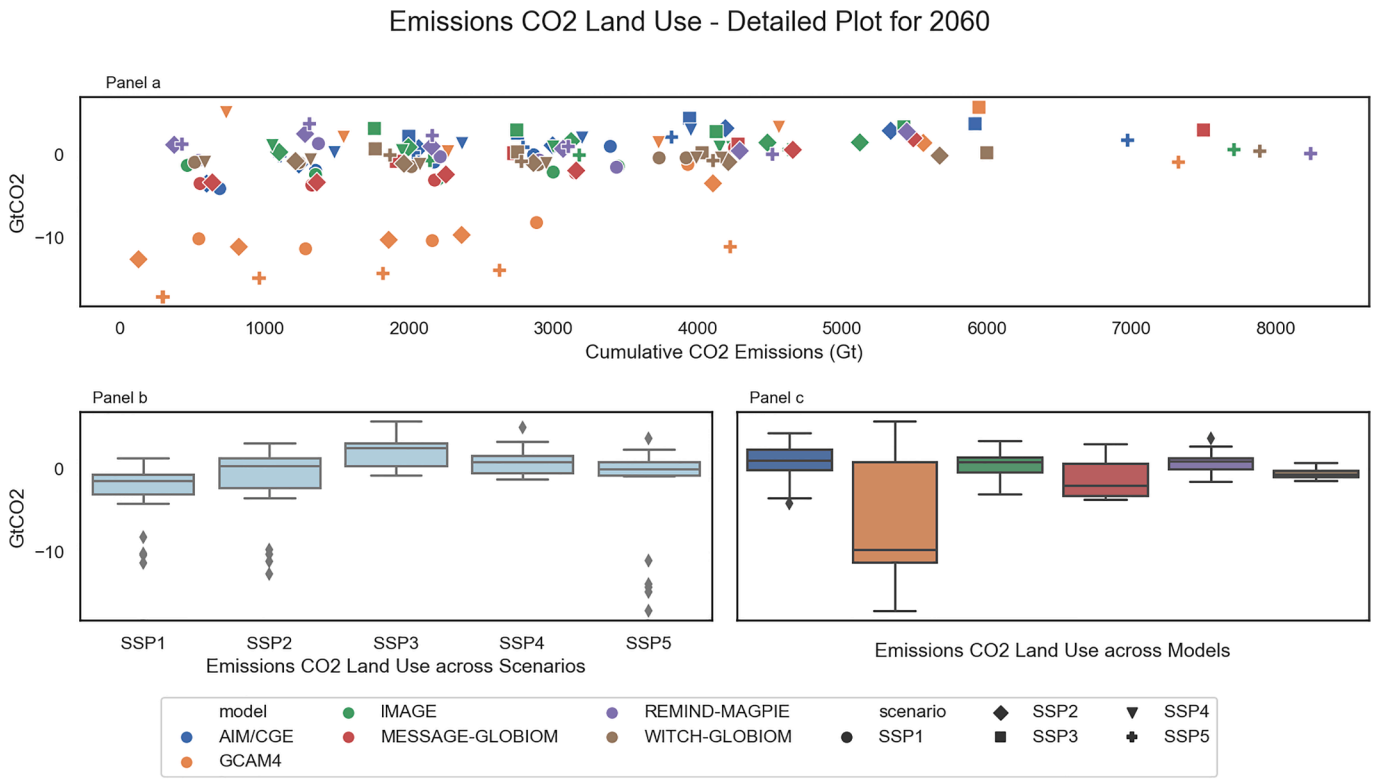

Fig. C18. The variability of land use CO_2 emissions across models and scenarios in the SSPs database, year 2060. As the figure here illustrates, the spread across (Panel c) and within the models is large due to the high uncertainties in measuring land use CO_2 emissions, as discussed in Section 3.7 above in relation to Fig. 10.

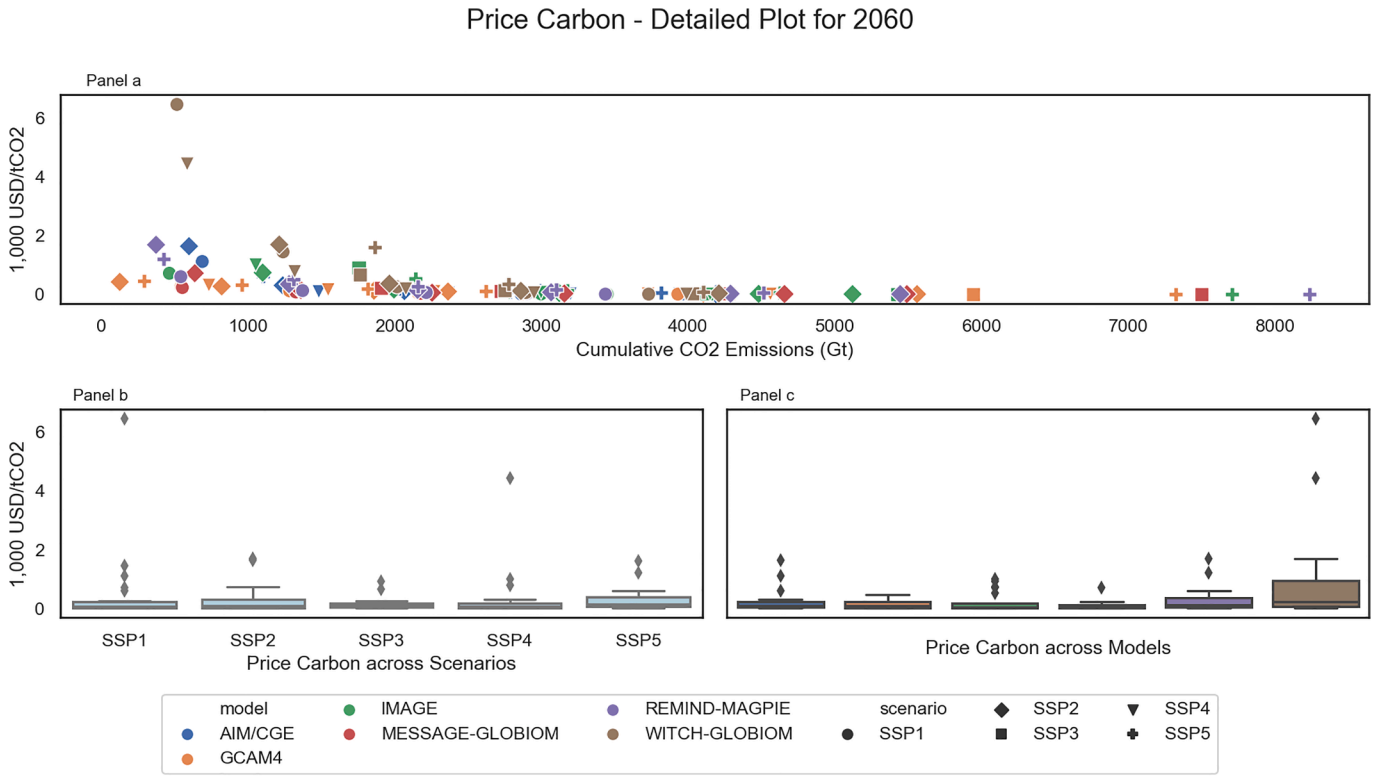

Fig. C19. The variability of carbon price across models and scenarios in the SSPs database, year 2060. Related to Section 3.8 above, Fig. 12.

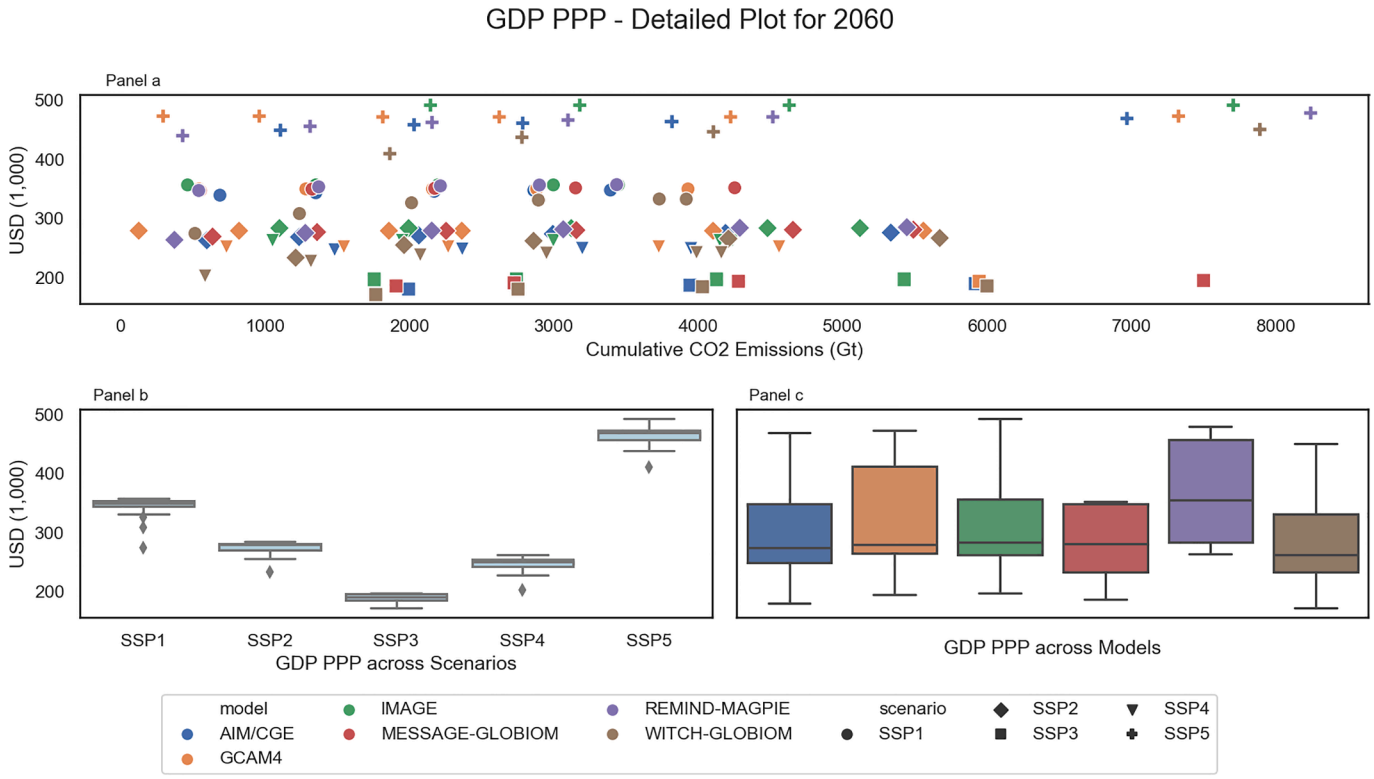

Fig. C20. The variability of GDP_{ppp} across scenarios and models in the SSPs database, year 2060. Related to Section 3.8 above, Fig. 12.

Appendix D Additional results on final energy

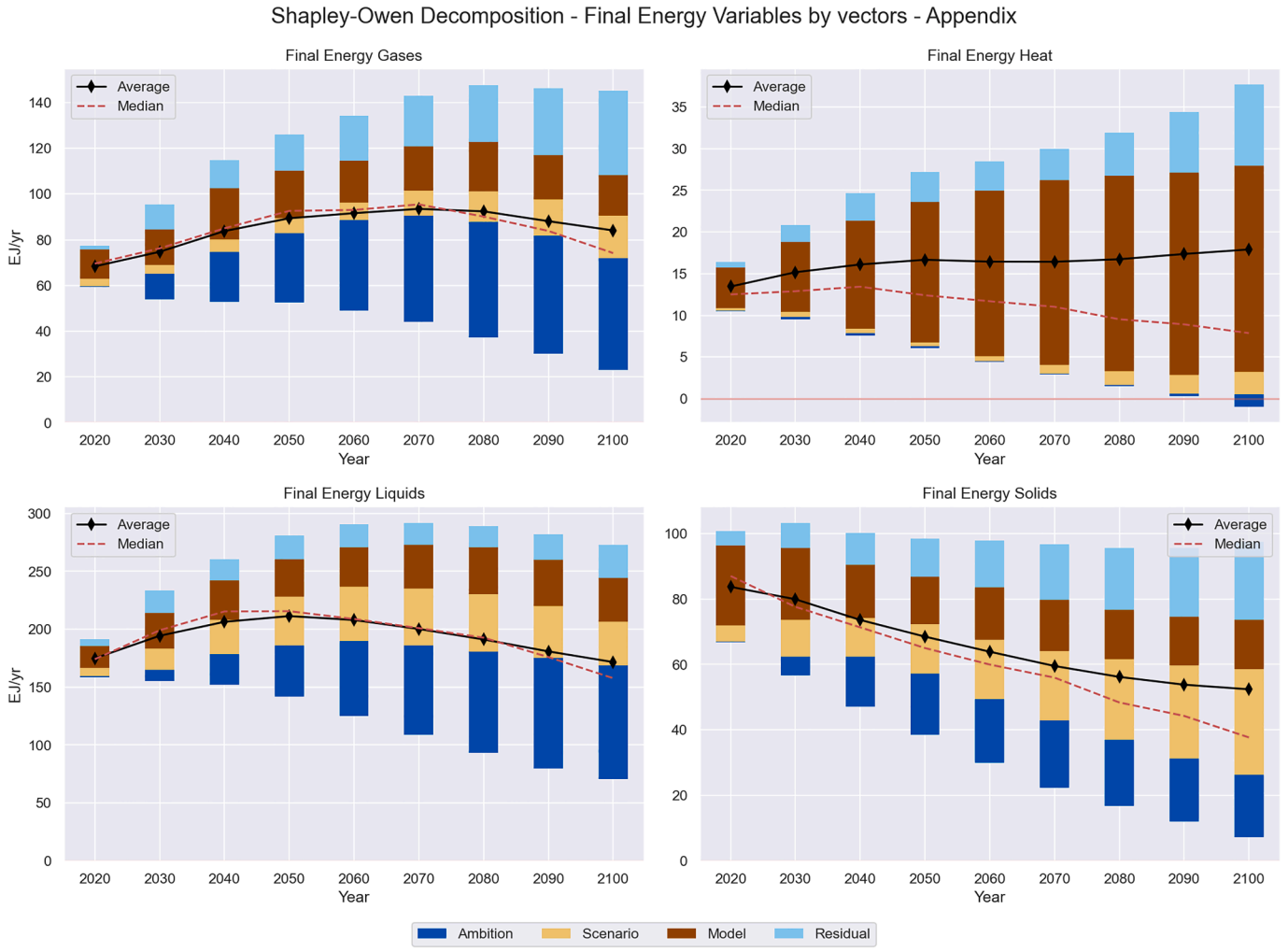

Fig. D1. Shapley–Owen decomposition - final energy for additional carriers. Top left panel shows gases, top right panel shows heat, and bottom left panel shows liquids, and bottom right panel shows solids. Notice that the y-axis differs between panels.

The discussion here relates to the main final energy carriers and variables discussed in Section 3.5 and Fig. 7 above, but also to the discussion on energy supply from fossil fuels in Section 3.3 and Fig. 4. As Fig. D1 above demonstrates variations in gases (top left panel) and liquids (bottom left panel) are largely driven by climate ambition, with some role for the model and background scenario factors. As discussed in the earlier sections, the role of climate ambition is not surprising given the importance of fuel switching in decarbonisation, coupled with models' assumptions and demand due to population and GDP [27]. The decomposition for solids (bottom right panel) is not dissimilar but with a more prominent role for the background scenario factor largely motivated by access to clean fuels in developing countries, which, as discussed in Section 3.6 above, is influenced by the levels of population and GDP growth [23].

Heat use (top, right panel) is almost entirely explained by difference between models, something that we verify in Fig. D2 below, due to the inconsistent and highly uncertain characterisation of the heating (and cooling) sector (e.g. residential vs. commercial) across models [38].

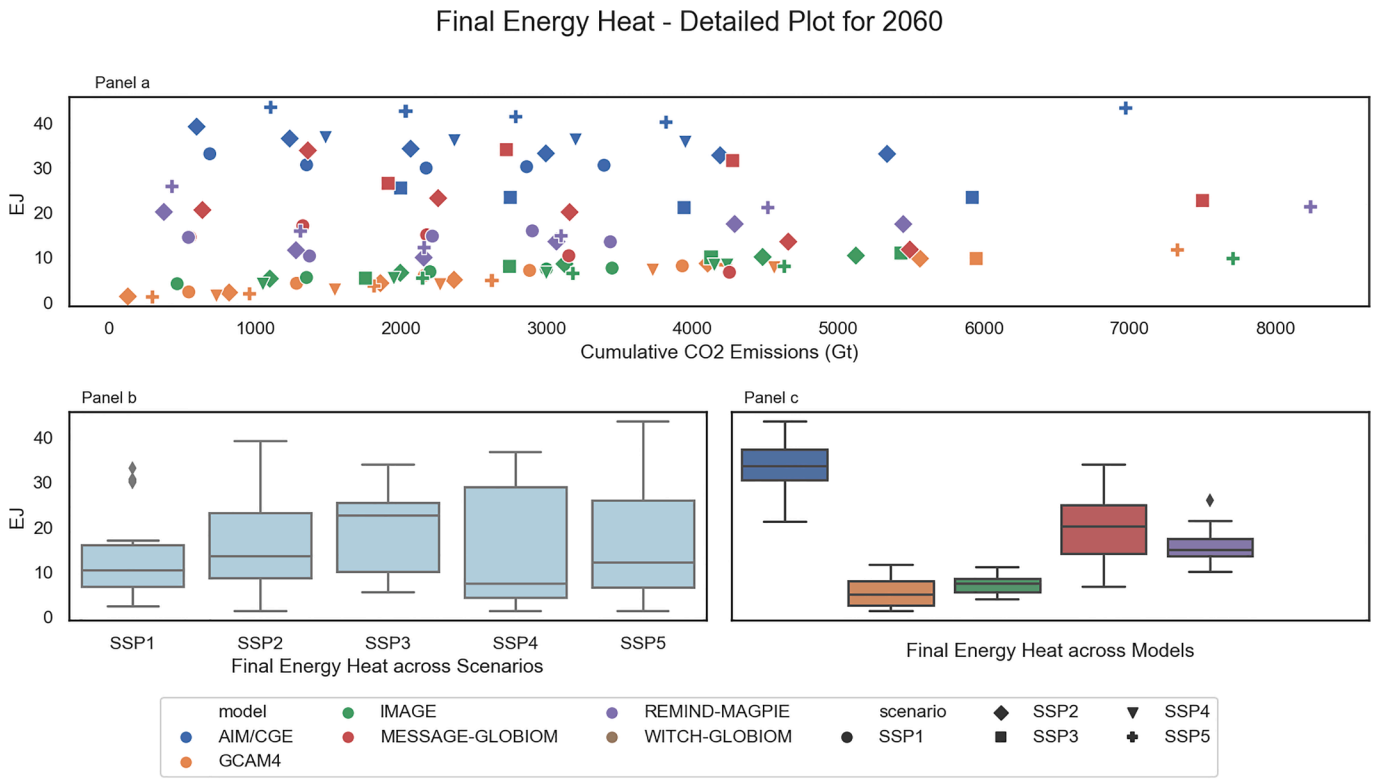

Fig. D2. The variability of heat use across models and scenarios in the SSPs Database, year 2060.

Appendix E Comparative diagnostics of climate ambition representation in Shapley–Owen decomposition: quadratic emissions function versus RCP dummy variables

In our analysis, the climate ambition factor is represented by a quadratic function of total cumulative CO_2 emissions over the 21st century and its square. An anonymous referee asked us to consider using the RCPs as dummy variables instead, and this appendix reports the results of doing so for our 2060 data. For most indicators, the choice makes little difference, as can be seen comparing the paired columns in Figs. E1, E2, E3, E4, E5, E6 below. However, when we use RCP dummy variables, the climate ambition factor explains less of the variation in unabated fossil fuels or final energy demand than when we use a continuous variable. For hydrogen as a final energy carrier, or primary solar energy production, however, the RCP dummy variables *increase* the proportion that is explained by the average effect of climate ambition.

Table E1 gives summary statistics for three of our indicators, split by RCP pathway: the number of runs we have, the mean value and the standard deviation.

Table E1
Summary statistics for selected climate indicators.

		Climate scenario RCP1.9	RCP2.5	RCP3.4	RCP4.5	RCP6.0	Baseline
Cumulative emissions, 2010–2100, Gt CO_2	Number	13	19	25	25	18	26
	Mean	452	1169	1988	2847	4155	5379
	S.D.	147	191	183	231	249	1445
Unabated fossil primary energy, 2060, EJ/yr	Number	13	19	25	25	18	26
	Mean	107.7	220.7	347.7	482.2	688.9	816.3
	S.D.	94.2	80.8	95.5	76.6	102.8	225.4
Hydrogen (Final energy), 2060, EJ/yr	Number	9	12	15	15	11	16
	Mean	23.3	9.5	8.1	4.9	4.4	4.4
	S.D.	17.0	4.4	7.5	1.8	1.9	1.6

Note that within each RCP, there is some variation in cumulative CO_2 emissions between model runs, but this is dwarfed by the variation across the baseline runs, in which the (shadow) CO_2 price is zero. Using RCP dummy variables, this inter-baseline variation is ignored, while it is captured with the quadratic measure of climate ambition that we use. The underlying cause of the variation in CO_2 emissions, of course, is variation in such indicators as the unabated use of fossil fuels, and the second part of the table confirms that for this indicator, there is more variation within the baseline runs than within any RCP. This is why the continuous measure of climate ambition is better at explaining the variation in unabated fossil fuel use than the RCP dummy variables, which implicitly suggest each baseline run is equally far from a sustainable climate. On the other hand, some low-carbon technologies need a strong carbon price before they rise in importance. The bottom block of the table shows that the use of hydrogen as a final energy carrier is predicted to be similar (in terms of mean and standard deviation) across the baseline runs, RCP 6.0 and RCP4.5 – it takes the higher carbon

prices associated with (some) runs under RCP3.4 to increase its average use by an important amount. It would take a much more complex function of cumulative emissions to capture this relationship as well as the dummy variable that can treat all model runs with a carbon price of zero as similar, whatever their cumulative emissions.

While we expected that any decrease in the explanatory power of climate ambition would be reflected by an increase in the model factor (since it is differences between models that give the different emissions within an RCP-SSP combination), the figures below show that it mainly results in an increase in the variation that is not explained by the average effect of our factors.

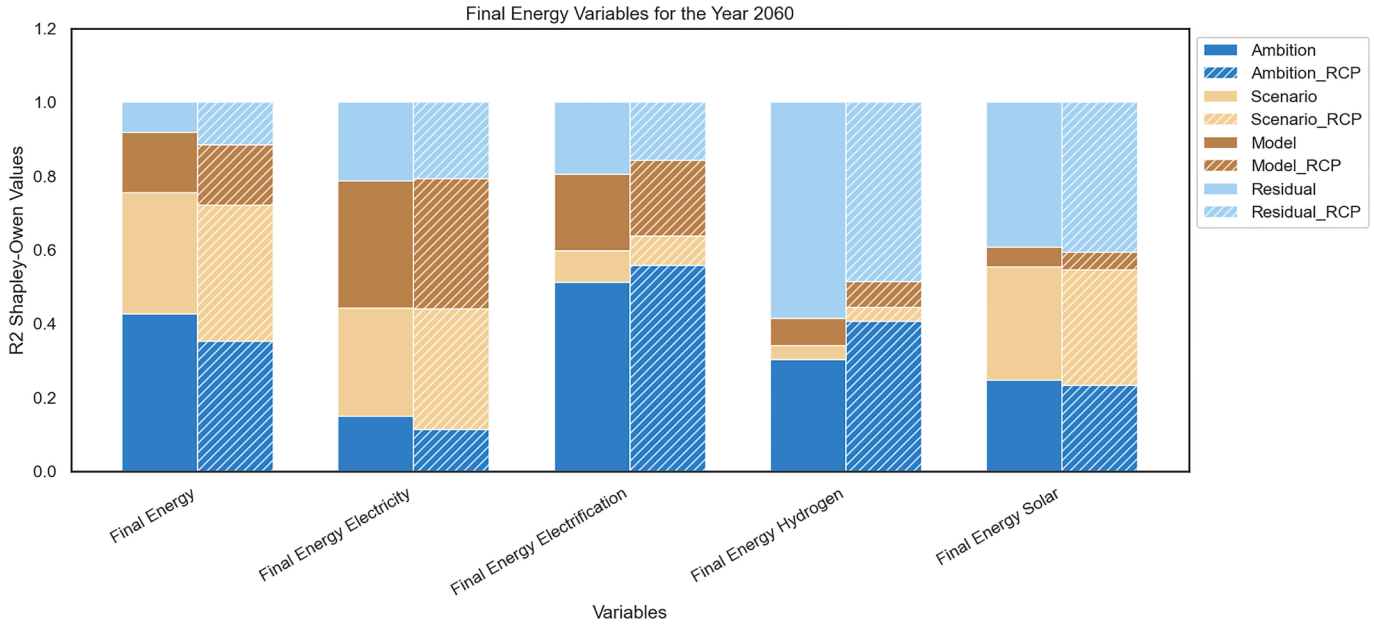

Fig. E1. The effects of using quadrative emissions versus RCPs to capture the climate ambition factor in Shapley–Owen decomposition – final energy variables, 2060.

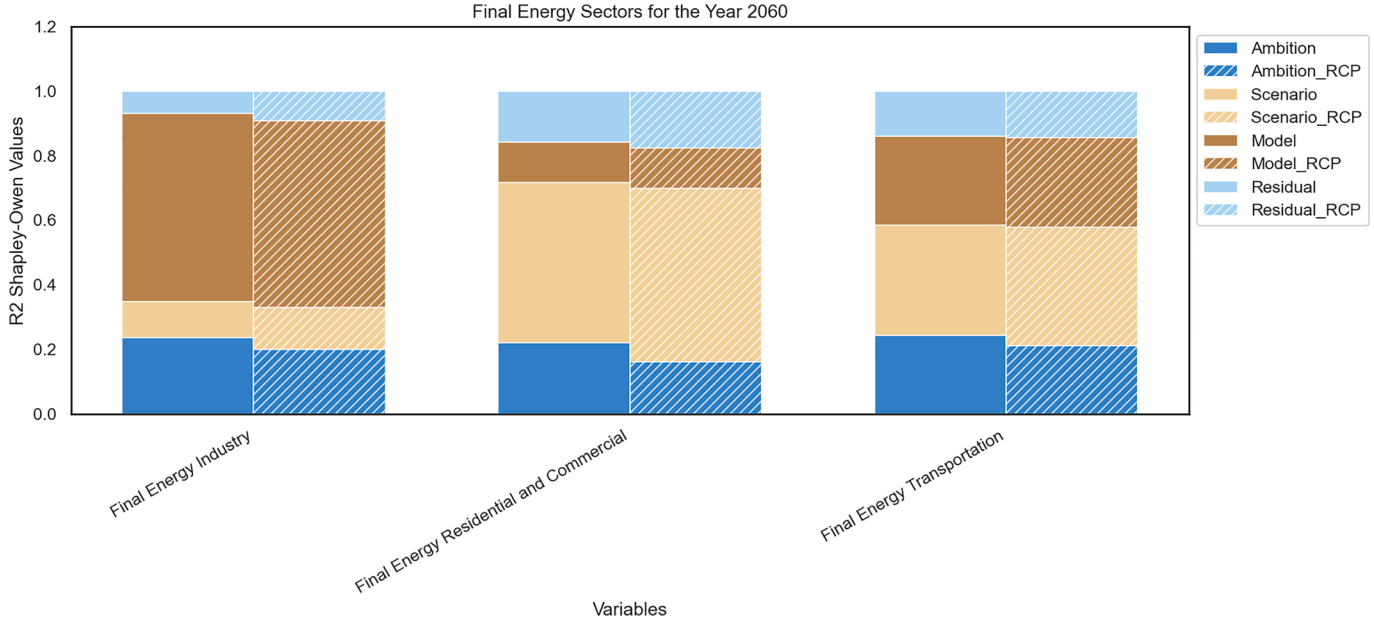

Fig. E2. The effects of using quadrative emissions versus RCPs to capture the climate ambition factor in Shapley–Owen decomposition – final energy sectors, 2060.

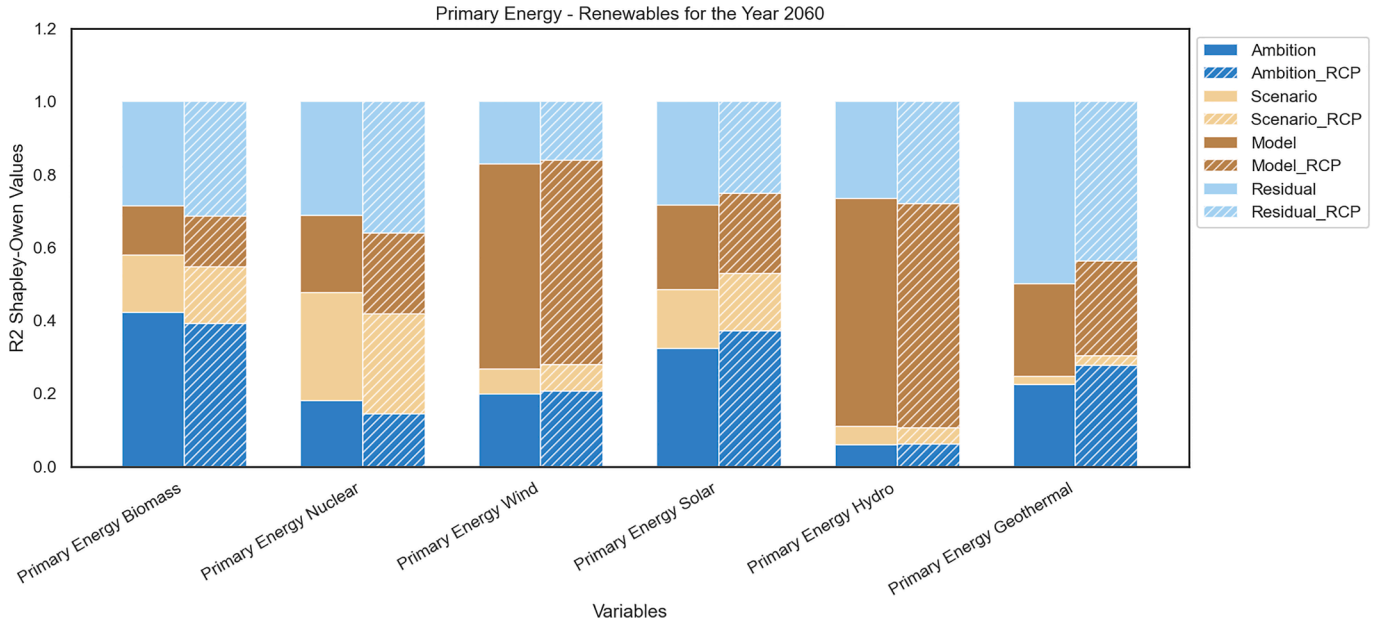

Fig. E3. The effects of using quadrative emissions versus RCPs to capture the climate ambition factor in Shapley–Owen decomposition – renewable sources for primary energy, 2060.

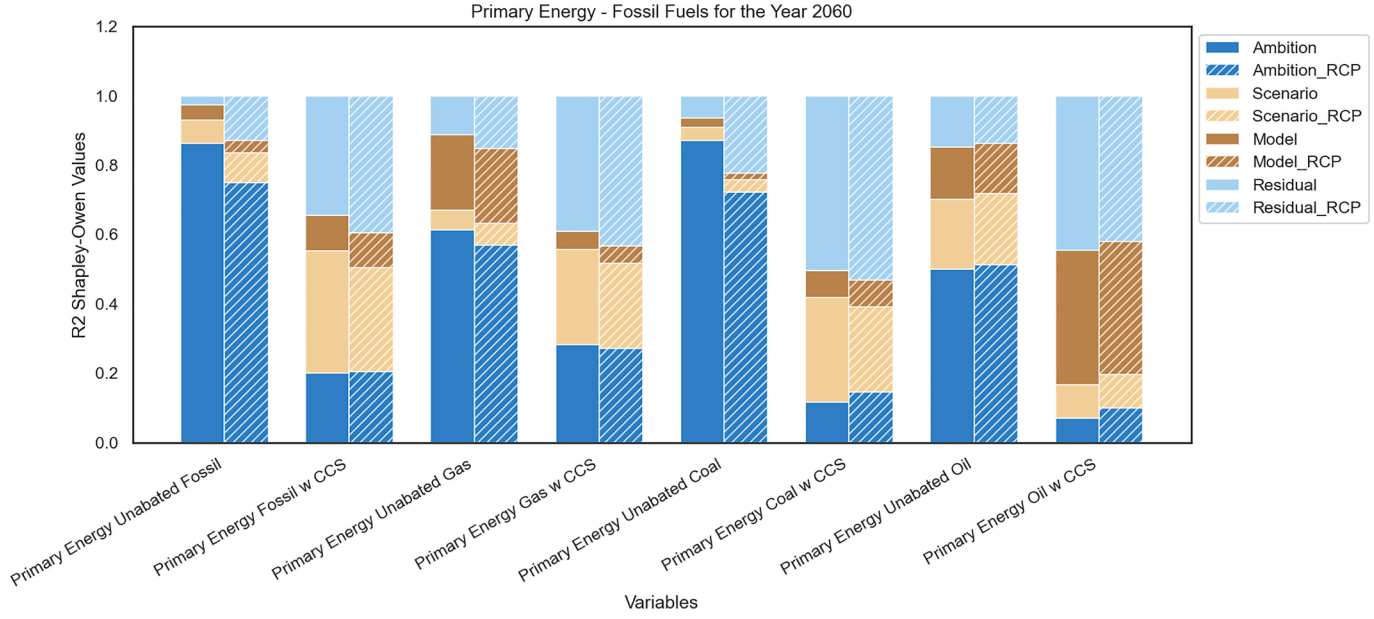

Fig. E4. The effects of using quadrative emissions versus RCPs to capture the climate ambition factor in Shapley–Owen decomposition – fossil fuel sources for primary energy, 2060.

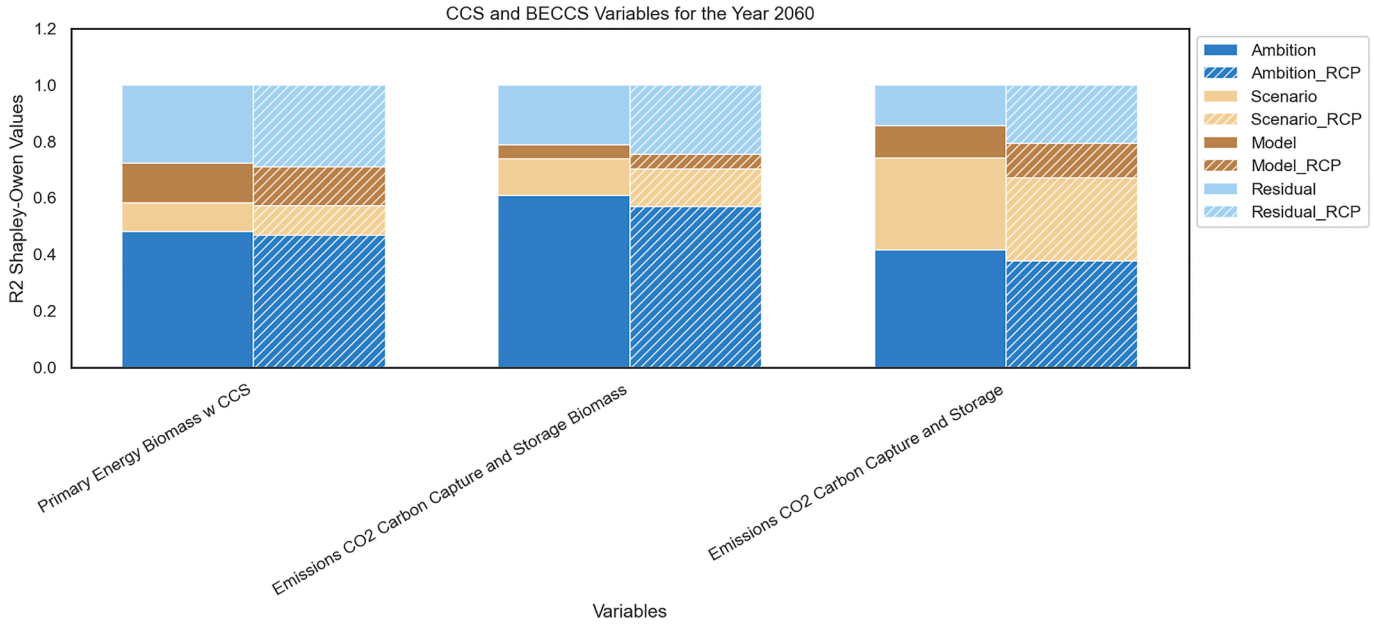

Fig. E5. The effects of using quadrative emissions versus RCPs to capture the climate ambition factor in Shapley–Owen decomposition – CCS and BECCS, 2060.

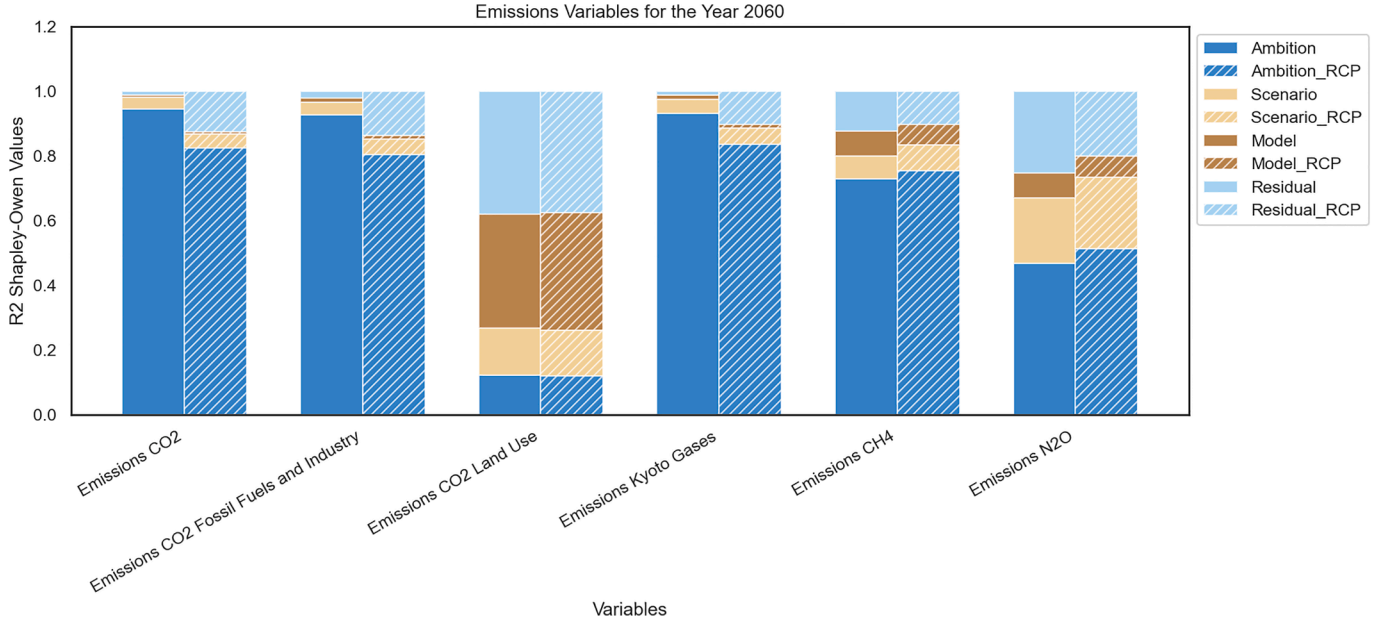

Fig. E6. The effects of using quadrative emissions versus RCPs to capture the climate ambition factor in Shapley–Owen decomposition – emissions variables, 2060.

Appendix F Code, data and visualisation availability

The code, output data for the decomposition analysis, decomposition and ternary plots and appendices plots are available on GitHub: https://github.com/AlKhourdajie/SSPs_decomposition.

References

[1] L. van Beek, M. Hajer, P. Pelzer, D. van Vuuren, C. Cassen, Anticipating futures through models: the rise of integrated assessment modelling in the climate science-policy interface since 1970, Glob. Environ. Change 65 (2020) 102191.

[2] IPCC, 2022. Annex III: scenarios and modelling methods. Guivarch, C., E. Kriegler, J. Portugal-Pereira, V. Bosetti, J. Edmonds, M. Fischedick, P. Havlík, P. Jaramillo, V. Krey, F. Lecocq, A. Lucena, M. Meinshausen, S. Mirasgedis, B. O'Neill, G.P. Peters, J. Rogelj, S. Rose, Y. Saheb, G. Strbac, A. Hammer Strømman, D.P. van Vuuren, N. Zhou (eds). In IPCC, 2022: Climate Change 2022: Mitigation of Climate Change. Contribution of Working Group III to the Sixth Assessment Report of the Intergovernmental Panel on Climate Change. P.R. Shukla, J. Skea, R. Slade, A. Al Khourdajie, R. van Diemen, D. McCollum, M. Pathak, S. Some, P. Vyas, R. Fradera, M. Belkacemi, A. Hasija, G. Lisboa, S. Luz, J. Malley, (eds.). Cambridge University Press, Cambridge, UK and New York, NY, USA. https://doi.org/10.1017/9781009157926.022.

[3] K. Riahi, C. Bertram, D. Huppmann, J. Rogelj, V. Bosetti, A.-M. Cabardos, A. Deppermann, L. Drouet, S. Frank, O. Fricko, S. Fujimori, M. Harmsen, T. Hasegawa, V. Krey, G. Luderer, L. Paroussos, R. Schaeffer, M. Weitzel, B. van der Zwaan, Z. Vrontisi, F. Dalla Longa, J. Després, F. Fosse, K. Fragkiadakis, M. Gusti, F. Humpenöder, K. Keramidas, P. Kishimoto, E. Kriegler, M. Meinshausen, L. P. Nogueira, K. Oshiro, A. Popp, P.R.R. Rochedo, G. Ünlü, B. van Ruijven, J. Takakura, M. Tavoni, D. van Vuuren, B. Zakeri, Cost and attainability of meeting

stringent climate targets without overshoot, Nat. Clim. Chang. 11 (12) (2021) 1063–1069.
[4] C. Guivarch, T. Le Gallic, N. Bauer, et al., Using large ensembles of climate change mitigation scenarios for robust insights, Nat. Clim. Chang. 12 (2022) 428–435, https://doi.org/10.1038/s41558-022-01349-x.
[5] G. Peters, A. Al Khourdajie, I. Sognnæs, B. Sanderson, AR6 scenarios database: an assessment of current practices and recommendations for future global assessments, npj Clim. Action 2 (2023) 31, https://doi.org/10.1038/s44168-023-00050-9.
[6] A. Gambhir, I. Butnar, P.-H. Li, P. Smith, N. Strachan, A review of criticisms of integrated assessment models and proposed approaches to address these through the lens of BECCS, Energies. (Basel) 12 (9) (2019) 1747, https://doi.org/10.3390/en12091747.
[7] J. Skea, P. Shukla, A. Al Khourdajie, &.D. McCollum, Intergovernmental panel on climate change: transparency and integrated assessment modeling, Wiley Interdiscip. Rev.: Clim. Change (2021), https://doi.org/10.1002/wcc.727 e727.
[8] K. Riahi, D.P. van Vuuren, E. Kriegler, J. Edmonds, B.C. O'Neill, S. Fujimori, N. Bauer, K. Calvin, R. Dellink, O. Fricko, W. Lutz, A. Popp, J. Crespo Cuaresma, S. KC, M. Leimbach, L. Jiang, T. Kram, S. Rao, J. Emmerling, K. Ebi, T. Hasegawa, P. Havlík, F. Humpenöder, L. Aleluia Da Silva, S. Smith, E. Stehfest, V. Bosetti, J. Eom, D. Gernaat, T. Masui, J. Rogelj, J. Strefler, L. Drouet, V. Krey, G. Luderer, M. Harmsen, K. Takahashi, L. Baumstark, J.C. Doelman, M. Kainuma, Z. Klimont, G. Marangoni, H. Lotze-Campen, M. Obersteiner, A. Tabeau, M. Tavoni, The shared socioeconomic pathways and their energy, land use, and greenhouse gas emissions implications: an overview, Glob. Environ. Change 42 (2017) 153–168, https://doi.org/10.1016/j.gloenvcha.2016.05.009. ISSN 0959-3780.
[9] M.M. Dekker, A.F. Hof, M. van den Berg, et al., Spread in climate policy scenarios unravelled, Nature 624 (2023) 309–316, https://doi.org/10.1038/s41586-023-06738-6.
[10] Byers, E., Krey, V., Kriegler, E., Riahi, K., Schaeffer, R., Kikstra, J., Lamboll, R., Nicholls, Z., Sandstad, M., Smith, C., van der Wijst, K., Al Khourdajie, A., Lecocq, F., Portugal-Pereira, J., Saheb, Y., Stromann, A., Winkler, H., Auer, C., Brutschin, E., Gidden, M., Hackstock, P., Harmsen, M., Huppmann, D., Kolp, P., Lepault, C., Lewis, J., Marangoni, G., Müller-Casseres, E., Skeie, R., Werning, M., Calvin, K., Forster, P., Guivarch, C., Hasegawa, T., Meinshausen, M., Peters, G., Rogelj, J., Samset, B., Steinberger, J., Tavoni, M., van Vuuren, D., 2022. AR6 scenarios database [Data set]. In Climate Change 2022: Mitigation of Climate Change (1.1). Intergovernmental Panel on Climate Change. https://doi.org/10.5281/zenodo.7197970.
[11] F. Huettner, M. Sunder, Axiomatic arguments for decomposing goodness of fit according to Shapley and Owen values, Electron. J. Stat. 6 (2012) 1239–1250, https://doi.org/10.1214/12-EJS710. ISSN: 1935-7524.
[12] U. Grömping, Estimators of relative importance in linear regression based on variance decomposition, Am. Stat. 61 (2) (2012) 139–147, https://doi.org/10.1198/000313007X188252.
[13] I.M. Sobol, Sensitivity estimates for nonlinear mathematical models, Math. Model. Comput. Exp. 4 (1993) 407–414.
[14] Looss, B., & Prieur, C., 2019. Shapley effects for sensitivity analysis with correlated inputs: comparisons with Sobol' indices, numerical estimation and applications. arXiv. Mathematics - Statistics Theory. https://doi.org/10.48550/arXiv.1707.01334.
[15] A.B. Owen, C. Prieur, On Shapley value for measuring importance of dependent inputs, SIAM/ASa J. Uncertain. Quantif. 5 (1) (2017) 986–1002, https://doi.org/10.1137/16M1097717.
[16] A.B. Owen, Sobol' indices and Shapley value, SIAM/ASa J. Uncertain. Quantif. 2 (1) (2014) 245–251, https://doi.org/10.1137/130936233.
[17] K.-I. van der Wijst, A.F. Hof, D.P. van Vuuren, On the optimality of 2 °C targets and a decomposition of uncertainty, Nat. Commun. 12 (2021) 2575, https://doi.org/10.1038/s41467-021-22826-5.
[18] G. Marangoni, M. Tavoni, V. Bosetti, E. Borgonovo, P. Capros, O. Fricko, D.E.H.J. Gernaat, C. Guivarch, P. Havlik, D. Huppmann, N. Johnson, P. Karkatsoulis, I. Keppo, V. Krey, E. Ó Broin, J. Price, D.P. van Vuuren, Sensitivity of projected long-term CO2 emissions across the shared socioeconomic pathways, Nat. Clim. Chang. 7 (2017) 113–117.
[19] D.P. van Vuuren, J. Edmonds, M. Kainuma, K. Riahi, A. Thomson, K. Hibbard, G. C. Hurtt, T. Kram, V. Krey, J.F. Lamarque, T. Masui, M. Meinshausen, N. Nakicenovic, S.J. Smith, S.K. Rose, The representative concentration pathways: an overview, Clim. Change 109 (2011) 5.
[20] X. Zhu, Comparison of four methods for handling missing data in longitudinal data analysis through a simulation study, Open J. Stat. 4 (11) (2014) 52855, https://doi.org/10.4236/ojs.2014.411088.
[21] M.A.E. van Sluisveld, M.J.H.M. Harmsen, D.P. van Vuuren, V. Bosetti, C. Wilson, B. van der Zwaan, Comparing future patterns of energy system change in 2 °C scenarios to expert projections, Glob. Environ. Change 50 (2018) 201–211, https://doi.org/10.1016/j.gloenvcha.2018.03.009.
[22] O. Fricko, P. Havlik, J. Rogelj, Z. Klimont, M. Gusti, N. Johnson, P. Kolp, M. Strubegger, H. Valin, M. Amann, T. Ermolieva, N. Forsell, M. Herrero, C. Heyes, G. Kindermann, V. Krey, D.L. McCollum, M. Obersteiner, S. Pachauri, S. Rao, E. Schmid, W. Schoepp, K. Riahi, The marker quantification of the shared socioeconomic pathway 2: a middle-of-the-road scenario for the 21st century, Glob. Environ. Change 42 (2017) 251–267, https://doi.org/10.1016/j.gloenvcha.2016.06.004.
[23] K. Riahi, F. Dentener, D. Gielen, A. Grubler, J. Jewell, Z. Klimont, V. Krey, D. McCollum, S. Pachauri, S. Rao, B. van Ruijven, D.P. van Vuuren, C. Wilson, Global Energy Assessment – Toward A Sustainable Future, Cambridge University Press and the International Institute for Applied Systems Analysis, Cambridge, UK and New York, NY, USA, and Laxenburg, Austria, 2012, pp. 1203–1306.
[24] M. Rogner, K. Riahi, Future nuclear perspectives based on MESSAGE integrated assessment modeling, Energy Strategy Rev. 1 (4) (2013) 223–232, https://doi.org/10.1016/j.esr.2013.02.006.
[25] K. Vaillancourt, M. Labriet, R. Loulou, J.P. Waaub, The role of nuclear energy in long-term climate scenarios: an analysis with the world-TIMES model, Energy Policy 36 (7) (2008) 2296–2307, https://doi.org/10.1016/j.enpol.2008.01.015.
[26] V. Krey, F. Guo, P. Kolp, W. Zhou, R. Schaeffer, A. Awasthy, C. Bertram, H.S. de Boer, P. Fragkos, S. Fujimori, C. He, G. Iyer, K. Keramidas, A.C. Köberle, K. Oshiro, L.A. Reis, B. Shoai-Tehrani, S. Vishwanathan, P. Capros, L. Drouet, J.E. Edmonds, A. Garg, D.E.H.J. Gernaat, K. Jiang, M. Kannavou, A. Kitous, E. Kriegler, G. Luderer, R. Mathur, M. Muratori, F. Sano, D.P. van Vuuren, Looking under the hood: a comparison of techno-economic assumptions across national and global integrated assessment models, Energy 172 (2019) 1254–1267, https://doi.org/10.1016/j.energy.2018.12.131. ISSN 0360-5442.
[27] E. Kriegler, N. Bauer, A. Popp, F. Humpenöder, M. Leimbach, J. Strefler, L. Baumstark, B.L. Bodirsky, J. Hilaire, D. Klein, I. Mouratiadou, I. Weindl, C. Bertram, J.P. Dietrich, G. Luderer, M. Pehl, R. Pietzcker, F. Piontek, H. Lotze-Campen, A. Biewald, M. Bonsch, A. Giannousakis, U. Kreidenweis, C. Müller, S. Rolinski, A. Schultes, J. Schwanitz, M. Stevanovic, K. Calvin, J. Emmerling, S. Fujimori, O. Edenhofer, Fossil-fueled development (SSP5): an energy and resource intensive scenario for the 21st century, Glob. Environ. Change 42 (2017) 297–315.
[28] N. Bauer, K. Calvin, J. Emmerling, O. Fricko, S. Fujimori, J. Hilaire, J. Eom, V. Krey, E. Kriegler, I. Mouratiadou, H.S. de Boer, M. van den Berg, S. Carrara, V. Daioglou, L. Drouet, J.E. Edmonds, D. Gernaat, P. Havlik, N. Johnson, D. Klein, P. Kyle, G. Marangoni, T. Masui, R.C. Pietzcker, M. Strubegger, M. Wise, K. Riahi, D.P. van Vuuren, Shared socio-economic pathways of the energy sector – quantifying the narratives, Glob. Environ. Change 42 (2017) 316–330, https://doi.org/10.1016/j.gloenvcha.2016.07.006.
[29] G. Luderer, S. Madeddu, L. Merfort, F. Ueckerdt, M. Pehl, R. Pietzcker, M. Rottoli, F. Schreyer, N. Bauer, L. Baumstark, C. Bertram, A. Dirnaichner, F. Humpenöder, A. Levesque, A. Popp, R. Rodrigues, J. Strefler, E. Kriegler, Impact of declining renewable energy costs on electrification in low-emission scenarios, Nat. Energy 7 (2022) 32–42.
[30] M. Isaac, D.P. van Vuuren, Modeling global residential sector energy demand for heating and air conditioning in the context of climate change, Energy Policy 37 (2) (2009) 507–521, https://doi.org/10.1016/j.enpol.2008.09.051.
[31] R. Zhang, S. Fujimori, The role of transport electrification in global climate change mitigation scenarios, Environ. Res. Lett. 15 (3) (2020).
[32] S. Dhakal, J.C. Minx, F.L. Toth, A. Abdel-Aziz, M.J. Figueroa Meza, K. Hubacek, I. G.C. Jonckheere, Yong-Gun Kim, G.F. Nemet, S. Pachauri, X.C. Tan, T. Wiedmann, Emissions Trends and Drivers, in: P.R. Shukla, J. Skea, R. Slade, A. Al Khourdajie, R. van Diemen, D. McCollum, M. Pathak, S. Some, P. Vyas, R. Fradera, M. Belkacemi, A. Hasija, G. Lisboa, S. Luz, J. Malley (Eds.), IPCC2022: Climate Change2022: Mitigation of Climate Change. Contribution of Working Group III to the Sixth Assessment Report of the Intergovernmental Panel on Climate Change, Cambridge University Press, Cambridge, UK and New York, NY, USA, 2022, https://doi.org/10.1017/9781009157926.004.
[33] Nabuurs, G.-J., R. Mrabet, A. Abu Hatab, M. Bustamante, H. Clark, P. Havlík, J. House, C. Mbow, K.N. Ninan, A. Popp, S. Roe, B. Sohngen, S. Towprayoon, 2022. Agriculture, forestry and other land uses (AFOLU). In IPCC, 2022: Climate Change 2022: Mitigation of Climate Change. Contribution of Working Group III to the Sixth Assessment Report of the Intergovernmental Panel on Climate Change. P.R. Shukla, J. Skea, R. Slade, A. Al Khourdajie, R. van Diemen, D. McCollum, M. Pathak, S. Some, P. Vyas, R. Fradera, M. Belkacemi, A. Hasija, G. Lisboa, S. Luz, J. Malley, (eds.). Cambridge University Press, Cambridge, UK and New York, NY, USA. https://doi.org/10.1017/9781009157926.009.
[34] E. Kriegler, J. Edmonds, S. Hallegatte, K. Ebi, T. Kram, K. Riahi, H. Winkler, D. van Vuuren, A new scenario framework for climate change research: the concept of shared policy assumptions, Clim. Change 122 (2014) 401–414, https://doi.org/10.1007/s10584-013-0971-5, pages.
[35] S. Lipovetsky, M. Conklin, Analysis of regression in game theory approach, Appl. Stoch. Models Bus. Ind. 17 (4) (2001) 319–330, https://doi.org/10.1002/asmb.446.
[36] S.K. Mishra, Shapley value regression and the resolution of multicollinearity, J. Econ. Bibliography 3 (3) (2016).
[37] B.C. O'Neill, T.R. Carter, K. Ebi, P.A. Harrison, E. Kemp-Benedict, K. Kok, E. Kriegler, B.L. Preston, K. Riahi, J. Sillmann, B.J. van Ruijven, D. van Vuuren, D. Carlisle, C. Conde, J. Fuglestvedt, C. Green, T. Hasegawa, J. Leininger, S. Monteith, R. Pichs-Madruga, Achievements and needs for the climate change scenario framework, Nat. Clim. Chang. 10 (2020) 1074–1084, https://doi.org/10.1038/s41558-020-00952-0.
[38] F.P. Colelli, E. De Cian, Cooling demand in integrated assessment models: a methodological review, Environ. Res. Lett. 15 (11) (2020) 113005, https://doi.org/10.1088/1748-9326/abb90a.